Essays on the Efficient Integration of Renewable Energies into Electricity Markets

Inauguraldissertation

zur

Erlangung des Doktorgrades

der

Wirtschafts- und Sozialwissenschaftlichen Fakultät

der

Universität zu Köln

2017

vorgelegt

von

Dipl.-Math. Frank Obermüller

aus

Köln

Referent	Prof. Dr. Felix Höffler
Korreferent	Prof. Dr. Marc-Oliver Bettzüge
Tag der Promotion	09.01.2018

Acknowledgment

First of all, I thank Prof. Dr. Felix Höffler as my mentor and supervisor during my doctoral studies. His fruitful comments and constructive critics strengthened my research as well as my academic career. I would also like to express my gratitude to Prof. Dr. Marc-Oliver Bettzüge for helpful academic feedback as well as enriching personal discussions.

Many thanks goes to my ewi/EWI family which supported me during the exciting time with joyful talks, relaxing lunch breaks, challenging projects, great vacation and working trips, and especially wonderful beer happenings. Each of you became unforgettable to me. I express my gratitude to Andreas Knaut, Florian Weiser and Philipp Henckes as the co-authors of my research papers.

Financial support is gratefully acknowledged by the Emerging Group on Energy Transition and Climate Change (ET-CC) funded by the DFG Zukunftskonzept (ZUK 81/1) and the Energy Storage Initiative funded through grant 03ESP239 by the German Federal Ministry for Economic Affairs and Energy (BMWi) and the German Federal Ministry of Education and Research (BMBF).

Finally, I thank my wonderful wife Nina and my son, my family and all my friends for the wonderful time in my life. You give me the strength and the motivation on the pursuit of happiness!

Frank Obermüller Cologne, September 2017

Contents

1 Introduction

The anthropogenic climate change involves the danger to be one major challenge for the world in the next century. The 2015 UN Climate Change Conference negotiated the Paris Agreement to tackle climate change, e.g. by the restriction of global warming to a maximum of 2°C . These targets translate to CO_2-reduction efforts, especially for the carbon-dioxide intense electricity sectors. The German effort is subsumed under the term *Energiewende* (engl. Energy Transition) which contains the transition from carbon-dioxide intense conventional or nuclear power plants to sustainable energies like wind, solar or hydro power.[1] The promotion of renewable energies seems promising to achieve the Energy Transition targets and reduce Germany's CO_2-emissions.

The promotion of renewable energies led to a significant renewable production share of 29% at the total German gross electricity production in 2016 (AG Energiebilanzen, 2017). However, renewable energies differ in production characteristics from conventional electricity production. Renewable energies like wind and solar power have almost zero marginal costs and strong production volatilities due to weather-dependence. Nevertheless, wind and solar power are two main technologies to promote renewable energies, especially in Germany. The different characteristics of renewable energies is still challenging for pure market integration. The impacts on market efficiency and strategic behavior are ex-ante not clear within the complexity of multiple sequential and regional electricity markets. This thesis sheds light on different aspects of electricity market efficiency which could strongly be influenced by renewable energies and their different characteristics. The efficiency can be separated to temporal and regional efficiency questions. The temporal efficiency is subject to the Chapters 2, 3 and 4. The regional aspect is subject to Chapter 5 and Chapter 6.

The sequential electricity market design serves as an excellent example for temporal efficiency. The concept of sequential market design should, among others, allow forward trading with the possibility of risk hedging. In electricity markets, where

[1] In fact, the German *Energy Transition* reaches further back and obtained greater visibility after the Fukushima nuclear accident in 2011.

the good is typically non-storable[2], this is even more important than for other goods. The day-ahead forward market serves typically as the reference market where most contracts are settled. Deviations from the day-ahead expectations can be traded in adjustment markets called real-time markets (PJM, ISO New England) or intraday-markets (Europe). This market setting works well for diversified competitive conventional producer portfolios which have limited incentive to deviate from their profit optimal marginal bidding strategy. However, this does not necessarily hold for renewable producers with zero marginal costs and uncertain production. **Chapter 2** examines the optimal bidding of renewable producers with zero-marginal costs and production uncertainty within an oligopoly. More precisely, the research question is investigated if oligopolistic renewable producers have an incentive to act strategically and withhold production in the forward market to increase prices and to sell the withheld production in the intraday-market. The assumption of an oligopolistic partitioning of the renewable producer seems counterintuitive under the fact that renewable energies are typically small-scale distributed generation like roof-top photovoltaic or regionally split wind parks. In fact, as a particular result of the electricity market liberalization, renewable aggregators entered the electricity market. The aggregators combine small-scale (private) renewable production within big (virtual) operators. The aggregation allows for effects of scale within different parts of the value chain, e.g. trading at different sequential markets. Thus, the aggregation leads to possible price influencing behavior and the danger of strategical bidding. This needs to be investigated and understand to ensure market efficiency under high shares of integrated renewable production.

The interaction between the day-ahead- and intraday-markets is also subject of **Chapter 3**. This chapter examines the forward premiums of renewable uncertainty. Forward premiums are price differences for a good between the forward market and a later (e.g. spot) market. They can occur due to risk hedging and price expectations. However, the reasons for forward premiums within sequential electricity markets are not fully understood and subject to current research. Typical research work investigates the effects of load uncertainty to forward premium effects. The temporal disaggregation such as seasonal or hourly differentiated forward premiums is examined as well in the literature. Chapter 3 extends the classical research literature by the effects of renewable uncertainty. With the increasing production share of renewable energies, this aspect becomes more relevant. To capture the renewable uncertainty effects, weather types are applied. This emphasizes the meteorological

[2]To a limited degree electricity storage is possible by batteries or physical transformation (pump storage, methanation) but not yet competitive in large scales.

weather implications to the current and future electricity markets.

Another view on the temporal market efficiency is examined in **Chapter 4** which focuses on the balancing market design. For Germany and several other European countries, the balancing markets serve as power provision for possible short-term deviations of supply and demand.[3] The purpose of the balancing markets is the stabilization of the transmission grid by short-run (seconds to minutes) production adjustments in case of unplanned deviations. In recent years, the balancing markets were dominated by conventional capacities. With the increasing share of renewables and the proceeding Energy Transition, those balancing markets should be opened to new players, e.g. renewable producers, batteries or demand side management. To reduce the entry barrier and further increase efficiency, the shortening of the weekly provision duration to shorter periods is politically discussed. Some research studies show the theoretical efficiency increase by shortened provision duration. On the other side, balancing markets could be subject to market concentration due to the limited participation possibility (technical operation prerequisites need to be fulfilled). The effect of a provision shortening on the market concentration is not yet well investigated. This is the focus of Chapter 4 which quantifies the efficiency gain and the market concentration effects.

Apart from the temporal efficiency aspects of the aforementioned chapters, the understanding of the regional implications of renewable energies is highly relevant within electricity markets. New challenges occurred with increasing renewable capacities. High wind situations could lead to grid congestion. This is the case for windy situations in Germany where northern wind production needs to be transferred to southern load centers. Additionally, transmission lines to neighboring countries have limited capacities. Windy hours could therefore lead to low electricity prices without the possibility of suitable exchange. On the other side, situations could arise where exceptional low wind is produced within one country. The situation in neighboring countries could be different due to the weather patterns. Thus, exchange would contribute to the level of secured capacity. Transmission extensions would allow lifting regional efficiency effects between countries as well as within countries. This extension is subject to current grid enforcement plans on national and European scale. However, the quantification of optimal transmission extension

[3]Note that the term *balancing market* is not consistently defined on an international level. Within this thesis, *balancing markets* denote the tender design to provide ex-ante reactions before or in the moment of physical delivery. These balancing markets are also known as (control) reserve markets. Sometimes *balancing market* refers to the ex-post market in which regional operators trade imbalance deviations after the physical delivery to reduce deviation penalties; these market are not focus of the analysis.

is a challenging task. One reason is the volatility of renewable production on hourly, seasonal or annual time scales.[4] These timescales need to be considered to estimate the welfare optimal electricity system extension. **Chapter 5** provides a temporal and regional high-resolution 20-year wind power dataset for total Europe to contribute an extensive dataset for this research field. The wind volatility of 20-years with its extreme values (high and low wind situations) as well as the average wind production is compared. Additionally, simultaneity of wind production across European countries is subject to the analysis. The focus lies on balancing effects in critical low wind situations.

Apart from the above mentioned wind balancing effects on a European scale, inner-country grid congestion could arise and distort the electricity market efficient outcome. The zonal market design in European countries, and especially in Germany, typically reimburses electricity production independent of the exact location within a country.[5] For the typical high northern wind production in congestion situations this implies that wind production regionally before the congested line has no additional value for the electricity system. In the German zonal market design, those northern wind production receives the same market prices as wind production regionally behind the congestion (assumed a fully market integration without a subsidy compensation).[6] This leads to a discrepancy between the market revenues (or the market value) of wind energy in comparison to its real contribution to the electricity system. One challenge of future renewable regulation is to design a subsidy scheme which incentivizes the optimal wind locations from the systems perspective (i.e. the electricity market with internalized grid congestions). **Chapter 6** contributes to solve this challenging task. It examines the regional incentives for wind production under a zonal pricing and under a nodal pricing regime. The zonal pricing is the current day-ahead market regime within Germany which does not internalize grid congestions in the wholesale market. The contrasting nodal pricing regime can be considered as the economic efficient benchmark market design since grid congestions would be internalized. The analysis sheds light on the question whether optimal wind locations under the current zonal pricing regime differ to

[4]Under the climate change, even longer investigation horizons are necessary covering up to 100 years or more.

[5]Regulatory price components could be implemented which is not the case for the exemplary German wholesale market. Ex-post adjustments like re-dispatch could be implemented with static efficiency but lack the market component in the current designs.

[6]A fully market integration without subsidies represents the goal of a future regulation regime. Renewables would face all market incentives and compete among each other for the most economical solution. But fully market integration becomes relevant right now. German subsidy schemes for wind and PV are designed to lasts for 20 years which implies that a certain part of the renewables fleet faces full market integration without subsidies.

optimal wind locations under the efficient nodal pricing. The implications support decision makers on efficient subsidy scheme towards a fully market integration of renewable energies.

The remaining structure of the introduction contains the methodology overview as well as the outline of each chapter. Each chapter represents a single research paper.

- Chapter 2: How to Sell Renewable Electricity - Strategic Interaction in Sequential Markets (based on Knaut and Obermüller (2016))
- Chapter 3: Explaining Electricity Forward Premiums - Evidence for the Weather Uncertainty Effect (based on Obermüller (2017b))
- Chapter 4: Tender Frequency and Market Concentration in Balancing Power Markets (based on Knaut et al. (2017))
- Chapter 5: The Benefit of Long-term High Resolution Wind Data for Electricity System Analysis (based on Henckes et al. (2018))
- Chapter 6: Build Wind Capacities at Windy Locations? Assessment of System Optimal Wind Locations (based on Obermüller (2017a))

If a research paper is conducted by more than one author, each author contributed equally to the research paper.

1.1 Methodology overview

The thesis investigates different efficiency aspects of renewable energy integration to electricity markets. Therefore different methodologies are required which address the research questions in the best suitable way. Concluding, the thesis relies on analytical equilibrium models, fundamental electricity market optimization models, empirical methods as well as statistical assessments.

Analytical models are applied in Chapter 2 and Chapter 3 for the profit optimal bidding strategy of renewable producers. In Chapter 2 the monopolistic or oligopolistic market equilibrium is subject to the investigation focus whereas Chapter 3 examines model results under perfect competition. Both analytical models optimize for traded quantities under renewable production uncertainty but with different focuses and assumptions, e.g. on the merit order shape.

Fundamental electricity market optimization models are applied in Chapter 4 and

Chapter 6. The objective function (total system cost minimization) is subject to typical electricity market constraints and assumptions. Chapter 4 extends the classical day-ahead market model for the European electricity markets by a representation of the German balancing markets. Here, the temporal provision duration is of high interest and will be varied to conduct new insight on efficiency gains and market concentration under a shortened provision duration. Chapter 6 focuses on the day-ahead market but examines inner-country locational incentives. Thus, the zonal electricity market model is extended to a nodal representation which also incorporates physical grid characteristics of direct current load-flow.

Empirical methods are necessary to analyze the forward premium effects within Chapter 3. The theoretical analysis is empirically tested based on time-series data (price, wind and solar production, load) in combination with weather type classifications. The cores are ordinary least square estimation which account for heteroscedastic and autocorrelation robust standard errors.

Statistical comparisons are mainly used in Chapter 5 to examine regional and temporal simultaneity effects of wind production between different countries across Europe.

1.2 Extended Abstracts

Chapter 2: How to Sell Renewable Electricity - Strategic Interaction in Sequential Markets

Chapter 2 examines the question if renewable producers with uncertain production and zero marginal costs have an incentive to strategically bid within the sequential day-ahead and intraday market design. The question becomes relevant for high shares of renewables which participate in electricity markets. This represents, for instance, electricity markets with (particular) market integrated renewable production (i.e. without fixed feed-in tariffs or after the subsidized period).

The research question is analyzed with an analytic two-stage profit optimization model. The model can be associated with the day-ahead market and subsequent intraday-market (which is similar to real-time markets). Conventional and renewable producers compete in order to satisfy the demand of consumers. In the day-ahead market, renewable producers face uncertainty about their production realization. The uncertainty resolves in the intraday-market. The model assumes conventional producers to act perfectly competitive. Renewable producers are assumed to act monopolistic or oligopolistic since market aggregators virtually combine small-scale renewable production.

The main result shows that renewable producers have an incentive to withhold production in the day-ahead market to increase prices and sell the withheld production in the intraday market. The analysis varies relevant aspects of the model as for instance the merit order shape, the level of renewables' competition, and the relation of the day-ahead to intraday merit order steepness. The main result holds true under each of these variations. The uncertainty has no impact to optimal bidding under a linear merit order curve but becomes relevant under a quadratic convex merit order shape. Nevertheless, welfare analyses are performed which prove that uncertainty has relevant distributional effects between conventional and renewable producers as well as consumers. Higher uncertainty decreases overall welfare. For an increasing number of renewable players, the withholding effect diminishes and the consumer surplus increases. Thus, implications for electricity markets under high shares of integrated renewables are the following. First, the regulator should pay attention that competition among renewable producers (and its aggregators) is high. This reduces the potential renewable production withholding in the day-ahead market. Second, reduced uncertainty has positive welfare effects. The uncertainty can be reduced by improved renewable production forecast quality or a day-ahead gate closure shift closer to physical realization. The latter needs to be investigated carefully, since further electricity market aspects (such as risk hedging, grid stability, etc.) are closely related.

Chapter 3: Explaining Electricity Forward Premiums - Evidence for the Weather Uncertainty Effect

This chapter sheds light on forward premium effects between the day-ahead- and intraday-market which could arise due to renewable production uncertainty. The research hypothesis states that positive forward premium effects are expected by higher renewable uncertainty. The analysis is motivated by an analytical model and examined with empirical hypothesis tests.

The analytical model is oriented at the model of Chapter 2 but extended to focus on a quadratic convex merit order function and perfect competition among all producers. The convexity of the merit order function leads to profit-optimal bidding strategies which sell less production to the day-ahead market than expected. The rationale is that potential overselling induces higher losses than potential underselling due to the merit order convexity.

This effect is examined empirically. Therefore, time-series data of the German electricity market is analyzed. The electricity market data is completed by weather type data from the German Weather Service. It is shown that weather type data could have significant influence on the forward premium level. Weather criteria like wind advection direction, cyclonality and humidity are identified as relevant indicators for forward premium effects. More important, the uncertainty of renewable forecasts can be clustered as to weather types. This allows estimating the forward premium effects of renewable forecast errors and renewable forecast uncertainty. The significant positive effect of both factors is quantified. That means that a higher renewable uncertainty leads to higher forward premiums as previously shown analytical. Hence, this finding extends the classical forward premium literature of load uncertainty, seasonal or hourly forward premium effects as well as scarcity effects on forward premiums by the effect of weather uncertainty.

The findings connect weather dependent renewable forecast uncertainty to forward premiums and support the consideration of weather types in price forecasting models. Therefore, results are highly-relevant for electricity market participants to understand interdependencies and accurately predict price effects.

Chapter 4: Tender Frequency and Market Concentration in Balancing Power Markets

Chapter 4 examines the market concentration effects of a shortened provision duration in German balancing power markets. The main question is whether a provision duration shortening increases unfavorable market concentration effects in contrast to the expected favorable efficiency gains.

The research question is of high relevance due to the current political discussion of a provision duration shortening to enable the participation of new technologies and to increase market efficiency. In the old-fashioned electricity systems, balancing markets were dominated by conventional producers. The current provision duration lasts for a whole week for primary and secondary balancing power (split into peak and off-peak products). To fulfill provision criteria, power plants are required to operate for the total provision duration. The possibility of pooling allows a suitable utilization of generation capacity within the power plant pool of an operator. This is beneficial for big portfolios by lower provision costs. Small providers face disadvantages.

The shift in electricity markets towards renewable producers by the Energy Transition requires opening balancing markets for new technologies like renewables, demand side management, or batteries. These technologies could provide balancing power for a certain time period but a weekly provision with its production and demand uncertainties seems too challenging. Therefore a provision duration shortening is discussed which is expected to increase efficiency simultaneously. However, the implications on market concentration by a shortening are ex-ante not clear. Due to the operator structure and the pooling possibility, a provision shortening could drastically impact market concentration. This trade-off is examined within this chapter.

To analyze the research question, a fundamental electricity market optimization model is applied and extended to consider balancing power markets as well as operator structures for Germany. The results indicate that shorter provision durations could reduce balancing costs by 15%. On the other side, market concentration is effected ambiguously. Specific situations lead to a relevant increase in market concentrations. Provision duration adjustments should therefore be performed with caution and market concentration should be monitored carefully.

Chapter 5: The Benefit of Long-term High Resolution Wind Data for Electricity System Analysis

Chapter 5 examines wind balancing effects with a novel high-resolution 20-year wind production dataset. The incorporation of such datasets becomes more important for electricity markets due to the increased share of weather-dependent renewable production. An understanding of production characteristics is essential for the functioning of future electricity systems. Critical low wind situations may endanger the security of supply. So far, historical observations of wind power production are limited to few recent historical years and may not suffice to quantify the expected overall wind contribution, its variability, and its regional balancing effects for future electricity systems.

To examine the wind characteristics and international balancing effects, statistical evaluations are performed. The results indicate three findings. First, the high-quality of the dataset is proven by comparisons to other wind datasets and real-world data. Second, the variation properties of annual wind production are investigated. Extreme situations (like high- and low-wind) as well as average wind productions have no obvious correlation and could strongly vary per year. A conclusion on a representative wind year cannot be drawn. Third, the potential beneficial balancing effects between countries are analyzed. Germany could highly benefit from neighboring countries in low-wind situations. The probability of simultaneous critical low-wind situations in multiple neighboring countries is comparable low.

The dataset and the results serve as input for further analyses (e.g. in Chapter 6). It supports evaluation of grid expansion discussions. Electricity market models benefit from a better comparison of wind input data.

Chapter 6: Build Wind Capacities at Windy Locations? Assessment of System Optimal Wind Locations

Chapter 6 examines the question of optimal wind locations under nodal and zonal pricing regimes. The installed wind capacities have steadily been increasing. However, the wind locations extensions have only limited incentive to consider grid congestions or market situations. The zonal pricing system in Germany favors wind production at windy locations (especially in combination with fixed feed-in tariffs or similar remuneration schemes). This led to high wind capacities at locations which could increase grid congestions and hence be system-unfriendly.

This chapter aims on identifying system optimal wind locations. Therefore a nodal electricity market model for Germany is applied (with connection to neighboring countries). The nodal market outcome is compared to the zonal market outcome. The analysis focuses on a pure market integration of wind production without distorting subsidy schemes. In a first step, wind revenues per node are compared between the nodal and zonal pricing regime. The focus on revenues is reasonable under assuming zero marginal costs and identical location costs across Germany. In a second step, the investigation was extended to the widely-used wind value factor, which represents the average market price that can be expected by wind producers.

The results identify optimal wind locations under efficient nodal pricing. The optimal wind locations under zonal pricing deviate from its comparable nodal pricing results. Thus, the zonal pricing optimal wind locations can be identified as inefficient since they do not consider grid congestion within its remuneration. The regional market values of wind production do not reflect the revenue-optimal locations. Thus, the value factor is not suitable as a detailed indicator and should only be considered for rough estimations and not for detailed analyses. Furthermore, the market value factor under zonal pricing overestimates windy locations in contrast to the nodal pricing regime.

The results contribute to a better understanding of optimal wind locations under zonal or nodal market design. Moreover, it is highly relevant for designing adequate wind production subsidy schemes which incentivize market optimal locations with consideration of grid congestion.

2 How to Sell Renewable Electricity - Strategic Interaction in Sequential Markets

Uncertainty about renewable production increases the importance of sequential short-term trading in electricity markets. We consider a two-stage market where conventional and renewable producers compete in order to satisfy the demand of consumers. The trading in the first stage takes place under uncertainty about production levels of renewable producers, which can be associated with trading in the day-ahead market. In the second stage, which we consider as the intraday market, uncertainty about the production levels is resolved. Our model is able to capture different levels of flexibility for conventional producers as well as different levels of competition for renewable producers. We find that it is optimal for renewable producers to sell less than the expected production in the day-ahead market. In situations with high renewable production it is even profitable for renewable producers to withhold quantities in the intraday market. However, for an increasing number of renewable producers, the optimal quantity tends towards the expected production level. More competition as well as a more flexible power plant fleet lead to an increase in overall welfare, which can even be further increased by delaying the gate-closure of the day-ahead market or by improving the quality of renewable production forecasts.

2.1 Introduction

A broad range of current electricity markets face an rapid increase in renewable energies to decrease carbon-dioxide emissions. These technologies were highly subsidized in the past and therefore not well integrated into the market. However, subsidies will run out and it is high on the European Union's policy agenda to integrate renewable generation into the market (EU Comission (2009), EU Comission (2013)). This means in the future, renewable producers are expected to sell their entire production at the existing sequential wholesale electricity markets, e.g. the day-ahead and the intraday market.[1]

[1]The long-term forward market is currently not a relevant market for volatile renewables due to the uncertain production in the long run.

The specific problem is that it is unclear how renewable energies sell their production between forward markets (like day-ahead) and real time markets (intraday). Most electricity markets are organized with a sequential structure in which competition in quantities á la Cournot is assumed. The fundamental work of Allaz and Vila (1993) shows that forward trading is beneficial for Cournot competitive producers. Additionally, the sequential structure allows for risk hedging in uncertain production or prices. This is relevant for renewable energies which face uncertainty of their realized production. Thus, their optimal quantity bidding behavior between short-term forward markets like the day-ahead market and real-time markets (e.g. the intraday market) are ex-ante unclear.

To analyze the research question, an analytic profit maximizing model is applied. This model allows insights into optimal bidding for the monopoly and the oligopoly case. One major investigation aspect is the effect of renewables' production uncertainty on optimal bids. The model results account for a linear merit order as well as a more realistic convex merit order. Additionally, the model allows quantifying distribution effects between producer surpluses and consumer surpluses as well as effects on the overall welfare.

Previous fundamental work on optimal Cournot bidding in sequential markets is given by Allaz (1992) and Allaz and Vila (1993). Within a sequential market framework, they show the existence of incentives for forward bidding to increase profits. They focus on the duopoly case under a linear merit order and abstract from uncertainty. The model was extended to electricity markets by Ito and Reguant (2016) which is probably the closest work to our research. They investigate strategic bidding behavior for a Cournot monopoly in a two-stage sequential market framework.[2] They assume a linear merit order function (i.e. supply curve) and perfect foresight. Ito and Reguant (2016) focus on the impact of arbitrage that participates between the two stages.

Although, the basic analytical model is quite similar, we extend the findings of Ito and Reguant (2016) in several ways. First, we derive our results for competitive oligopolies since this is a more realistic assumption in electricity markets. Arbitrage is thus handled as additional producers (for a discussion of this see Section 2.7.1). Second, our investigation focus is production uncertainty which is not considered in Allaz and Vila (1993) or Ito and Reguant (2016). Third, we emphasize the case of a supply function increases from day-ahead market to intraday-market as motivated

[2] Note that the model of Ito and Reguant (2016) additionally incorporates a competitive fringe which results in downward sloping inverse demand function for the monopoly player.

and investigated by Knaut and Paschmann (2017b) or Kiesel and Paraschiv (2017). A major distinction is our additional analysis of distribution effects and welfare derived from the equilibrium results.

The latter of the paper is organized as followed: In Section 2.3 we develop the basic model framework. Section 2.4 analyzes the Cournot competition and the basic model is applied to the monopolistic as well as the oligpolistic case. Section 2.5 focuses on the impact of flexibility constraints for conventional power technologies. Section 2.6 sheds light onto the incentives of renewable producers to withhold capacity in the intraday market. In Section 2.7 we show the effects on welfare, producer and consumer surplus. In Section 2.8 we conclude our results and discuss possible policy implications.

2.2 Background and literature

This section gives detailed information about the background on electricity markets as well as relevant literature.

2.2.1 Background

In electricity markets, demand and supply need to be balanced at all times. Therefore it is essential for all market participants to announce their foreseeable production and consumption in advance. The largest share of electricity is currently traded in the day-ahead market, which can be considered as a kind of forward market. Trading commonly takes place at noon one day before physical delivery. This is necessary to signal the regional supply and demand situations to the transmission system operators in advance, such that they can guarantee grid stability. In contrast, the intraday market provides the opportunity to trade electricity down to 30 minutes before physical delivery. Hence, adjustments to the day-ahead market clearing result can be traded which may occur due to (uncertain) short term deviations in electricity systems (e.g. demand forecast errors, renewable forecast errors, and unforeseen power plant shortages).

The characteristics of renewable electricity generation have increased the importance of sequential short-term trading and are affecting the competition in electricity markets. Renewable energy technologies differ in two important aspects from classic conventional technologies. First, renewables produce electricity at short run marginal costs of zero whereas conventional technologies have short run marginal costs greater than zero. Second, renewable electricity production depends on weather conditions that can only be predicted to a certain level. The uncertainty diminishes with a shorter time duration to the physical delivery. Thus, volatile renewable producers have a higher uncertainty if they trade in the day-ahead market. Therefore, the optimal bidding strategy for renewable energy producers in the intraday and day-ahead market under uncertainty is not clear and in the focus of the following investigations.

Electricity markets are known to be especially vulnerable to the potential abuse of market power (Borenstein et al., 2002, Green and Newbery, 1992). The demand can be regarded as very price inelastic in the short-run and therefore participants could be able to increase prices above the competitive level. While this has been an issue of large conventional generators in the past, we also can expect large renewable producers as being able to act strategically in sequential electricity markets. The size of renewable aggregators who aggregate renewable generation plants and sell the production in the market is steadily increasing especially because they are able to lift significant scale effects by increasing their renewable portfolio (e.g. reduction in costs of trading and reduction of forecast uncertainty).

In this paper, we analyze the competition between conventional and renewable producers that interact in two sequential stages by using an analytic model. The first stage is considered as the day-ahead and the second as the intraday market. The electricity production of the renewable producer is uncertain in the first stage and is realized in the second stage. In particular, this affects renewable producers in choosing the optimal quantity to trade in both stages. Furthermore, we account for flexibility constraints of conventional power producing technologies, because not all conventional technologies are flexible enough to change their production schedules in short time intervals (e.g. 30 minutes before physical delivery). These flexibility constraints are included in our model to measure effects on profit maximizing quantities and prices. We analyze the results based on different levels of competition for the renewable producers, ranging from a monopoly to oligopolies under a flexible and less flexible power plant fleet.

2.2.2 Literature overview

Our investigation is strongly related to the branch of two-stage Cournot games as well as the literature of optimal bidding strategies for renewable producers. A general overview of existing literature as to optimal bidding approaches and competition in electricity markets is given by von der Fehr and Harbord (1998). Concerning two-stage Cournot games, fundamental work is given by Allaz (1992) and Allaz and Vila (1993) who investigate Cournot competition of a duopoly in sequential markets. Their subject of investigation is the forward market which, however, can be transferred to our idea of a day-ahead auction before the market is finally cleared in an intraday auction. The setting differs to our model with respect to the type of players. In Allaz and Vila (1993) both players have increasing marginal costs of production and no uncertainty associated with their level of production. In Allaz (1992), uncertainty is incorporated in the two-stage model such that risk hedging influences the optimal production. However, Allaz (1992) and Allaz and Vila (1993) assume implicitly infinite production possibility, which is not true for our renewable producer. Similar to Allaz and Vila (1993), Saloner (1987) developed an extension of the classical Cournot one-shot duopoly to a model with two production stages in which the market clears only once after the second stage. In this framework Saloner showed the existence of a unique Nash-Cournot equilibrium under the possibility of a second stage response action. Nevertheless, the model does not account for different player types or uncertainty of production. Bushnell (2007) extents the general Cournot duopoly of Allaz and Vila (1993) to oligopoly competition which is similar to our Section 2.4.3 but without consideration of renewable producers or production uncertainty. Bushnell (2007) support their analytical finding of production withholding under imperfect competition with empirical results for US electricity markets (PJM, New England and California). Similar to Allaz and Vila (1993), they assume no-arbitrage behavior between sequential markets such that forward and spot prices are identical. Twomey and Neuhoff (2010) transfer the general theoretical findings to the case of electricity markets in which renewable producers and conventional producers are competing. They analyze the case when conventional players use market power to increase prices. With their model they are able to show that renewable producers are worse off in settings with market power of conventional producers. They assume a convex supply function of conventional producers which is similar to hour assumption in Section 2.4.2. In contrast to our analysis they do not consider the strategic behavior of renewable producers and abstract from uncertainty. The work of de Frutos and Fabra (2012) focus on symmetric and asymmetric oligopolies and the impact of different forward contract distributions among the producers to their bidding behavior. They find, that a symmetric forward contract distribution under symmetric firms decrease the forward prices and increase market efficiency. This is relevant for our oligopoly investigation which assumes symmetric players and thus a symmetric forward contract distribution (i.e. forward contract bidding). In our model setup, we confirm the price decreasing and efficiency increasing results of de Frutos and Fabra (2012). Acemoglu et al. (2017) apply a Cournot model and distinct between Cournot competitive conventional producers and perfect-competitive renewable producers. They deviate from classical models by the assumption of incomplete information. However, in their model framework renewable producers do not act competitive. This is one critical assumption as discussed previously which we address in our theoretical model.

In parallel but independent work, which was just published while our paper was about to be finalized, Ito and Reguant (2016) deal with a similar problem and come to very similar conclusions. Our basic model setup is essentially identical to Ito and Reguant (2016) and therefore also many of the theoretical insights coincide. Their case of "no arbitrage" is similar to our monopolist case and the case of strategic arbitrage is similar to the introduction of additional renewable players. Our work nevertheless, adds some important insights to the topic that cannot be found in Ito and Reguant (2016). We explicitly consider the role of uncertainty in our model. While this has no effect (at least for linear marginal costs) on the optimal strategies, we are able to quantify the effect of uncertainty on overall welfare and distribution effects. We find that welfare is decreased if uncertainty about final production levels is large. This signifies the importance of forecast uncertainty and market design for the efficient functioning of electricity markets. In addition, we also consider the effect of a convex marginal cost function and show that this increases the incentive for strategic withholding of quantities. Furthermore, our analysis sheds light on the role of strategic behavior in oligopolistic markets instead of focusing solely on the monopolist case (as in Ito and Reguant (2016)). We are therefore able to illustrate distributional and welfare effects for different numbers of strategic players, which cannot be found in Ito and Reguant (2016). Besides providing additional intuitions for the results of Ito and Reguant (2016), the paper is also able to shed light on some important additional aspects.

The other branch of relevant literature covers optimal bidding strategies under uncertain production of one single player. Many papers in this field analyze numerical models from a price taker perspective and focus on wind power producers. For instance, Botterud et al. (2010) numerically analyze the optimal bidding for a wind power producer in a two-stage market (day-ahead and real time market) under certain risk assumptions.[3] They find that the optimal bid on the day-ahead market

[3]Here, *real time market* means the ancillary grid services for balancing supply and demand.

depends on risk behavior and the respective market prices. Furthermore, it tends towards the expected production as a deviation penalty between the day-ahead and the real time market is introduced. Botterud et al. (2010) focus on one specific wind power producer without considering the implications of adjusted bidding strategies on the market equilibrium. Those effects can influence the optimal bidding strategy as we will show in the investigated oligopoly cases. Further literature similar to Botterud et al. (2010) can be found in Bathurst et al. (2002), Usaola and Angarita (2007), Pinson et al. (2007), and Morales et al. (2010).

2.3 The Model

We consider two players that interact at two stages in the wholesale market for electricity, namely, conventional producers (c) and renewable producers (r). The consumers are assumed to behave completely price-inelastic in the short-run and demand a quantity D. The demand of consumers is satisfied already in the first stage, since we assume consumers as being myopic and risk-averse. On the supply side, we distinguish between conventional producers and renewable producers.

Conventional producers in the model are represented as competitive fringe. They are able to produce electricity at total costs of $C(q_c)$ where q_c is the quantity produced. These quantities are sold into the market at a uniform price of the marginal production costs. The conventional producers also act as market makers which means they always satisfy the residual demand in both stages[4].

Renewable producers produce electricity at zero marginal costs. Their final production level Q is uncertain in the first stage with the probability density function $f(Q)$. The uncertainty about the production level resolves over time (from stage 1 to 2; cf. Figure 2.1).

Throughout our analysis we assume the probability function $f(Q)$ as symmetric. In our view this assumption is reasonable, since well-behaved forecasting models should be able to produce a symmetric distribution.[5]

Conventional and renewable producers can trade electricity in the two stages ($t =$

[4]Conventional producers have a strong incentive to sell their production in a market as long as the price is above their marginal production costs. This makes it seem to be a reasonable assumption that conventional producers always satisfy the residual demand when prices are above or equal to their marginal generation costs.

[5]Of course the distribution would not be symmetric in cases where production is expected to be extreme in the sense of a very low (close to zero) or very high (close to the capacity limit) production. Further information on wind forecasts and uncertainty can be found in Zhang et al. (2014).

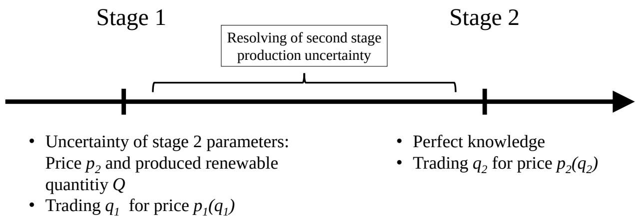

Figure 2.1: Basic two-stage model

1 and $t = 2$). For the conventional producers quantities are denoted by q_{ct} and for the renewable producer by q_{rt}. Here, we allow for q_{ct} and q_{rt} to be positive or negative. This allows producers, e.g. to sell too much production in the first stage and buy back quantities in the second stage. As already mentioned, we assume the demand of consumers (D) to get satisfied in the first stage. In the second stage, conventional and renewable producers can adjust their positions, e.g. conventional producers buy quantities from the renewable producer in order to replace their more expensive conventional production with renewable electricity. In this setting it is unclear what quantity (q^*_{r1} and q^*_{r2}) is optimal to trade in the first and second stage for the renewable producer.

The market clearing conditions at both stages can be written as

$$\text{Stage 1:} \qquad D = q_{c1} + q_{r1} \tag{2.1}$$

$$\text{Stage 2:} \qquad D = q_{c1} + q_{c2} + q_{r1} + q_{r2}. \tag{2.2}$$

The conventional producers produce electricity based on linear increasing marginal cost functions in both stages. A linear marginal cost abstracts from real cost functions in electricity markets in two important assumptions. The first model assumption is the linearity. In reality, the cost function is usually a monotonic increasing function (with a mainly stepwise convex-similar shape). Therefore, in theory, a usual simplifying assumption is a convex cost function. In contrast to this, we assume linearity since it simplifies the theoretical analysis. Similar results can be obtained with a convex cost function (e.g. arbitrary second order quadratic functions monotonic increasing in $\mathbb{R}^+$). However, this increases the complexity without generating significant further insights.

Second, in reality, marginal costs of production may change with time, which can have multiple reasons. In electricity markets this may be due to technical constraints of power plants (start-up costs, minimum load restrictions or partload-efficiency losses) or due to transaction costs of participants that do not engage in short-term trading in short intervals before production. In the end, this may lead to a reduction of electricity supply that is available on short notice.

We account for a change of the supply side by considering two different marginal cost functions $MC_1(q)$ and $MC_2(q)$ with different inclinations a_1 and a_2. Since the number of flexible power plants is lowered the closer we get to physical delivery (or less power plant operators participate in the second market), a_2 has to be greater than a_1. As explained before, the supply curve may change due to two reasons. First, technical constraints of power plants which are not able to adjust their power output in short intervals before production can lead to reduced supply. Second, there may be transaction costs for power plant operators to participate in the intraday market which is why supply is also reduced. This approach is similar to Henriot (2014) and has been empirically verified for the German intraday market by Knaut and Paschmann (2017b).

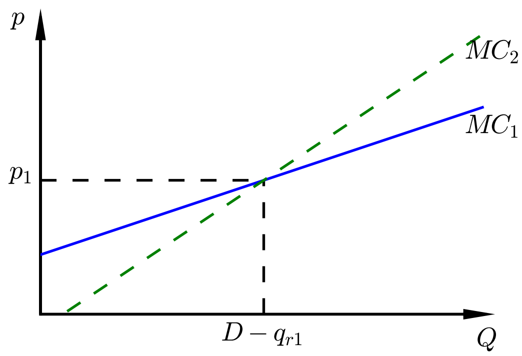

Figure 2.2: Marginal cost function in the first and second stage

For the analysis we have to define the properties of the marginal cost function in the second stage. Besides the increase of the slope to a_2, the whole curve needs to cross the market clearing point from the first stage. Because if there are no adjustments in quantities, the price of the first and second stage are identical. Thus the marginal cost function for the second stage can be obtained by a rotation around the market clearing point from stage 1 (cf. Figure 2.2). This means an increase in production comes at additional costs and a decrease in production at fewer savings of production costs. In combination with the market clearing conditions, this leads to the following two equations for price formation in the two stages:

$$p_1(q_{r1}) = a_1\,(D - q_{r1}) + b_1 \tag{2.3}$$

$$\mathbb{E}[p_2(q_{r1}, q_{r2})] = a_2(D - q_{r1} - q_{r2}) + b_1 + (D - q_{r1})\,(a_1 - a_2)\,, \tag{2.4}$$

where b_1 is the offset, a_1 the gradient in the first stage and a_2 the gradient in the second stage of the marginal cost function.

In a next step, we will derive the respective profit functions for the conventional and renewable producer. The conventional producer's profit function is defined as

$$\Pi_c(q_{c1}, q_{c2}) = p_1(q_{r1})q_{c1} + p_2(q_{r1}, q_{r2})q_{c2} - C_1(q_{c1}) - C_2(q_{c1} + q_{c2}) + C_2(q_{c1}). \tag{2.5}$$

Revenues in both stages are the products of the respective prices and quantities. Production costs depend on the power plants utilized for production. Since the marginal costs of production may change with time, the costs consist of the sum of quantities planned for production in each stage.

The profit function of the renewable producer

$$\Pi_r(q_{r1}, q_{r2}) = p_1(q_{r1})q_{r1} + p_2(q_{r1}, q_{r2})q_{r2} \tag{2.6}$$

consists of the quantities traded at the respective prices in the first and second stage without associated production costs.

We are able to show how competition between renewable producers and conventional producers can be modeled by applying this framework to different settings. In this paper, we will consider three cases:

- Competition in the first stage with identical cost functions: $q_r = Q$, $a_1 = a_2 = a$
- Competition in the first stage with changing cost functions: $q_r = Q$, $a_2 > a_1$
- Competition in the first and second stage with changing cost functions: $q_r \leq Q$, $a_2 > a_1$.

2.4 Cournot Competition of Renewable Producers

Throughout this paper we focus on a linear marginal cost function which can be regarded as the simplest case.[6] In this section, we will first give an intuition for the results of the model based on the simple case of identical cost functions and a renewable monopolist who acts strategically in the first stage. For this part of the analysis, we assume that the renewable producer sells the complete remaining production in the second stage, meaning $q_r = Q$.[7] In a next step, we will extend the analysis from the renewable monopoly to an oligopoly.

We can parametrize the linear marginal cost function $MC(q_c) = aq_c + b$ by the gradient $a \in \mathbb{R}_{>0}$ and an offset $b \in \mathbb{R}_{\geq 0}$ with variable $q_c \in \mathbb{R}_{\geq 0}$ as the produced quantity from conventional producers. Because demand is assumed to be price inelastic, we can write the prices in both stages a function of renewable quantities:

$$p_1(q_{r1}) = a(D - q_{r1}) + b \tag{2.7}$$

and

$$p_2(Q) = a(D - Q) + b. \tag{2.8}$$

2.4.1 Renewable Producer Monopoly

First, we look at the simple case in which all renewable production is traded by one firm. From economic literature it is well known that under the assumptions of Cournot competition, the monopolist has incentives to deviate from welfare optimal behavior in order to maximize its own profits. In our sequential market setting, this can be observed as well. By Proposition 2.1 we show that the optimal bidding strategy for a renewable producer under a monopoly is to bid half the expected production in the first stage.

Proposition 2.1. *The profit maximizing quantity for a renewable monopolist is* $q^*_{r1} = \frac{\mu_q}{2}$ *with* μ_q *the expected renewable production.*

---

[6] The main results also hold for convex second-order cost functions. However, the exact results may slightly deviate (i.e. it has a slightly shifting influence to the profit maximizing bidding strategy, but comparable small impact on the main results).

[7] Note that we assume additionally $Q \leq D$. If $Q > D$ and renewable producers have to sell their whole production in stage 2, we would force producers to bid negative prices. In such cases, we would expect that renewable producers reduce their production to avoid too low prices, e.g. below 0. This will be discussed in Section 2.6 in which we extend the model and allow for $q_r \leq Q$.

Proof. The basic profit function of a renewable producer in our theoretical model framework is described in (2.6). For identical marginal cost functions, we derive the following expected profit function

$$\mathbb{E}[\Pi_r(q_{r1})] = q_{r1}\,(a(D - q_{r1}) + b) + \int (Q - q_{r1}) f(Q)\,(a\,(D - Q) + b)\; dQ. \quad (2.9)$$

Where the first derivative results in

$$\frac{\mathrm{d}}{\mathrm{d}q_{r1}}\mathbb{E}[\Pi_r(q_{r1})] = a(D - q_{r1}) + b - aq_{r1} - Da \int f(Q)\,dQ + a \int Qf(Q)\,dQ - b \int f(Q)\,dQ. \quad (2.10)$$

Since $f(Q)$ is symmetric and the marginal cost function is linear, we can further simplify the expected profit function by the following substitutes:

$$\text{Expected value for } Q: \quad \int Qf(Q)\,dQ = \mu_q \quad (2.11)$$

$$\text{Distribution function has a total probability of 1:} \quad \int f(Q)\,dQ = 1 \quad (2.12)$$

This leads to the simplified necessary condition for the profit maximizing quantity q^*_{r1} as

$$\frac{d}{dq_{r1}}\mathbb{E}[\Pi_r(q_{r1})] = -Da + a\mu_q - aq_{r1} + a(D - q_{r1}) \overset{!}{=} 0. \quad (2.13)$$

Now we can solve this equation for q_{r1} which results in the profit maximizing quantity

$$q^*_{r1} = \frac{\mu_q}{2}. \quad (2.14)$$

In order for this being a maximum the second derivative has to be negative. This can easily be checked by calculating

$$\frac{d^2}{dq^2_{r1}}\mathbb{E}[\Pi_r(q_{r1})] = -2a. \quad (2.15)$$

Since a is defined as the slope of the marginal cost function and is positive by definition, $q^*_{r1} = \frac{\mu_q}{2}$ indeed describes the profit maximizing quantity for the renewable producer. □

The motivation of the renewable producer to bid half her expected quantity in the first stage becomes clear by analyzing Figure 2.3. Since we consider a linear marginal cost function, we can abstract from the uncertainty in renewable production $f(Q)$

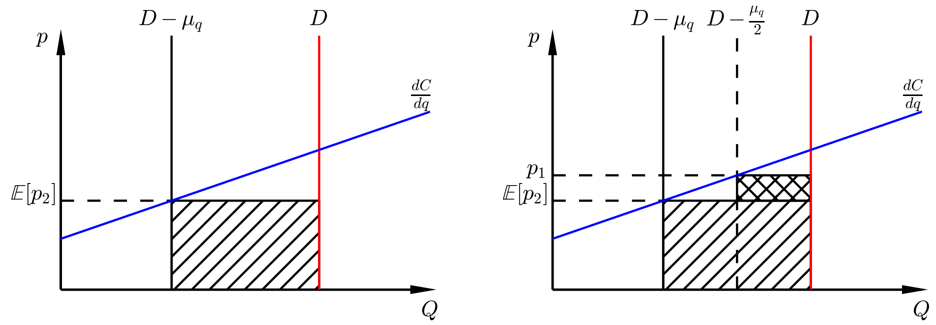

(i) Lower bound for the profit of the renewable producer

(ii) Profit of the renewable producer from the first and second stage

Figure 2.3: Optimal quantity of the renewable monopolist

and only consider the expected production μ_q. The profit of the renewable producer can be split into two parts. One part stems from selling the expected production into the market, as can be seen in Figure 2.3i (single hatched area). This part can be considered as a lower bound to the profit of the renewable producer and does not depend on the strategy of the renewable producer because she has to sell all production to the market in the final stage. The resulting price in the second stage is thus given by $\mathbb{E}[p_2]$. The second part of the renewable producer profit can be obtained by selling a quantity forward in the first stage at a price p_1. In order to increase her profit, the quantity in the first stage needs to be between $D - \mu_q$ and D to obtain a higher price compared to $\mathbb{E}[p_2]$. Since the marginal cost function is linear and we have a monopolist selling forward, it is optimal to sell half her expected production because it maximizes the additional profit in Figure 2.3ii (cross hatched area).

Proposition 2.2. *The optimal strategy of a renewable monopolist selling its renewable production in sequential markets with multiple stages is to sell it in small quantities at decreasing prices.*

Proof. The triangle in Figure 2.3i can be considered as the maximum profit which can be gained by selling the expected production of the renewable producer. When the renewable producer is able to sell this production in multiple stages, it is optimal to sell it little by little in order to maximize her profit. This means prices in multiple sequential market stages would be declining until the price of $\mathbb{E}[p_2]$ is reached in the final stage. In this case, the renewable producer would be able to increase its profit by the triangle in Figure 2.3i compared to selling the expected quantity already in the first stage. $\square$

For the case of multiple market stages also conventional producers would be able to increase their profit. In this case, they would be able to obtain a higher profit in the first stage, where they can sell a larger quantity at a higher price. On the other hand, consumer surplus would be lowered due to higher prices.

This leads us to the conclusion that with a renewable monopolist, different market designs can have a large impact on distributional effects between producers and consumers. Consumers loose if producers trade electricity in multiple stages. Thus, continuous trading in short-term markets lowers consumer surplus. From the view of consumers, a few separate auctions should be preferred to a continuous auction since this limits strategic behavior of a renewable monopolist.

Strategic production withholding is commonly observed by market participants at the margin (see, for instance, Fabra et al. (2006), Ausubel et al. (2014), Ito and Reguant (2016)). The reason is that it is most profitable to reduce the production at the margin if the corresponding price increase overcompensates the production withholding.[8] The production close to the margin has generally the lowest profits and thus the profit for the whole production fleet can be increased. In contrast to this, our results show that strategic production withholding may also occur for infra-marginal production with our underlying model assumptions (two-stage trading possibility, zero marginal costs for the renewable producers, positive marginal costs for the perfect competitive conventional producers). Unlike usual, it is not dependent on a higher steepness of the cost function for extra-marginal production but also holds for the basic case of a linear cost function. This spans a new dimension of strategic behavior and could also be investigated in further research.

2.4.2 Renewable Producer Monopoly in the Context of a Strict Convex Marginal Cost Function

The results, so far, stem from an analysis with a linear marginal cost function for conventional producers. This has been mainly due to practical reasons, in order to show first effects. In reality, however, the assumption of a linear marginal cost curve may not be valid in every situation. The marginal cost curve in electricity markets is generally assumed to be strict convex and monotonic increasing.[9] Whereas the

[8]Additional to pure production withholding, strategic behavior at the margin can also be excerted with bids above marginal costs to increase the market clearing price.

[9]This is due to the different cost structures of power plants. For example in high demand situations gas turbines are needed to satisfy the demand with high variable costs. This leads to a steep increase of the marginal cost function.

parametrization of a linear function is straight forward, a strict convex and monotonic increasing function can be parametrized in various ways. One way, for example, can be using a quadratic second order function.

In this section we will analyze the general effects of a strict convex marginal cost function on our results for the case of a renewable monopolist. By Bessembinder and Lemmon (2002), we know that a convex marginal cost function could have significant impacts to forward prices. They show, that for quadratic convex marginal cost functions the forward price tends to be lower than the real-time price for a limited demand uncertainty. Within our analysis, there are basically two important differences between the case of a linear and a quadratic marginal cost function which stem from the different shapes. One difference is that the expected price in the second stage is greater than the price for the realization of the expected production ($\mathbb{E}[p_2(Q)] > p_2(\mu_q)$). Whereas in the case of a linear marginal cost function both were equal and we could abstract from the uncertainty in renewable production, this is not the case for a different marginal cost shape. Realizations below the expected production (μ_q) lead to a higher increase in the second stage price (p_2), compared to higher realization than the expected production. Therefore, the expected price ($\mathbb{E}[p_2]$) in the strict convex case will be greater than the price for a realization of the expected production. The second difference is that the shape has also an impact on the optimal quantity (q^*_{r1}). The optimal quantity will always be below the result from the linear case ($q^*_{r1} < \frac{\mu_q}{2}$).

We will try to give the intuition for the second difference based on Figure 2.4. In Figure 2.4i we plot the profit when the renewable producer bids the optimal quantity from the linear case ($\frac{\mu_q}{2}$). This is compared to the case of optimal trading in Figure 2.4ii in the first stage under a strict convex marginal cost function.

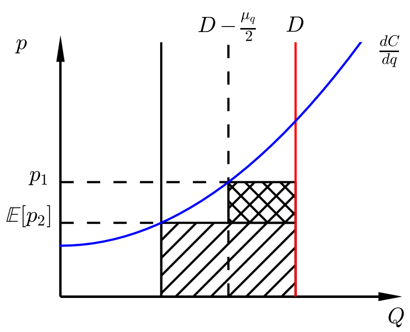

(i) Trading half the expected production

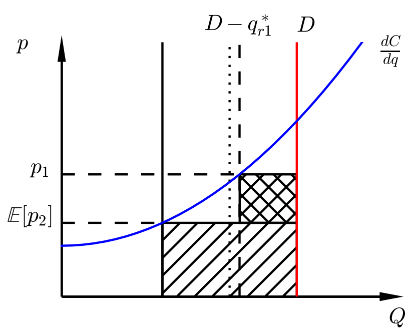

(ii) Optimal trading decision (dotted line is former result of trading $q_{r1} = \mu/2$)

Figure 2.4: Difference in trading for the renewable producer under a convex merit order

The single hatched area represents the lower bound for the expected profit, as explained in Section 2.4.1. This area is equal in both settings, regardless of the traded quantity in the first stage.

The double hatched areas represent the additional profit that can be obtained from trading a quantity in the first stage. In Figure 2.4i, $\frac{\mu}{2}$ is traded in the first stage which is the result of the former optimal amount under a linear merit order.

Now, in the case of a convex merit order, the profit can further be increased by trading even less than half the expected production $\mu_q/2$ (as it can be seen in Figure 2.4ii). The double hatched area is greater than in Figure 2.4i). The magnitude of the impact depends on the shape of the merit order, the demand, and the expected renewable production as well as the uncertainty (standard deviation) of the renewable production. This reasoning can also be proofed for a strict convex polynomial of second order and results in Proposition 2.3.

Proposition 2.3. *For a quadratic merit order, the optimal first stage offer q_{r1} of a renewable monopolist is strictly below $\mu_q/2$.*

Proof. See Appendix 2.9.1. □

We show that a strict convex merit order leads to a stronger withholding of quantities in the first stage compared to the linear case. This is in line with the results of Bessembinder and Lemmon (2002) which focus on conventional producers within a two-stage Cournot competition. Based on our results, the optimal quantities of the renewable producers, which we derive for the linear marginal cost curve can be considered as an upper bound. For the sake of simplicity we will stick to the analysis of a linear marginal cost curve in the following sections. But based on the results from Figure 2.4 we have to keep in mind, that the results from this special case should be considered as an upper bound to the optimal quantities of renewable producers.

2.4.3 Renewable Producer Oligopoly

In this section, we extend the monopoly case to the case of multiple symmetric renewable producers that form an oligopoly. The symmetry implies that the renewable producers have perfectly correlated generation as well as forecast errors. The remaining approach and notation are similar to previous sections. As we learned from before, the conventional producer reacts to the decision of the renewable producers and can be considered as a price taker. So we can focus on the optimal quantities of the renewable producers. We still consider a linear marginal cost function $MC(q) = aq + b$ and define the players $i = 1, ..., N$ with their corresponding quantities in stage 1 as q_{ir1}. Furthermore, we define the sum of the quantities of all players but i as $q_{-ir1} = \sum_{j \neq i} q_{jr1}$. We find that the optimal bid of a renewable producer in the first stage is still driven by strategic behavior but tends towards the expected production level as the number of producers increases.

Proposition 2.4. *The optimal quantity traded in the first stage for each player is* $q^*_{ir1} = \frac{1}{N+1}\mu_q$ *with* μ_q *the total expected renewable production of all players.*

Proof. See Appendix 2.9.2. □

As a direct implication from the optimal first stage bid we see that for the linear marginal cost function, the optimal strategy is still independent of the gradient or the uncertainty of production.

Corollary 2.1. *The profit maximizing traded quantity in stage 1 of the above setting is identical for all players. Furthermore,* q^*_{ir1} *is independent of the steepness* $a \in [0, \infty)$ *of the marginal cost function, the offset* $b \in [0, \infty)$ *of the marginal cost function, and the probability distribution function* $f(Q_i)$.

According to Proposition 2.4 it is optimal for renewable producers to always trade less than the expected production in the first stage since this maximizes their profits. The overall quantity tends towards the overall expected quantity as the number of players increases.[10]

In stage 1, this leads to an overall traded quantity of renewable production of

$$q_{r1} = \sum_{j=1}^{N} q_{jr1} = \frac{N}{N+1}\mu_q \tag{2.16}$$

with $\mu_q := \sum_{j=1}^{N} \mu_{jq}$. In two sequential markets, renewable producers have an incentive to trade less than the total expected renewables production in the first stage. The more players enter the market the stronger the competition and thus the traded amount in the first stage tends towards the expected production. Our results of the first stage show that, under the described setting, a renewable producer acts exactly as predicted in a standard one-shot oligopolistic Cournot game.

[10]Note that, for the moment, we assumed a linear marginal cost function which does not change between the first and the second stage.

2.5 Flexibility and its Role in Short-term Markets

In this section we shed light on the implications of changing cost functions in short-term markets. As mentioned before, this can happen for essentially two reasons. One reason is that not all conventional power plants are flexible enough to adjust their production capacity in stage 2 in the short run. The second reason is that there can be transaction costs for power plant operators associated with the trading in the intraday market.

The difference between the cost function of the first and second stage has implications for the optimal quantity of the renewable producers in the first stage, which we analyze here in more detail. The nomenclature corresponds to the previous sections.

Proposition 2.5. *The optimal quantity traded in the first stage for each renewable player is $q^*_{ir1} = \frac{1}{N+1}\mu_{iq}(N+1-\frac{a_1}{a_2})$, with the ratio $\frac{a_1}{a_2}$ representing the degree of flexibility of the supply side in both stages.*[11]

Proof. In a first step we will derive the optimal quantity of a player i who competes against $N-1$ identical players[12]. According to the setup, the prices in the first and second stage can be defined as:

$$p_1(q_{ir1}, q_{-ir1}) = a_1(D - q_{ir1}) - q_{-ir1} + b_1 \tag{2.17}$$

$$p_2(q_{ir1}, q_{-ir1}) = a_2(D - Q_i N) + b_1 + (a_1 - a_2)(D - q_{ir1} - q_{-ir1}). \tag{2.18}$$

Again, we can define the expected profit function for player i, take the first derivative and integrate over f_i (which is assumed as being identical for all players). Setting the first derivative equal to zero leads us to the necessary condition for an optimal quantity:

$$-a_1\mu_{iq} + a_2\mu_{iq}N + a_2\mu_{iq} - a_2 q_{-ir1} - 2a_2 q_{ir1} \overset{!}{=} 0 \tag{2.19}$$

Under the assumption that all players are identical we can set $q_{-ir1} = (N-1)q_{ir1}$ and solve for q_{ir1} which leads to:

$$q^*_{ir1} = \left(1 - \frac{1}{N+1}\frac{a_1}{a_2}\right)\mu_{iq}. \tag{2.20}$$

The second derivative of the expected profit function is negative, which proves q^*_{ir1} being a maximum for the expected profit function. □

[11] Small values of $\frac{a_1}{a_2}$ represent a very inflexible supply side in the second stage.
[12] The sum over all other players is still denoted by the quantity $q_{-ir1} = \sum_{j \neq i} q_{jr1}$

This means that all renewable producers together submit a quantity of

$$q_{r1}^{*} = \mu_q - \frac{1}{N+1}\frac{a_1}{a_2}\mu_q \tag{2.21}$$

in the first stage (with $a_2 > a_1$).

From Equation (2.21) we can conclude the following: (1) q_{r1}^{*} increases if conventional producers are less flexible ($a_2 \gg a_1$); (2) q_{r1}^{*} increases with an increasing number of renewable producers N. For a perfectly competitive market (with $N \longrightarrow \infty$) it is optimal for each player to trade its share of the total expected quantity in the first stage.

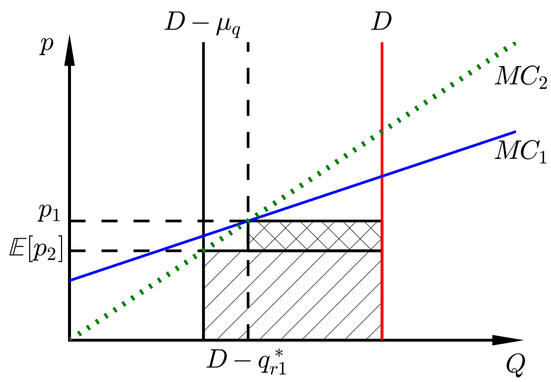

Figure 2.5: Profit of a renewable monopolist facing a inflexible conventional producers

By looking at the example of a renewable monopolist in Figure 2.5, we can get a deeper understanding of the motives for a renewable producer who faces a market with inflexible conventional producers. As explained before, the marginal cost curve for the second stage rotates around the market clearing point of the first stage. The total production of the renewable producer that needs to be sold after both stages however does not change. Thus, the renewable producer has to decide what quantity to sell at a respective price in the first stage and sell the remaining quantity at a lower price in the second stage. The price is lower in the second stage due to the additional renewable quantities that are sold by the renewable producer. Basically, in Figure 2.5, the sum of the cross hatched area and the single hatched area needs to be maximized. The renewable producer is able to maximize both areas by a parallel shift of the marginal cost function for stage 2 (green dotted line). This means, the renewable producer has to optimize the quantity in the first stage in such a way that the profit from both stages is maximized. Summarizing, a more flexible power plant fleet shifts the total optimal first stage bidding quantity of a renewable producer towards the expected production.

The described effects on the optimal quantity hold true for different numbers of renewable producers and different degrees of flexibility. This is shown exemplarily in Figure 2.6. Here, the optimal quantity converges more slowly to the expected production in the perfectly flexible case ($\frac{a_2}{a_1} = 1$) compared to a highly inflexible conventional power plant mix ($\frac{a_2}{a_1} = 4$). An increase in the number of renewable producers leads to a similar effect of a higher overall renewable quantity in the first stage.

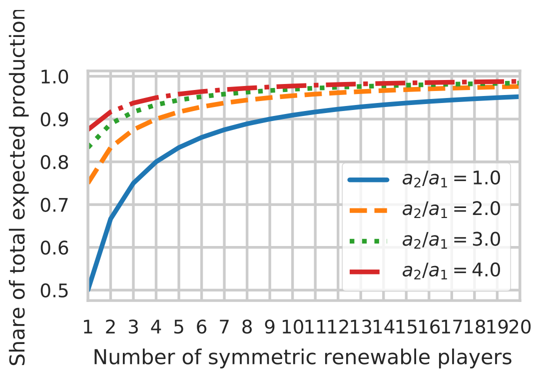

Figure 2.6: Optimal renewable quantity q_{r1} dependent on the number of players N and the ratio a_2/a_1

2.6 Incentives of Renewable Producers to Withhold Production

In this section we extend the analysis of strategic competition in the first stage by investigating the case in which renewable producers are allowed to withhold production in the second stage. Therefore, we relax the assumption that the renewable producer needs to sell all her realized production in the second stage. This means $q_{r1} + q_{r2} \leq Q$ instead of $q_{r1} + q_{r2} = Q$. We still assume that renewable producers strictly avoid being short after stage 2, i.e. selling more production than they produce. The rational is that high financial penalties need to be payed in case of an imbalance. All other model assumptions stay the same.

The motivation for the relaxation of the second stage restriction to sell the whole production is threefold. First, we note that, in general, it is technically possible to reduce production for renewable producers. This happens for photovoltaic in critical grid situation if the voltage level extends a critical value (automatic shut down around 50.2 Hertz) or for wind turbines during storms. Second, a reduced production could be economically profitable in specific situation. Especially if prices are negative or, like in the investigated case, if market prices could be increased profitably by withholding production. Third, market manipulation by a withhold of renewable production is not easy to prove by the regulator. It is hard to detect whether a wind turbine does not produce due to maintenance, local wind conditions or strategic production withholding.

We extend the model with cost functions by replacing the constraint $q_{r1}+q_{r2}=Q$ with $q_{r1}+q_{r2}\leq Q$. Based on this model we obtain the following results.

Proposition 2.6. *If renewable producers are allowed to withhold production, they only withhold production after the second stage if the expected production of all producers is high compared to the demand D, i.e. if* $\mu_q > \frac{a_2N(N+1)}{a_2(N+1)^2-a_1N}D + \frac{a_2N(N+1)}{a_1\left(a_2(N+1)^2-a_1N\right)}b$. *This means the expected renewable production needs to be at least* $\frac{D}{2}$. *Otherwise, renewable producers sell the total realized production into the market (same result as of Proposition 2.5).*

Proof. We use the same model as in Section 2.5 (and corresponding Proposition 2.5). The only difference is the relaxed constraint $q_{r1}+q_{r2}=Q$ by $q_{r1}+q_{r2}\leq Q$. This allows the renewable producer to withhold production and to increase prices in the second stage. Since we adjusted an equality constraint by an inequality constraint, we face now a convex optimization problem with inequalities and can use the Karush-Kuhn-Tucker (KKT) conditions to solve it. The full proof can be found in the appendix. □

The main finding is that renewable producers have an incentive to withhold production after the second stage only if the (expected) production exceeds a threshold value which is at least $\frac{D}{2}$ (but dependent on a_1, a_2, b and N).[13] The exact threshold value is

$$Q_{threshold} := \frac{a_2N\left(N+1\right)}{a_2\left(N+1\right)^2-a_1N}D + \frac{a_2N\left(N+1\right)}{a_1\left(a_2\left(N+1\right)^2-a_1N\right)}b. \tag{2.22}$$

As long as the (expected) production is below this threshold, the renewable producers will sell their total realized production in the second stage. Nevertheless, the

[13] In stage 1, the expected production is the relevant quantity while in stage 2 the realized production is the relevant quantity. If both, expected and realized production, deviate from each other, it is possible that the renewable producers pursue a different strategy in each stage.

production is split between first and second stage to increase profits. By analyzing this threshold we find the following

- $Q_{threshold}$ is increasing in N: The more producers exist, the higher the threshold. Therefore, more competition between renewable producers limits the incentive for renewable producers to withhold quantities in the second stage.
- $Q_{threshold}$ is decreasing in a_2 (with a_1 fixed): The more inflexible the power plant fleet, the lower is the threshold. Therefore, renewable producers start to withhold production at a lower level of expected renewable production.
- $Q_{threshold}$ converges to $\frac{N}{N+1}\left(D + \frac{b}{a_1}\right)$ for $a_2 \to \infty$ but is strictly above $\frac{D}{2}$.

To sum up, renewable producers only have an incentive to withhold quantities in situations with very high renewable generation compared to the demand. Additional renewable producers as well as more flexible conventional producers increase the threshold ($Q_{threshold}$) to withhold production quantities.

2.7 Prices, Welfare, Producer Surplus and Consumer Surplus

Trading in the day-ahead and intraday market has implications for overall welfare, producer surplus and consumer surplus. So far, we focused on the quantities of the renewable producers that maximize their respective profits. They determine the quantities that are traded by the conventional producers and thereby the prices in both stages. In order to disentangle the effects on overall welfare, producer and consumer surplus, we will first analyze the effects on prices in the two stages.

Since we found in Section 2.6 that renewable players only withhold production at very high production levels compared to demand D, we focus on the case in which renewable producers sell all their production after stage 2 (the case $q_{r1}+q_{r2}=Q$).[14]

2.7.1 Prices and the Role of Arbitrageurs

By plugging in the optimal quantity from Equation (2.20) into the price equations for the case with flexibility constraints (Equation (2.3) and (2.4)) we obtain the

[14] For a realistic number of renewable players $N > 5$ and an arbitrary ratio of a_2 to a_1, the threshold $Q_{threshold}$ is at least $0.85D$.

following prices:

$$p_1 = Da_1 + b_1 - \frac{a_1}{a_2}\frac{\mu_q}{N+1}(a_2(N+1) - a_1) \tag{2.23}$$

$$\mathbb{E}[p_2] = Da_1 + b_1 - \frac{a_1}{a_2}\frac{\mu_q}{N+1}(a_2(N+2) - a_1). \tag{2.24}$$

From these two equations we can already see that the price in the first stage is higher than in the second stage. This becomes obvious by taking the difference between the two prices:

$$p_1 - \mathbb{E}[p_2] = \frac{a_1\mu_q}{N+1}. \tag{2.25}$$

We can observe the following implications: First, the price difference between stage 1 and 2 is independent of the change in the slope of the marginal cost function (a_2). The renewable producers choose their quantity dependent on the slope (a_2). This has an effect on the absolute prices in the two stages but the price delta stays constant. Second, with a higher overall expected production from renewables (μ_q) also the price difference increases. The quantity that is withheld from trading in the first stage increases with the expected production and, thereby, the price difference increases. Third, the price difference decreases with an increasing number of renewable producers (N). In a perfectly competitive market (with $N \longrightarrow \infty$), prices in both stages are equal. As we can observe in Figure 2.6, the quantity in the first stage tends towards the overall expected quantity and hereby prices in both stages converge.

Based on the price difference in both stages one could suspect arbitrageurs to be entering the market. By obtaining a short position in the day-ahead market and adjusting their position in the intraday market, they would be able to make a profit. The optimal strategy of an arbitrageur is therefore identical with the strategy of the renewable players. The only difference is that arbitrageurs do not necessarily own production assets. Each additional arbitrageur that would enter the market can nevertheless be regarded as an additional renewable player. This would in turn decrease the price difference between the day-ahead and intraday market (cf. Figure 2.7).

Still, electricity markets have some unique features that may prevent arbitrageurs from engaging in short-term electricity markets. First, the assets that are traded are not only financial but physical obligations to produce and deliver electricity. Therefore, some short-term market platforms restrict the participation to firms with physical production assets. This prevents for example banks from entering these mar-

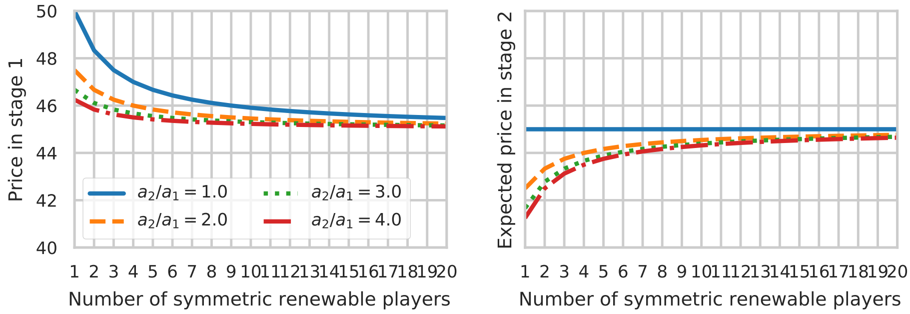

Figure 2.7: Prices in the two stages for an example with $D = 70$, $\mu_q = 20$, $\sigma_q = 5$, $b_1 = 20$ and $a_1 = 0.5$

kets. Second, there may be information asymmetries between renewable producers and arbitrageurs that may be hard to overcome. For example renewable producers can be assumed as having better knowledge about the expected production level of their assets. For the following discussions we will thus not focus on the case of additional arbitrageurs entering the market. Nevertheless, the implications of arbitrageurs entering the market can be observed implicitly by considering an increase in the number of renewable players (N).

In order to gain a deeper understanding of the effects from changing cost functions and increased competition on prices, we plot this relationship in Figure 2.7 for an exemplary case. The direction of the effects will stay the same for arbitrary a_1, a_2 with $a_2 \geq a_1$ and arbitrary D, Q and b with $(D-Q)a_1 + b \geq 0$ ($Q \sim \mathcal{N}(\mu_q, \sigma_q)$).

In Figure 2.7, we chose the values such that one can easily find similarities to the German electricity market. A demand D of 70 GW can be observed during peak times, where also an expected renewable production μ_q of 20 GW is quite common. Furthermore the parameters of the marginal cost function were chosen such that they represent common price levels.[15]

We can see that the prices in stage 1 and 2 converge to the same value with an increasing number of players. This benchmark is set by the perfectly flexible case ($\frac{a_2}{a_1} = 1$), where the price in the second stage stays constant. In the next sections we will analyze the effects on producer surplus, consumer surplus and overall welfare.

[15]Of course a linear marginal cost function is a crude assumption in this case, but it allows us to show the overall effects.

2.7.2 Producer Surplus

The producer surplus is defined as the sum of the renewable producer surplus and the conventional producer surplus. For the case with a changing marginal cost function, the conventional producer surplus can be defined as

$$\mathbb{E}[\Pi_c(q_{r1})] = p_1(D - q_{r1}) + p_2 \int (q_{r1} - Q) f(Q) dQ - C_1(q_{r1}) - \int C_2(q_{r1}) f(Q) dQ. \tag{2.26}$$

It is the difference between the income from sold quantities in stage 1 and 2 and the associated costs with the production of electricity.

The first stage costs C_1 in our model depend on the quantities offered by the renewable producers q_{r1}. We can thus obtain the costs in the first stage by integrating over the marginal cost function MC_1

$$C_1(q_{r1}) = \frac{1}{2} a_1 (D - q_{r1})^2 + b_1(D - q_{r1}). \tag{2.27}$$

The formulation is more complex for the costs that are associated with the second stage of production. First, it depends on the quantity that is traded in the first stage by the renewable producer q_{r1}. Second, it depends on the realization of the final renewable production Q. In the first stage, the conventional producers plan to produce a certain quantity $D - q_{r1}$. In the second stage, this quantity has to be adjusted to meet the total residual demand of $D - Q$. This means if the renewable production turns out to be higher than the traded quantity in the first stage, the conventional producers need to reduce their planned production and can buy back quantities at a lower price. Meanwhile the slope of the cost function has changed from a_1 to a_2. This leads us to the following expected cost function for the second stage:

$$\mathbb{E}[C_2(q_{r1})] = \int \int_{q_{r1}}^{D-Q} (a_2 q_{c2} + (a_1 - a_2)(D - q_r 1) + b_1) dq_{c2} f(Q) dQ \tag{2.28}$$

$$= (Da_1 - a_1 q_{r1} + b_1)(\mu_q - q_{r1}) + a_2 q_{r1}(\mu_q - \frac{q_{r1}}{2}) - \frac{a_2 n^2}{2}\left(\mu_{iq}^2 + \sigma_{iq}^2\right). \tag{2.29}$$

What is especially noticeable in this equation, is that for the first time in our analysis also the standard deviation (σ_{iq}) of the expected renewable production plays a role. The reason for this lies in the non-linear cost function of the conventional producers. Here, deviations from the expected value are not multiplied by a linear curve and weighted equally but weighted by the non-linear function. This is why the standard deviation plays an important role. By inserting Equation (2.27) and (2.29) in (2.26), we obtain the total conventional producer surplus.

In the same way, we can also derive the producer surplus for the renewable producers.

$$\mathbb{E}[\Pi_r(q_{r1})] = p_1 q_{r1} + \int p_2(Q - q_{r1}) f(Q) dQ \tag{2.30}$$

By plugging in the results from Equation (2.20) it is possible to quantify the renewable and conventional producer surplus. We plot this for an exemplary cases in Figure 2.8.

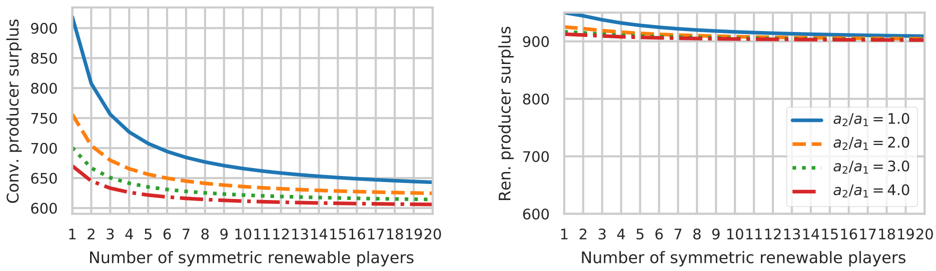

(i) Expected conventional producer surplus

(ii) Expected renewable producer surplus

Figure 2.8: Expected producer surplus for an example with $D = 70$, $\mu_q = 20$, $\sigma_q = 5$, $b_1 = 20$ and $a_1 = 0.5$.

As we could already see from Figure 2.7, prices in the first stage decrease with an increase in competition or a less flexible supply curve. At the same time prices in the second stage increase. This results in both, a dampening and an increasing effect on producer surplus. From Figure 2.8 we can observe that the decreasing effect of the first stage outweighs the increasing effect in the second stage. Overall, we see that the producer surplus decreases with the number of renewable producers N and with a less flexible power plant mix. Especially the decrease in conventional producer surplus is noticeable. For renewable producers the decrease in surplus is not as prominent, since they are able to reduce the effects by adjusting their optimal quantity q_{r1}. For example the overall quantity traded by renewable producers (q_{r1}^*) is increased when more renewable producers compete in the first stage. Also a less flexible power plant mix leads to a higher optimal quantity for renewable producers in the first stage (cf. Figure 2.6).

2.7.3 Consumer Surplus

In our model, consumers are represented as being completely inelastic in their demand behavior. In electricity markets it is common practice to assume consumers as completely price inelastic and consuming electricity up to the point when the price exceeds the value of lost load (VOLL). We therefore slightly adjust our assumptions by introducing the price p^{VOLL} which can be regarded as the upper limit for the willingness-to-pay for electricity consumption.

As consumers are assumed to be risk-averse, demand is already satisfied in the first stage at price p_1, as long as $p_1 < p^{VOLL}$. The consumer surplus can therefore be expressed as $(p^{VOLL} - p_1)D$. By plugging in the price formulation for the first stage from Equation (2.3), we get

$$CS = D\left(p^{VOLL} - Da_1 - b_1 + \frac{a_1}{a_2}\frac{\mu_q}{N+1}(a_2(N+1) - a_1)\right). \tag{2.31}$$

We can now compare the consumer surplus for the different combinations of N and a_2/a_1. In order to circumvent an assumption for the upper price limit p^{VOLL}, we focus our analysis on changes in consumer surplus compared to a reference point. We therefore choose the reference point where consumer surplus is the lowest. This is the case for a renewable monopolist and perfectly flexible conventional producers ($a_1 = a_2$).

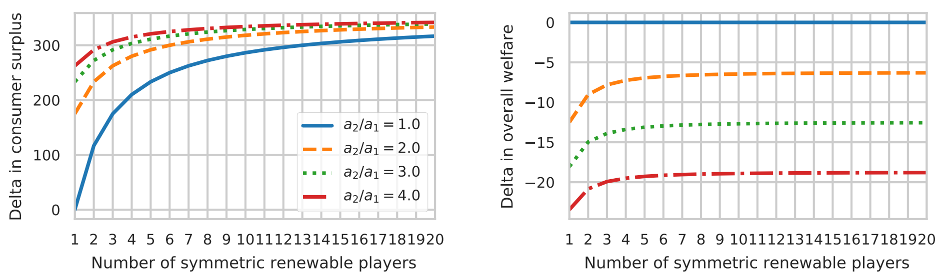

(i) Delta in consumer surplus

(ii) Delta in expected overall welfare

Figure 2.9: Delta in consumer surplus and expected overall welfare for an example with $D = 70$, $\mu_q = 20$, $\sigma_q = 5$, $b_1 = 20$ and $a_1 = 0.5$

As one could already expect from decrease in prices with an increasing number of players in Figure 2.7, the consumer surplus increases with the number of players. What may be counter intuitive is that consumers can profit from a less flexible power plant mix. The lower flexibility of conventional producers leads renewable producers to adjust their quantity, which has a price dampening effect for the first stage. Consumers can therefore profit from the lower prices in the first stage as it is shown exemplarily in figure 2.9i.

2.7.4 Welfare

Combining the effects on producer and consumer surplus leads to changes in overall welfare. As we can only analyze differences in consumer surplus this also holds for the case of overall welfare. Again, we define the perfectly flexible case with a monopolistic renewable producer as a reference point for the analysis (cf. Section 2.7.3). The difference in overall expected welfare to the monopolistic case can be defined as

$$\Delta\mathbb{E}[\mathbb{W}(q_{r1})] = -\Delta\mathbb{E}[CE(q_{r1})] + \Delta\mathbb{E}[\Pi_p(q_{r1})]. \tag{2.32}$$

In Figure 2.9ii we can observe these effects on overall welfare. The overall welfare stays constant for the case of a perfectly flexible power plant mix. In this case, the demand is always satisfied at the same costs which do not lead to a change in overall welfare. Negative effects on overall welfare occur only if the total production costs for electricity increase, i.e. if conventional power producers are less flexible. Especially if the power plant mix is highly inflexible, as in the case with $\frac{a_2}{a_1} = 4$, it will lead to a substantial decrease in overall welfare. Generally we can observe two effects. First, the effect on welfare has a smaller magnitude than the isolated effects on producer surplus or consumer surplus. The increase in consumer surplus and decrease in producer surplus counteract each other and lead only to a slightly reduced effect on overall welfare. Second, the welfare is generally decreased in a setting with less flexible power plants.

In a last step, we analyze the effects of uncertainty on overall welfare. So far, we assumed the production of the renewable producer in the final stage to be forecasted with a standard deviation of $\sigma_q = 5$ in the numerical examples. Now, we assume that if forecasts are improved or trading time is delayed, the standard deviation decreases, as to Foley et al. (2012). A decrease in standard deviation could also be accomplished by delaying trading of the first stage (e.g. by trading in the evening of the day before physical delivery instead of at noon). We quantify the welfare effects by comparing them to the case with no uncertainty ($\sigma_q = 0$) and a perfectly competitive market ($q_{r1} = \mu_q$). From Figure 2.10 we can observe that a larger standard deviation results in welfare losses. From this we can conclude that it is desirable to increase the quality of forecasts or to change the timing of trading in order to increase overall welfare.

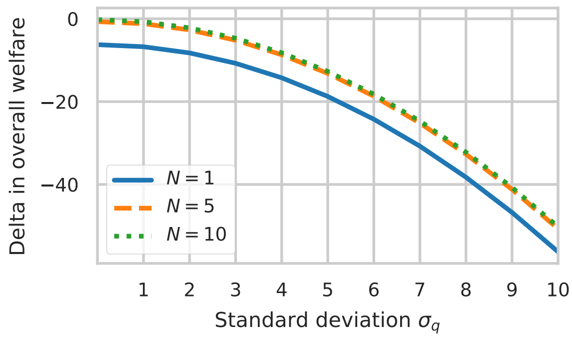

Figure 2.10: Delta in expected overall welfare for varying standard deviation of the forecast σ_q ($D = 70$, $\mu_q = 20$, $b_1 = 20$, $a_1 = 0.5$ and $a_2 = 1$)

2.8 Concluding Remarks

We derive the optimal quantities for renewable producers that are strategically selling their production in a two-stage game with uncertainty about production in stage 1 and knowledge about the realization of their production in stage 2. It is profit maximizing for renewable producers to bid less than their expected total quantity in the first stage, which we consider as the day-ahead market. Renewable producers are able to increase their profits by selling only part of their expected production in the first stage and thus raising the price in the first stage. The optimal quantity in the first stage tends towards the overall expected quantity with an increasing number of renewable producers. Conventional producers are considered as a competitive fringe that satisfies the residual demand in both markets. If conventional power producers are less flexible in their operation, renewable producers have a larger incentive to increase the traded quantity in the first stage. In general, prices in the first stage (day-ahead) are higher compared to the second stage (intraday), but with an increasing number of renewable producers or with arbitrageurs entering the market this difference decreases. In situations with very high production levels, that are at least able to serve half of the demand, renewable producers have an incentive to withhold production in the second stage. This effect is decreased by an increasing number of players but increases in a setting with low flexibility of conventional producers.

A reduced forecast uncertainty leads to an increase in overall welfare. This leads us to two conclusions. First, overall welfare can be increased by delaying the trade in the day-ahead market closer to the time of physical delivery. For example by shifting the auction from noon to the evening. Second, an increase in forecast quality has a positive effect on overall welfare.

Based on the results it becomes obvious that in a future electricity system with high shares of renewables, regulators need to pay attention to the possible abuse of market power by large renewable producers. In situations with low liquidity and the absence of arbitrageurs this could lead to significant distributional effects and even welfare losses.

In our whole analysis, we assumed the generation of all renewable producers to be perfectly correlated, as well as their forecast errors. This is not the case in reality and could be further investigated. Additionally, it would be possible to quantify welfare implications of improved forecast quality and alternative market designs at concrete examples.

The role of uncertainty only plays a minor role in our analysis since we mainly focus on the case of linear marginal cost functions and risk-neutrality. In reality, however, participants may be acting more risk-averse which would increase the importance of accounting for uncertainty. This could be especially interesting when the analysis is extended to players with mixed portfolios of renewable and conventional power production. The optimization within a generation portfolio (maybe in combination with risk-averse behavior) could lead to interesting insights on the potential use of market power in electricity markets in a more realistic setting.

2.9 Appendix

2.9.1 Proof of Proposition 2.3

Proof. Let $MC(q) = aq^2 + bq + c$ with $a > 0$ and $b, c \geq 0$ be a strictly monotonic increasing convex (quadratic) marginal cost function. The optimal first stage trading amount for a monopolistic renewable producer is

$$q_{r1}^* = \frac{2}{3}D + \frac{1}{3}\frac{b}{a} - \frac{2}{3}\sqrt{\left[D - \frac{3}{4}\mu_q + \frac{1}{2}\frac{b}{a}\right]^2 + \frac{3}{16}\mu_q^2 + \frac{3}{4}\sigma_q} \tag{2.33}$$

(this can be derived analogously to the optimal amount of the linear case in Proposition 2.1). Then the following holds:

$$\begin{aligned} q_{r1}^* &= \frac{2}{3}D + \frac{1}{3}\frac{b}{a} - \frac{2}{3}\sqrt{\left[D - \frac{3}{4}\mu_q + \frac{1}{2}\frac{b}{a}\right]^2 + \frac{3}{16}\mu_q^2 + \frac{3}{4}\sigma_q} \\ &< \frac{2}{3}D + \frac{1}{3}\frac{b}{a} - \frac{2}{3}\sqrt{\left[D - \frac{3}{4}\mu_q + \frac{1}{2}\frac{b}{a}\right]^2} \\ &= \frac{1}{2}\mu_q. \end{aligned} \tag{2.34}$$

The inequality is strict since the square root is a strict monotonic function on positive numbers. Therefore, under a convex merit order, it holds that $q_{r1}^* < \frac{1}{2}\mu_q$. Note that we assumed $\mu_q < D$ in the model setup. □

2.9.2 Proof of Proposition 2.4

Proof. Because all players are symmetric we can denote the total traded renewable production of all players in stage 1 by $q_{r1} = q_{ir1} + q_{-ir1}$ (where q_{-ir1} aggregates all players but not player i), the realized production in stage 2 by $Q = NQ_i$, and the expected quantity by $\mu_q = N\mu_{iq}$. With these definitions, Equation (2.7) and (2.8) still hold for the oligopoly case.

The profit function of renewable producer i can be derived by plugging in those values into

$$\Pi_{ir}(q_{ir1}) = p_1(q_{r1})q_{ir1} + p_2(D - Q)q_{ir2} \tag{2.35}$$

so that the profit function results in

$$\Pi_{ir}(q_{ir1}) = (a(D - q_{ir1} - q_{-ir1}) + b)q_{ir1} + (a(D - NQ_i) + b)(Q_{ir} - q_{ir1}). \tag{2.36}$$

Remember that $q_{ir2} = Q_i - q_{ir1}$ and that we assume Q_i to be uncertain. In order to derive the expected profit function we have to integrate for Q_i over the distribution $f(Q_i)$, where $f(Q_i)$ is the probability density function for Q_i. After taking the first derivative, setting it equal to zero and replacing the expected values (analogous to Equations (2.11) and (2.12)), we get the necessary conditions

$$\frac{d}{dq_{ir1}}\mathbb{E}[\Pi_{ir}(q_{ir1})] = a(N\mu_q - 2q_{ir1} - q_{-ir1}) \stackrel{!}{=} 0 \tag{2.37}$$

and the corresponding solution is

$$q_{ir1}^* = \frac{1}{2} N \mu_{jq} - \frac{1}{2} q_{-ir1} \tag{2.38}$$

for $i = 1, ..., N$.

In an equilibrium of identical players we have identical solutions which results in $q_{-ir1} = (N-1) q_{ir1}$. With this, we derive

$$q_{ir1}^* = \frac{1}{2} N \mu_{iq} - \frac{1}{2}(N-1) q_{ir1}^* \tag{2.39}$$

$$\Leftrightarrow \qquad q_{ir1}^* = \frac{1}{N+1} \mu_q . \tag{2.40}$$

Because the second derivative of Equation (2.36) is negative, we found the profit maximizing quantity q_{ir1}^* □

2.9.3 Proof of Proposition 2.6

Proof. As before, we assume N identical (symmetric) renewable producers. Let us define our inequality constraint for producer i by

$$g(q_{ir1}, q_{ir2}) := q_{ir1} + q_{ir2} - Q_i \leq 0 \tag{2.41}$$

Then the Lagrange function is

$$\begin{aligned} L(q_{ir1}, q_{ir2}, \lambda) := \; & q_{ir1} \left(a_1 \left(D - q_{ir1} - q_{jr1} (N-1) \right) + b \right) + \\ & q_{ir2} \left(a_2 \left(D - q_{ir1} - q_{ir2} - q_{jr1} (N-1) - q_{jr2} (N-1) \right) \right) + \\ & q_{ir2} \left(b + (a_1 - a_2) \left(D - q_{ir1} - q_{jr1} (N-1) \right) \right) \int \mathrm{f_i} (Q_i) \, dQ_i + \\ & \lambda \left(Q_i - q_{ir1} - q_{ir2} \right), \end{aligned} \tag{2.42}$$

which is the corresponding profit function of the first and second stage minus the function g. The conditions of the KKT which need to be fulfilled are

$$\begin{aligned} \text{Stationarity:} \quad & \frac{\partial L}{\partial q_{irk}} = 0 \, , \qquad k = \{1, 2\} && (2.43) \\ \text{Primal feasibility:} \quad & q_{ir1} + q_{ir2} \leq Q_i && (2.44) \\ \text{Dual feasibility:} \quad & \lambda \geq 0 && (2.45) \\ \text{Complementary slackness:} \quad & \lambda (q_{ir1} + q_{ir2} - Q_i) = 0. && (2.46) \end{aligned}$$

We need to consider two cases: $\lambda = 0$ or $q_{ir1} + q_{ir2} = Q_i$ (binding capacity constraint).

To case 1 ($\lambda = 0$):

From (2.43) we derive two equations which we can solve for q_{ir1} and q_{ir2}. Since we focus on symmetric probability distribution functions f_i for the renewable production, we can substitute $\int \mathrm{f_i}(Q_i)\, dQ_i = 1$. Furthermore, due to symmetric renewable producers, we can plug in $q_{ir1} = q_{jr1}$ and $q_{ir2} = q_{jr2}$ for all renewable producers i and j. Therefore, the equilibrium solution aggregated for all identical renewable producers are

$$q_{r1}^* = \frac{a_2 N(N+1) - a_1 N}{a_2 (N+1)^2 - a_1 N} D + \frac{1}{a_1} \frac{a_2 N(N+1) - a_1 N}{a_2 (N+1)^2 - a_1 N} b \tag{2.47}$$

$$q_{r2}^* = \frac{a_1 N}{a_2 (N+1)^2 - a_1 N} D + \frac{N}{a_2 (N+1)^2 - a_1 N} b. \tag{2.48}$$

Note that the individual quantities are $q_{irk} = q_{rk}/N$ for $k = \{1, 2\}$.

Now, we can plug the optimal quantities into the equation of the investigated case, i.e. into $q_{r1} + q_{r2} < Q$. This gives us the threshold value above which the renewable producers start to withhold production to increase prices. The threshold is

$$Q_{threshold} := \frac{a_2 N(N+1)}{a_2 (N+1)^2 - a_1 N} D + \frac{a_2 N(N+1)}{a_1 \left(a_2 (N+1)^2 - a_1 N\right)} b. \tag{2.49}$$

If the overall expected renewable production μ_q exceeds this threshold, the renewable producers withhold production. Otherwise, the sold quantities are constraint and we are in case 2.

Note that the expected production has to reach a high level relative to the demand such that renewable producers withhold production. μ_q has to be at least $\frac{D}{2}$ (for the monopoly situation with a infinite inflexible power plant fleet) but increases with increasing number of players or more flexible power plant fleet (for a duopoly it is at least $\frac{2D}{3}$).

To case 2 ($q_{ir1} + q_{ir2} = Q_i$): This is the same case as shown in Proposition 2.5. Therefore the optimal quantities for each individual renewable producer is

$$q_{ir1}^* = \frac{1}{N+1} \left(N + 1 - \frac{a_1}{a_2} \right) \mu_{iq} \tag{2.50}$$

$$q_{ir2}^* = \frac{1}{N+1} \frac{a_1}{a_2} \mu_{iq}. \tag{2.51}$$

and for all renewable producers together are

$$q_{r1}^* = \mu_q - \frac{a_1}{a_2(N+1)}\mu_q \tag{2.52}$$

$$q_{r2}^* = \frac{a_1}{a_2(N+1)}\mu_q \tag{2.53}$$

if $\mu_q \leq \frac{a_2 N(N+1)}{a_2 N(N+1)^2 - a_1 N} D + \frac{a_2 N(N+1)}{a_1\left(a_2(N+1)^2\right) - a_1 N} b$. Remember that $N\mu_{qi} = \mu_q$. This closes the proof. □

3 Explaining Electricity Forward Premiums - Evidence for the Weather Uncertainty Effect

With the increasing share of volatile renewable energies, weather prediction becomes more important to electricity markets. The weather-driven uncertainty of renewable forecast errors could have price increasing impacts. This research sets up an analytic model to show that the day-ahead optimal bidding under uncertain renewable production is below the expected production and thus price increasing. In a second step, the price increasing effect on forward premiums by specific weather types and their renewable production uncertainty is proved via empirical methods. Weather types are identified in which renewable production is harder to predict. The findings connect weather dependent renewable forecast uncertainty to forward premiums and support the consideration of weather types in price forecasting models.

3.1 Introduction

Renewable energies like wind and solar are one major pillar in order to reach CO_2-emission targets in the electricity sector. The production of wind and solar energy is weather dependent and hence volatile. This volatility induces uncertainty to wholesale electricity prices. In several countries, like Germany, renewable energies have reached a significant capacity share which increases uncertainty in the electricity markets to a relevant degree. It is thus highly relevant to have insights how electricity prices are affected by wind and solar uncertainty.

Most electricity markets are organized as sequential markets, see for instance Cameron and Cramton (1999) for PJM market or Viehmann (2017) and Knaut and Paschmann (2017b) for Germany. The sequential market structure allows for risk hedging by selling or buying electricity forward. Risk hedging becomes more important under a high share of volatile wind and solar production. This weather-dependent wind and solar production can accurately be predicted to a limited time horizon, e.g. 24 hours. Thus, the relevant markets are (1) the short-term forward market, in this case the day-ahead market, and (2) the real-time market, also known as intraday-market. However, planned production and demand in the (day-ahead) forward market can deviate from the final realization in the real-time market. As a risk-neutral renewable producer, it is questionable if it is profit optimal to sell the total expected production in the day-ahead forward market. Under a non-linear convex merit order, strategic underselling could be optimal for producers to avoid re-buying forward sold quantities. The (forward) production withholding would lead to higher forward market prices. The specific problem in this paper is to identify if and to what extent wind and solar uncertainty lead to positive forward price premiums.

This essay examines the research question both theoretical and empirical. The theoretical result is based on a two-stage profit-maximizing framework under perfect competition. Renewable producers have zero marginal costs and uncertain production realization. With uncertain production and a convex, quadratic merit order curve, the optimal first-stage (i.e. forward) production is below the expected production realization. The production withholding tends to increase first stage prices and is dependent on the production's standard deviation. The empirical evaluation supports the theoretical findings within the German electricity market. The German market is considered due to its high share of wind and solar production.[1] Weather type definitions of the German Weather Service are applied to determine the forward premium effects. The weather types are also applied to classify the wind and solar uncertainty. The empirical findings confirm that weather types can be utilized to indicate forward price premiums and to classify production uncertainty. Thus, it is highly recommended to incorporate wind and solar uncertainty in price forecasting models. The results suggest that a potential classification is based on weather types.

The conducted research is based on fundamental work of Allaz (1992) as well as Bessembinder and Lemmon (2002). Allaz (1992) shows analytical that there is a general incentive within a Cournot oligopoly (with uncertain production) to sell production in forward markets. Bessembinder and Lemmon (2002) derives similar results for electricity producers under demand uncertainty. They find positive price premiums for demand uncertainty within their theoretical model and empirical support. Their scope is on a monthly granularity which was extended by the work of Longstaff and Wang (2004) to day-ahead and real-time markets. The underlying research extends the theoretical work of Bessembinder and Lemmon (2002) and the empirical analysis of Longstaff and Wang (2004) by the consideration of production uncertainty of wind and solar energy. Additionally, the underlying research focuses on perfect competition since today's electricity markets have widely reached high

[1] Wind and solar production had a share of 18.3% of Germany's gross electricity production in 2015 (cf. Bundesnetzagentur (2016)).

supplier diversity.

The major distinction of this research to existing literature is the classification of wind and solar uncertainty by weather types. To the best of my knowledge, the underlying research is the first which applies weather type classifications to derive insights on forward price premiums and price deviations. Thus, this research supports electricity market participants by new insights. First, market participants get information on the general forward premium effects by each weather type, whereas weather types can be predicted accurately several days before realization. Some weather types indicate higher forward premiums than others. The information of the weather type situation allows for an approximation of the (mean) forward premium level. Second, the increasing effect on forward premiums by wind and solar uncertainty is quantified. A reduction in uncertainty would translate to reduced forward premiums. Third, market participants can incorporate weather types in forecasting models to consider uncertainty and derive a more accurate range of their price forecasts.

The remainder of this paper is structured as follows: Section 3.2 provides the fundamental theoretical and empirical literature as well as background information on the weather types. The theoretical analysis and findings are stated in Section 3.3. It covers the analytical model settings and assumptions as well as the theoretical finding of optimal production underselling under uncertainty. The empirical analysis is presented in Section 3.4. This section is the core of the paper. It contains the data, the empirical model setup and the results of the hypothesis tests. Section 3.5 concludes the present research.

3.2 Background

This section provides the background for the subsequent analysis. First, the literature regarding the theory is outlined. Then, previous work on the empirical background is briefly discussed. Afterwards, weather type classifications and their utilizations are presented. Within this work, *forward premiums* are defined as the price difference between the forward market and the real-time market, which corresponds to the definitions of Bessembinder and Lemmon (2002) or Douglas and Popova (2008).

3.2.1 Theoretical model

Fundamental analytic work on pricing and behavior in forward markets is given by Allaz (1992) (general) and Bessembinder and Lemmon (2002) (for electricity markets). Allaz (1992) sets up a two-stage Cournot oligopoly model with a homogeneous product. He considers uncertainty of the second stage price realization. He derives his results of forward trading incentives under the assumption of oligopolistic behavior as well as a linear inverse demand function and a linear cost function. As it is shown by Knaut and Obermüller (2016) as well as Bessembinder and Lemmon (2002), a non-linear (convex) cost function is an essential prerequisite such that uncertainty leads to forward premiums. Hence, this research assumes a convex quadratic linear cost function (called merit order). The inverse demand function is inelastic as widely assumed in short-run electricity market models. Additionally, the underlying research extends the model of Allaz (1992) to perfect competition and shows that the results still hold true.

Bessembinder and Lemmon (2002) analyzes a similar two-stage model as to Allaz (1992) (forward and spot market). They show analytical and empirical evidence of the demand uncertainty effect to forward premiums. However, their focus is demand uncertainty on a monthly basis. The present research focuses on weather-dependent wind and solar production uncertainty in the short-run (day-ahead to realization). Additionally, this research focuses on perfect competition because the number of actors in electricity markets has rapidly increased since the liberalization (cf. Jamasb and Pollitt (2005) or Joskow and others (2008)). The work of Bessembinder and Lemmon (2002) is widely accepted and the model is extended in several ways, e.g. to consider gas storages (Douglas and Popova (2008), Bloys van Treslong and Huisman (2010)) or capacity restrictions (Cartea and Villaplana, 2008).

The underlying theoretical model is oriented on the basic work of Ito and Reguant (2016) and Knaut and Obermüller (2016). Ito and Reguant (2016) find evidence for price premiums under imperfect competition (i.e. strategic behavior) and restricted entry of arbitrage (or speculators). They set up a two-stage model and assume perfect foresight, i.e. no uncertainty. In contrast to their model assumptions, this research accounts for uncertainty under perfect competition. Evidence for price premiums is shown. Thus, this work complements the results of Ito and Reguant (2016) by the finding that uncertainty has influences on price premiums as well.

The work of Knaut and Obermüller (2016) was conducted parallel to Ito and Reguant (2016) with a similar analytical two-stage strategic bidding model. They focus on renewable producers which have in general zero marginal costs but uncertainty about their production realization. They find theoretical evidence for the incentive of strategic production withholding on the forward market to increase prices. Additionally, they find that under a linear merit order function uncertainty has no influence on the strategic bidding. Production uncertainty (e.g. of renewable producers) becomes relevant with a higher order merit order function. Bessembinder and Lemmon (2002) come to similar findings within their theoretical framework.

The present analytical model extends the model of Knaut and Obermüller (2016) by (1) perfect competition and (2) a convex quadratic merit order function. Under this model setting, uncertainty becomes a relevant price driver for profit maximization. Based on that, theoretical insights on optimal bidding under uncertainty are derived in Section 3.3.

3.2.2 Empirical evaluation

Herein before mentioned theory will be supported by empirical evidence of forward premiums. This is in line with several papers which estimate risk premiums empirically. Similar to the theoretical model of Bessembinder and Lemmon (2002), Longstaff and Wang (2004) empirically analyzed forward premiums in the day-ahead and real-time market of PJM. They find empirical evidence for forward premiums dependent on demand uncertainty. Additionally, they show that the forward premium might deviate by hour and season and could also be negative. Similar findings are confirmed by Paraschiv et al. (2015) for the German electricity market. Focus of Paraschiv et al. (2015) is on the time-varying structure of forward premiums (hourly, weekday/weekend, season). They find that risk premiums are higher during weekdays and in winter. In contrast to Paraschiv et al. (2015), the underlying research does not aim to identify or quantify hourly forward premiums. The underlying research focuses on the uncertainty classification by weather types and their effect on forward premiums.

Bunn and Chen (2013) provides an overview of different explanation approaches for drivers of forward premiums. They do not consider weather types. They state that results are to some extent ambiguous since they are strongly related on the underlying markets, competition, as well as spatial and temporal resolution. An extensive overview of further literature on risk premiums is given by Ito and Reguant (2016) and Furió and Meneu (2010). However, forward premiums are not fully explained by existing research. Recent work of Paschmann (2017) explains forward premiums to some extent by restricted possibility of trading in the real-time market instead of purely rely on hedging incentives and the merit order convexity. This indicates the necessity of further research in the field of forward premiums. Most research is focused on demand uncertainty. The present work extends the classical approaches to consider renewable (i.e. wind and solar) production uncertainty. The renewable production uncertainty becomes more relevant under the proceeding energy transition towards volatile renewable energies. Thus, it is highly relevant to consider the effects of weather-dependent uncertainty. This work incorporates weather type classifications which are described subsequently.

Throughout this paper, the focus lies on *ex-post* forward premiums. Ex-post forward premiums rely on observed price differences whereas *ex-ante* forward premiums are based estimated price realization. For a detailed discussion on ex-post and ex-ante forward premiums see Furió and Meneu (2010).

3.2.3 Weather classification

This research incorporates weather-dependent volatile wind and solar energies on forward premium effects. An increase in zero marginal costs renewable production has in general a price dampening effect. This effect is widely known as merit order effect and analyzed for instance in Kiesel and Paraschiv (2017), Sensfuß et al. (2008) or Hirth (2013). Besides the classical long-term merit order effect, short-term deviations have influences on real-time prices (compared to day-ahead forward prices). Positive production deviations, i.e. more production than estimated day-ahead, lead to a decrease in real-time prices. This price decreasing effect is shown exemplarily in Figure 3.1 for the German electricity market. The figure shows price forecasts and realizations (upper graph) in comparison to wind and solar production forecasts and realizations (two lower graphs). A remarkable drop in real-time prices can be observed at 12:00am on 09.08.2014 (horizontal center of the plot). The underestimated production realization of wind energy and to some extent solar energy seem to be a driver for the extensive price drop from +20 EUR/MWh down to -25 EUR/MWh.

For the underlying empirical analysis (Section 3.4), it is necessary to capture the uncertainty of wind and solar production, e.g. by clustering situations of similar uncertainty. This clustering is performed based on weather types. Other research which applies weather type classifications are for instance Lange and Waldl (2001) or Couto et al. (2015) for wind as well as Chen et al. (2011) or Shi et al. (2012)

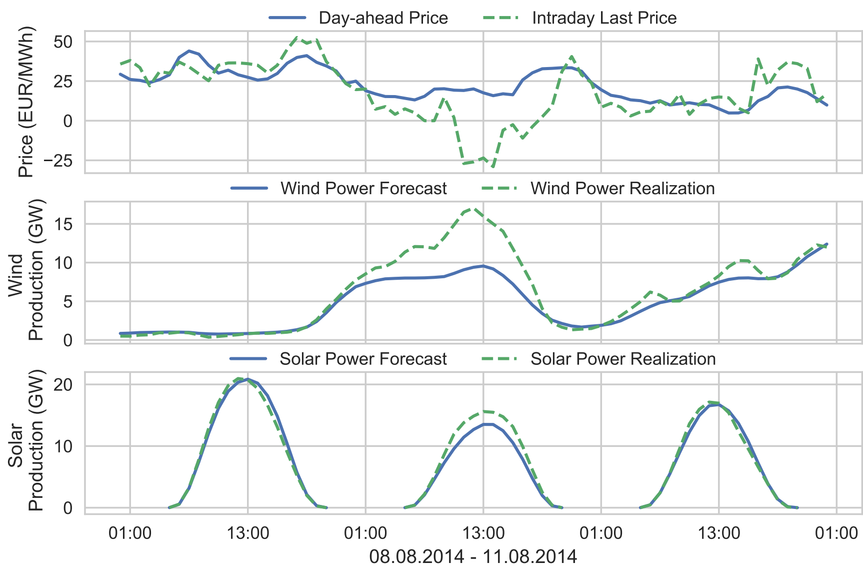

Figure 3.1: Forecasts and realizations for (a) electricity prices, (b) wind production and (c) solar production in Germany from 08. Aug. 2014 to 11. Aug. 2014. It shows wind and solar production forecasts and realizations in comparison to price forecasts and realizations. Realized wind production at 12:00h, 09. Aug. (center of the plot), is 16 GW and thus almost twice as high as forecasted. A simultaneous price drop to -25 EUR/MWh in intraday-prices can be observed.

for solar. None of those research works focuses on forward price premiums. Couto et al. (2015) propose a weather clustering approach to identify and characterize weather types with high wind power ramps (i.e. strong increase in hourly wind differences). They propose that large scale weather types are a suitable clustering possibility for wind ramps. Lange and Waldl (2001) shows that the wind prediction error differ with respect to weather types. Their research is limited to two wind sites for two weather types. The applied weather type classification within this present research considers 40 different weather types to account for Germany's wind and solar prediction errors (or uncertainty). Chen et al. (2011) shows that an artificial neural network (ANN) to predict PV power production performs better if a weather type separation is applied before. They categorize as to three weather types (sunny, cloudy, rainy). Similar, Shi et al. (2012) shows that the PV power forecasting precision depends strongly on the weather type and can be improved by selection of the adequate estimation model. They differentiate between four classes (sunny, cloudy, foggy, rainy). The aforementioned research is limited to either wind or solar prediction errors. In contrast to that research, the underlying work applies weather type classifications to derive information about both wind and solar production uncertainty.

The weather types within the present research are clustered based on the 40 objective Weather Type Classifications of the German Weather Service (cf. Bissolli and Dittmann (2001)). A similar number of weather types (29) is used in James (2007) by a clustering of ERA40 re-analysis data. However, the focus of James (2007) is on the comparison between his weather type classifications and the traditional classification of Gerstengarbe et al. (2010) (which reaches back to the 1950s).

3.3 Theory

The theoretical findings are based on an analytical model similar to Ito and Reguant (2016), Knaut and Obermüller (2016), and Zhang et al. (2015). The model setup consists of two stages. Stage 1 is the day-ahead forward market. Stage 2 is the real-time market (or intraday market). Three groups of players interact with each other, renewable producers r, conventional producers c and the consumers:

- The *renewable producers* r have zero marginal costs of production. In stage 1, they face uncertainty of their final electricity production in stage 2. In stage 2, the uncertainty for the renewable producers resolves. The renewable players form an oligopoly. They compete in order to maximize profits with respect to production (similar to the Cournot competition). However, the focus is on a competitive outcome, which corresponds to the solution for which the number of renewable producers N tends to infinity. All renewable players are assumed to be symmetric. Note that this assumption is a simplification and can be relaxed similar to Knaut and Obermüller (2016).
- The *conventional producers* c act perfectly competitive. They have positive marginal costs (> 0) and do not deviate from bidding their marginal costs. An underbidding of their marginal costs would lead to losses whenever the electricity price is below marginal costs and production was sold. An overbidding is prohibited by the German Monopolies Commission which controls and inspects significant bidding behavior above marginal costs (Bundeskartellamt, 2011).
- The *consumers* have an electricity demand D. The demand is assumed to be inelastic in the short-run. This is a typical assumption for stylized short-run

electricity market models (cf. Ito and Reguant (2016)).[2]

- All players are assumed to be risk-neutral.

The marginal cost function MC (or supply function) is assumed to be quadratic, i.e. convex and strictly monotonic increasing: $MC(q) = aq^2+bq+c$. In some analytic electricity market models, a linear marginal costs function is assumed as simplification ($a = 0$). This is a strong simplification. As shown by Knaut and Obermüller (2016), under a linear merit order function, only the first momentum (expected production) has an impact on optimal bids. Under a quadratic (convex) merit order, the first and the second momentum (standard deviation) have an impact on optimal bids. The standard deviation can be interpreted as a measure of uncertainty. In order to capture the uncertainty effects, a more realistic quadratic merit order is used. An empirical evaluation of the order of the merit order function can be found in Appendix 3.6.1. It indicates that the German merit order function can be estimated by a linear to quadratic function.

The first stage bid of the renewable producer i is denoted as q_{ir1}. For each renewable producer i, the combined first stage and second stage bids have to be equal to the total realized production Q_{ir}: $q_{ir1} + q_{ir2} = Q_{ir}$ The realized production Q_{ir} of player i in stage 2 is uncertain in stage 1 with a probability density function $f(Q_{ir})$. The uncertainty resolves in stage 2.

The aggregated first and second stage bids as well as the aggregated production of *all* renewable producers are denoted as following: $q_{r1} = \sum_i q_{ir1}$, $q_{r2} = \sum_i q_{ir2}$, $Q_r = \sum_i Q_{ir}$.

Each renewable player $i = 1, \ldots, N$ maximizes her profit function Π_{ir} under consideration of the bids of the other $(N-1)$ symmetric renewable players which results in

$$\begin{aligned}\Pi_{ir}(q_{ir1}, q_{ir2}) = p_1\left(q_{ir1}, (N-1)q_{jr1}\right) q_{ir1} \\ + p_2\left(q_{ir1}, (N-1)q_{jr1}, q_{ir2}, (N-1)q_{jr2}\right) q_{ir2}.\end{aligned} \tag{3.1}$$

Within this model setup, the following proposition holds.

Proposition 3.1. *Under above assumptions, the optimal amount of sold renewable*

[2] Short-run inelastic demand is a simplifying assumption for the theoretical analysis. For the German day-ahead market, Knaut and Paulus (2017) shows a demand elasticity of maximum −0.13 in certain hours. Due to recent developments of (battery) storages and demand side management, this effect is expected to grow.

production in the first stage is

$$q_{r1}^{*} = D + \frac{1}{2}\frac{b}{a} - \sqrt{\left[\left(\left(D + \frac{1}{2}\frac{b}{a}\right) - \mu\right)^2 + \sigma^2\right]}. \tag{3.2}$$

Proof. At this point, a brief outline of the approach is given. The detailed proof can be found in Appendix 3.6.2. The profit equation for one producer i is maximized. After taking the first derivative, setting it equal to zero and substituting the integrals of the distribution functions by the expectation and standard deviation, the necessary optimality conditions are derived. Then, the symmetry assumptions of the N firms are applied to derive the joint equilibrium solution. □

Equation (3.2) shows the competitive first stage renewables' bid. It corresponds with the expected outcome under perfect information.

Corollary 3.1. *Without uncertainty, the optimal first stage bid of all renewable players is* $q_{r1}^{*} = \mu$.

Proof. Without uncertainty, the production in the second stage is identic to the expected production in stage 1. Thus, no standard deviation exists. Set $\sigma = 0$ in the Equation (3.2). The remaining optimal bid becomes $q_{r1}^{*} = \mu$. □

In the proof of Proposition 3.1, two production withholding effects can be encountered. First, the potential oligopolistic behavior and second the withholding due to production uncertainty. Since the focus lies on the perfect competition case, the oligopolistic production withholding cancels out while the number of producers tends to infinity for the perfect competition case. However, Equation (3.20) in the Appendix 3.6.2 shows that production uncertainty leads to production withholding also for the oligopoly case. This can be found by the uncertainty-driven standard deviation σ which influences optimal oligopolistic first stage production bids. Thus, the findings can easily be transferred to oligopolies (which is not covered within this research).

The optimal first stage bid q_{ir1}^{*} of Equation (3.2) is dependent on σ. With higher standard deviation, the optimal bid is decreasing as stated in Proposition 3.2.

Proposition 3.2. *Under above assumptions, an increased uncertainty decreases the optimal production bid for renewable producers in the first stage.*

Proof. Take the first derivative of Equation (3.2) with respect to σ:

$$\frac{\partial}{\partial \sigma} q_{r1} = -\sigma \underbrace{\left(\left(\left(D + \frac{1}{2}\frac{b}{a}\right) - \mu\right)^2 + \sigma^2\right)^{-1/2}}_{>0} < 0 \qquad \text{, for } \sigma \neq 0 \tag{3.3}$$

which is strictly negative or equal to 0. It becomes zero if and only if $\sigma = 0$, i.e. no uncertainty exists. Since the first derivative is negative, the function is decreasing in σ. □

Figure 3.2 visualizes the result of Proposition 3.2 with typical numbers inserted. The figure shows that the increase in uncertainty (i.e. increasing σ) diminishes the

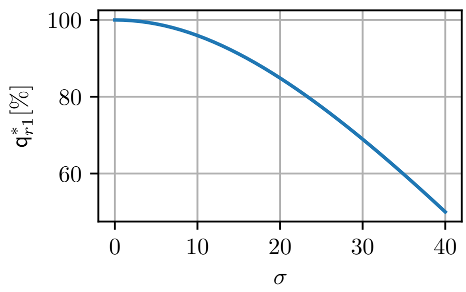

Figure 3.2: Impact on an increasing uncertainty via σ on the optimal first stage renewable bid q^*_{r1} relative to the expected outcome $\mathbb{E}[q_{r1}]$. The parameter to derive the figure were the aforementioned equations with $D = 70$, $\mu = 40$, $a = 0.01$, $b = 0$.

optimal first stage bid. The slope of the curve is dependent on the merit order parametrization as well as the demand intersection and expected renewables' production.

The rationale for Proposition 3.2 is the following: The representative renewables supplier aggregates price-taking behavior of many, small renewables suppliers. Each of these suppliers does not expect that her quantity choice will affect the second period price. However, each renewable producer knows that if she produces relative little energy in stage 2, also all other renewables producers will produce little as well (assuming perfect correlation, for simplicity). Thus, she knows that whenever she is overselling (i.e., more than the expected production), she will have to buy missing quantities at a higher intraday price. Vice versa when underselling with lower intraday prices. Under a non-linear convex merit order, an overselling (i.e. selling more day-ahead than intraday produced) is more expensive than an underselling.

The behavior of conventional producers differ from the renewable producers' behavior: The production ability of a conventional producer is independent of the market situation, i.e. without weather-dependence and correlation effects. Whenever the intraday market price is above her marginal costs, she will want to extend her production by one additional (marginal) unit if remaining production capacity is available. Whenever the intraday market price is below her marginal costs and she has sold production forward for at least her marginal costs, she is willing to demand one additional (marginal) unit electricity from the intraday market to fulfill her delivery responsibilities with lower costs. In all other situations (prices below marginal costs in both markets; or sold day-ahead above marginal costs and intraday-price is between marginal costs and day-ahead price), she has no incentive to deviate.

Note that the aforementioned behavior for renewable producers would not occur with a linear merit order. With a linear merit order, positive and negative price deviations would compensate each other. This compensation requires that the merit order in the forward market and in the real-time market is identic. Knaut and Obermüller (2016) shows, that a steeper real-time market merit order would result in a stronger shift towards selling more production in the first stage (under a competitive oligopoly). Knaut and Paschmann (2017b) shows that a steeper real-time merit order can occur due to inflexible production capabilities. Overall, an optimal bid under uncertainty is below the expected production to avoid cost-intense re-buying of sold but non-realized production.

The quantity deviation in the first stage expected production (based on Proposition 3.1) translates to a price deviation effect. The theoretical result is stated in Proposition 3.3.

Proposition 3.3. *Under the above assumptions and the optimal derived first stage quantity q_{r1}^*, the corresponding first stage equilibrium price is*

$$p_1^* = a((D-\mu)^2 + \sigma^2) + b(D-\mu) + c. \tag{3.4}$$

This optimal first stage wholesale price exceeds the price of trading the expected production (without uncertainty) solely by the term $a\sigma^2$.

Proof. Under the above assumptions, plug in the optimal quantity to the marginal costs function. Thus, $p_1^* = MC(D - q_{r1}^*) = D^2a - 2Da\mu + Db + a\mu^2 + a\sigma^2 - b\mu + c = a((D-\mu)^2 + \sigma^2) + b(D-\mu) + c$. Without uncertainty, the variance σ^2 in the optimal quantity equals 0. The price delta with and without uncertainty is $a\sigma^2$ (which is positive). Thus, uncertainty increases the first stage prices. $\square$

Note that Equation (3.4) is the risk neutral equilibrium result. Thus, arbitrage behavior should not lead to converging day-ahead and intraday-prices. Proposition 3.3 shows the price increasing effect of uncertain production. Figure 3.3 visualizes the findings.

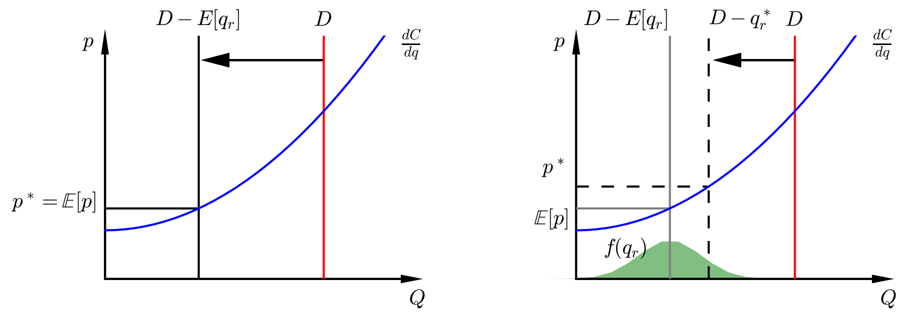

(i) Optimal first stage bid and price with perfect foresight.

(ii) Optimal first stage bid and price under uncertainty.

Figure 3.3: Optimal day-ahead wholesale price and residual demand under (a) perfect foresight and (b) uncertainty. D is the demand, q_r the renewable production, $f(q_r)$ a normal distribution of renewable production, p the price, dC/dq the first derivative of the cost function (i.e. the merit order). The parameter to derive the figure were $D = 70$, $\mu = 40$, $\sigma = 30$, $a = 0.01$, $b = 0$, $c = 20$. Note that neither the normal distribution nor the standard deviation of $\sigma = 30$ are realistic; they are chosen to simplify the illustration.

The uncertainty reduces the optimal first stage bid. This increases the residual demand and thus prices. The profit optimal day-ahead price deviates from the expected day-ahead price. The plotted distribution in this figure is a normal distribution. However, the theoretical proof has no specific assumptions according to the distribution function.

The subsequent section gives empirical evidence of this price increasing effect in the German electricity markets (day-ahead to intraday). The uncertainty is measured via standard deviations within weather types.

3.4 Empirical evidence

This section examines the empirical evidence for the provided theoretical results of Section 3.3. More precisely, two hypotheses are validated:

- *Hypothesis A*: The mean level of the forward premiums can be categorized by weather types.

- *Hypothesis B*: An increased wind and solar production uncertainty leads to an increase in forward premiums.

Hypothesis A allows an ex-ante indication for higher forward premium levels in electricity markets. Simultaneously, Hypothesis A motivates the classification of uncertainty with respect to weather types. This classification is utilized in Hypothesis B. Both hypotheses are evaluated via regression models. The analysis focuses on the German/Austrian electricity market due to its comparable high share of wind and solar energy. Both electricity markets are organized as a fully coupled bidding zone.

In the subsequent, the underlying data is described firstly. Then, the effect of weather types on the mean forward premiums is tested (Hypothesis A). Afterwards, the motivation for the uncertainty classification by weather types is given which uses the standard deviation as uncertainty measure.[3] Finally, empirical tests are performed to verify the impact of higher uncertainty on forward premium increases (Hypothesis B).

3.4.1 Data

Four different sources provide the data for the empirical analysis. First, wind and solar forecast and realization data is derived from the EEX Transparency platform. Second, price data (day-ahead and intraday) is obtained from EPEX Spot. The ENTSO-E Transparency platform provides the load data. Fourth, the weather type classification dataset is derived from the German Weather Service (DWD). Detailed description can be found subsequently. An overview is given in Table 3.1. Descriptive numbers are listed in 3.6.3. The analyzed timespan covers July 2015 to December 2016.

Wind and solar production data

The wind and solar production data is published by the EEX Transparency platform (Transparency, 2017). The focus lies on the provided wind and solar data for Germany *and* Austria due to the same bidding zone. The production data is provided by the Transmission System Operators (TSOs). The data has a quarter-hourly resolu-

[3]As to the theory section, the standard deviation is the relevant measure. Thus, the subsequent analysis focuses on the standard deviation as the indicator for forecast uncertainty. Other indicators like the Root Mean Squared Error (RMSE) or the Mean Absolute Error (MAE) would be possible as well but include similar information. Hence, they are redundant and the focus on the standard deviation is preferred.

Table 3.1: Overview of applied data. Regional focus is the joint German/Austrian bidding zone. The timespan covers July 2015 to December 2016.

Data	**Source**	**Used Resolution**
Wind and Solar Production	EEX Transparency	Hourly
Day-ahead and Intraday Prices	EPEX Spot	Hourly
Load	ENTSO-e	Hourly
Weather Type Classifications	DWD	Daily

tion, which is aggregated within this analysis to hourly mean values for comparison reasons. In the remaining paper, the forecast error is applied which is defined as $realization - prediction$ according to Morales et al. (2013). For wind and solar production, the forecast error is normalized by the monthly installed capacity $(realization - prediction)/InstalledCapacity$. This accounts for the fact of continuously increasing capacity and ensures comparability over time. The capacity data source is the German regulator Bundesnetzagentur (`www.Bundesnetzagentur.de`). For the ease of readability, the forecast error is denoted with Δ throughout this paper. The (normalized) wind forecast error in hour h, for instance, is given by $\Delta Wind_h$.

The reported data by the TSOs is not based on exact metering for each production utility. They use extrapolations from specific metered utilities in combination with weather data; see for instance 50Hertz (2017), Amprion (2017), Tennet (2017), TransnetBW (2017) and APG (2017). The TSOs are responsible for grid stability and coordinate the market participation for a certain share of wind and solar production (especially household production). Additionally, they closely collaborate with weather forecasting institutes. Thus, the TSOs' forecasts and extrapolated realizations are the best available wind and solar production data for Germany. Nevertheless, minor biases could exist.

Price data

The price data is published by the EPEX Spot (EPEX SPOT, 2017). The data contains the day-ahead electricity price and the intraday electricity price. The day-ahead price can be considered as the price forecast. Additionally, the day-ahead price determines the reference point for short-run price deviations of the expected information. The price covers the joint bidding zone of the German/Austrian electricity market.

The intraday price data is the volume weighted average price of the last three hours, which is called *ID3* at EPEX Spot. The ID3-price allows comparing the day-ahead price to the final intraday price level. The average price is taken since the last accepted intraday price in the continuous intraday market might be biased due to market overreactions, open positions before gate closure and irrational trader decisions. Thus, the last bid is not necessarily a valid indicator for the fundamental price level of the intraday market. The following analysis focuses on the ID3-price. The ID3-price index is available since July 2015 which restricts the total dataset time-span.

EPEX denotes for the intraday prices that the "German and Austrian areas might be disconnected temporarily due to necessary measures done by responsible TSOs. Hence displayed values might not be common German/Austrian market data in all cases but isolated German only or isolated Austrian only market data." (EPEX SPOT, 2017). Other countries cannot participate in the intraday auction. The disruptive effects of the intraday participant restriction are investigated in Knaut and Paschmann (2017b), Knaut and Paschmann (2017a) and Paschmann (2017).

In some rare situations, price differences between the day-ahead and intraday market become exceptional large. This cannot be explained fundamentally by wind, solar or load deviations. Reasons could be for instance power plant outages or unbalanced portfolios which cause high penalties in the balancing market and lead to corresponding trader behavior. To avoid biased estimations by not fundamentally driven price differences, those observations are handled as outliers and dropped from the analysis. An observation is categorized as an outlier if the price difference exceeds three times its standard deviation. Thus the remaining data covers 99.7% of the observations. The threshold for price differences has a value of ±37 EUR/MWh around the average day-ahead price level of 30.30 EUR/MWh in the observation period.

Load data

Corresponding load data for the joint bidding zone of Germany and Austria is derived by ENTSO-E. Both, a forecast and a realization value are published. The load values do not incorporate exports or imports. The current market design does not allow foreign production to participate in the intraday market (cf. Knaut and Paschmann (2017b)). Thus, it is consistent within this analysis to neglect trade in the delta comparison. In order to derive prices, instead of price differences, the foreign production needs to be considered within the day-ahead market. Since the latter analysis focuses on price deltas, this is not necessary within this framework.

Weather type classification data

The weather type classification data is published by the German Weather Service DWD (DWD, 2017). Current weather types are published daily including forecasts for the next seven days. Detailed information as to the classification scheme can be found in Bissolli and Dittmann (2001). The objective weather type classifications are a daily categorization of the German weather situations. That means each day is categorized to one weather type. The weather types are defined according to the following criteria:

- Advection type (no prevailing direction, northwest, northeast, southwest, southeast)
- Cyclonality in 950 hPa (cyclonic, anticyclonic)
- Cyclonality in 500 hPa (cyclonic, anticyclonic)
- Humidity of the atmosphere (wet, dry)

Note that 500 hPa and 950 hPa correspond to an approximate height of 5.5 km and 0.5 km above sea level, respectively. The advection type reflects the majority of horizontal wind directions on the 750 hPa level. An advection direction is prevailing if it covers at least two thirds of the measured (weighted) wind directions (cf. Bissolli and Dittmann (2001)).

The above combinations result in 40 possible weather types. Statistics (e.g. frequency) can be found in the 3.6.3. Data exists back to 1979. Due to price data availability reasons, the focus of this research is on the timespan from July 2015 to December 2016.

3.4.2 Effect of the weather types on the mean forward premium level (Hypothesis A)

This section examines Hypothesis A. The question is answered if and to what extent weather types have an effect on the mean forward premium levels. This question is analyzed by an effect coding approach which is one specific type of contrast coding. Here, the analysis provides the difference of each sub-groups' mean to the grand mean forward premium. The grand mean is defined as the mean of all observations. A general overview of contrast coding and effect coding can be found in Davis

(2010) and McClendon (1994). The method dates back to former work of Overall and Spiegel (1969). In a first step, the effect of the weather types on the mean level of forward premiums is analyzed. In a second step, the criteria to define and distinguish the weather types (advection direction, cyclonality, humidity) are subject to the effect coding analysis.

Forward premium effects by each weather type

The analyzed effect coding model reads as following

$$ForwardPremium_h = Intercept + \sum_i \beta_i WeatherType_{i,h} + \epsilon_h \tag{3.5}$$

for each hourly observation h. Here, $WeatherType_{i,h}$ is a categorical dummy variable with i the weather type index 1 to 40. The weather types are defined per day and therefore matched to the corresponding hours h. For each hourly observation h, at most one dummy variable $WeatherType_i$ can be equal to one whereas all other dummies equal zero. If all dummy variables are equal to zero, the pure intercept is estimated which represents the grand mean. The ϵ_h represents the hourly error term, i.e. the difference between the estimated sub-groups' mean forward premium and the hourly observations.

The results of the effect coding how the group mean deviates from the grand mean can be found in Table 3.2. The overall mean is highly-significant but slightly negative over the observation period with a value of -0.14 EUR/MWh. This indicates on average lower day-ahead prices than intraday-prices. Based on the results of the theory section, this seems counterintuitive since positive day-ahead forward prices are expected. In fact, other forward premium effects could influence the overall forward premium mean. Further effects are for instance restricted participation which leads to steeper intraday merit order curves and thus higher intraday-prices (cf. Paschmann (2017)), hourly forward price deviations which could be negative (investigated by Longstaff and Wang (2004) and Viehmann (2011)), seasonal forward premium effects (Bessembinder and Lemmon, 2002), scarcity effects (low reserve margins) which could be price influencing (Bunn and Chen, 2013). If other effects outweigh the forward premium effect of production uncertainty, the overall forward premium can become negative.

The reported values of Table 3.2 are the deviations of the groups' mean value to the grand mean. For instance, the weather type 1 has a 1.02 EUR/MWh higher mean

Table 3.2: Differences of each weather types' mean to the grand mean estimated by the effect coding approach $ForwardPremium_h = Intercept + \sum_i \beta_i WeatherType_{i,h} + \epsilon_h$. Number of observations is 13040 hourly values from July 2015 to December 2016. Significance levels denoted by * p<.1, ** p<.05, ***p<.01. Significance and estimations of the grand mean indicates the difference to a zero mean value. Note that five weather classes are omitted due to too less observations in the investigated time horizon.

Weather Type	Wind direction	Cyclonalitity in 950 hPa	Cyclonalitity in 500 hPa	Humidity	Difference to grand mean
Grand mean					−0.140***
1	no direction	anticyclonic	anticyclonic	dry	1.015***
2	northeast	anticyclonic	anticyclonic	dry	0.391
3	southeast	anticyclonic	anticyclonic	dry	1.347**
4	southwest	anticyclonic	anticyclonic	dry	0.802***
5	northwest	anticyclonic	anticyclonic	dry	−0.942***
6	no direction	anticyclonic	anticyclonic	wet	0.664**
9	southwest	anticyclonic	anticyclonic	wet	0.488***
10	northwest	anticyclonic	anticyclonic	wet	0.366**
11	no direction	anticyclonic	cyclonic	dry	1.461***
12	northeast	anticyclonic	cyclonic	dry	0.207
14	southwest	anticyclonic	cyclonic	dry	0.904***
15	northwest	anticyclonic	cyclonic	dry	−0.024
16	no direction	anticyclonic	cyclonic	wet	2.072*
17	northeast	anticyclonic	cyclonic	wet	−3.773***
19	southwest	anticyclonic	cyclonic	wet	−0.737**
20	northwest	anticyclonic	cyclonic	wet	−0.046
21	no direction	cyclonic	anticyclonic	dry	−0.375
23	southeast	cyclonic	anticyclonic	dry	1.032**
24	southwest	cyclonic	anticyclonic	dry	−0.740
25	northwest	cyclonic	anticyclonic	dry	0.413
26	no direction	cyclonic	anticyclonic	wet	−5.076***
27	northeast	cyclonic	anticyclonic	wet	1.182
28	southeast	cyclonic	anticyclonic	wet	−1.383***
29	southwest	cyclonic	anticyclonic	wet	−1.102***
30	northwest	cyclonic	anticyclonic	wet	1.759**
31	no direction	cyclonic	cyclonic	dry	−0.170
32	northeast	cyclonic	cyclonic	dry	−0.256
33	southeast	cyclonic	cyclonic	dry	2.607***
34	southwest	cyclonic	cyclonic	dry	0.419
35	northwest	cyclonic	cyclonic	dry	1.163**
36	no direction	cyclonic	cyclonic	wet	−3.792***
37	northeast	cyclonic	cyclonic	wet	−0.312
38	southeast	cyclonic	cyclonic	wet	−1.907***
39	southwest	cyclonic	cyclonic	wet	0.718***
40	northwest	cyclonic	cyclonic	wet	−0.080

than the grand mean and this deviation is highly significant for the observations. The absolute mean forward premium of the Weather Type #1 is thus 0.88 EUR/MWh, derived as the delta of both aforementioned values.

In total, the mean forward premiums of 22 weather types are significantly different from the grand mean; among them 14 weather types with a significance level of 1% or below and seven weather types with a significance level between 1% and 5%. Overall, 14 of the 22 significantly deviating means of the weather types are positive whereas eight are negative deviating. Some weather types as for instance Weather Type #26 or #33 have remarkable high deviations from the grand mean of −5.07 EUR/MWh or +2.61 EUR/MWh, respectively. However, there is no weather type criteria such as advection direction, cyclonality or humidity which has only significant positive or negative mean deviations. Thus, no exact causality can be derived but trends of the criteria could exist. Dry weather, for instance, seems to have more often a positive significant effect whereas wet weather seems to have more often a negative significant effect. The independent effects of the separated weather type criteria are analyzed in the subsequent section.

Foward premium effects by the weather types' separated criteria

This section puts emphasis on the separated weather type criteria (a) advection direction, (b) cyclonality (at 950 hPa and 500 hPa) and (c) humidity. The same effect coding approach as in Equation (3.5) is performed in which the categorical variables are the clustered weather types' sub-criteria.

(a) Advection direction Table 3.3 reports the mean differences of the advection directions to the grand mean. The separated wind directions have only two significant coefficients: *Southwest wind* and *no prevailing wind direction*. Both coefficients deviate from the grand mean on a 10% significance level. For southwest wind, the mean forward premium is 0.19 EUR/MWh higher than the grand mean of −0.14 EUR/MWh. Without a prevailing wind direction, the forward premium mean is 0.25 EUR/MWh lower than the overall mean. Based on these statistics and the fact that all other wind directions show no significant contribution, the wind direction indicates limited implications on the mean forward premium.

Table 3.3: Results of the effects coding approach for the weather types' criteria *advection direction* for the model $ForwardPremium_h = Intercept + \sum_i \beta_i AdvectionDirection_{i,h} + \epsilon_h$. The estimated values indicate the difference of the criterias' mean value to the grand mean. Number of observations is 13040 hourly values from July 2015 to December 2016. Significance levels denoted by * p<.1, ** p<.05, ***p<.01. Significance and estimations of the grand mean indicates the difference to a zero mean value. Note that five weather classes are omitted due to too less observations in the investigated time horizon.

Advection	Difference to grand mean
Grand Mean	−0.140***
Northeast	0.108
Northwest	−0.116
Southeast	0.105
Southwest	0.191*
No prevailing direction	−0.249*

(b) Cyclonality on 950 hPa Table 3.4 indicates high relevance of the cyclonality on 950 hPa on the mean forward premium levels. Anticyclonic weather types increase the mean forward premium by a mean of 0.27 EUR/MWh whereas cyclonic weather types have a decreasing effect of −0.53 EUR/MWh. Both effects are highly significant at the 1% level.

Table 3.4: Results of the effects coding approach for the weather types' criteria *cyclonality on 950 hPa* for the model $ForwardPremium_h = Intercept + \sum_i \beta_i Cyclonality950hPa_{i,h} + \epsilon_h$. The estimated values indicate the difference of the criterias' mean value to the grand mean. Number of observations is 13040 hourly values from July 2015 to December 2016. Significance levels denoted by * p<.1, ** p<.05, ***p<.01. Significance and estimations of the grand mean indicates the difference to a zero mean value. Note that five weather classes are omitted due to too less observations in the investigated time horizon.

Cyclonality on 950 hPa	Difference to grand mean
Grand Mean	−0.140***
Anticyclonic	0.270***
Cyclonic	−0.526***

The cyclonality on 500 hPa (approximately 5.5 km above sea level) has no significant coefficients. Therefore, the higher level cyclonality cannot be confirmed to have relevant effects on the forward premium. The corresponding results can be found in Appendix 3.6.5. As a reason for the non-significance, the relationship between the forward premium and the near-surface renewable production can be expected. Higher level weather conditions seem to have reduced impact for the electricity markets.

(c) Humidity The effect of the weather type criteria *humidity* on the mean forward premium level is reported in Table 3.5. Both, Dry and Wet, have a significantly deviating forward premium mean compared to the grand mean. Dry has a 0.25 EUR/MWh higher mean forward premium whereas Wet has a -0.27 EUR/MWh reduced mean forward premium.

Table 3.5: Results of the effects coding approach for the weather types' criteria *humidity* for the model $ForwardPremium_h = Intercept + \sum_i \beta_i Humidity_{i,h} + \epsilon_h$. The estimated values indicate the difference of the criterias' mean value to the grand mean. Number of observations is 13040 hourly values from July 2015 to December 2016. Significance levels denoted by * p<.1, ** p<.05, ***p<.01. Significance and estimations of the grand mean indicates the difference to a zero mean value. Note that five weather classes are omitted due to too less observations in the investigated time horizon.

	Difference to grand mean
Grand mean	-0.140***
Dry	0.254***
Wet	-0.271***

Discussion of the mean deviating effects of weather types on the forward premiums

The above analyses show distinguishable effects of the weather types and its subgroups to the mean level of the forward premiums. The analysis of the separated weather type criteria (advection direction, cyclonality and humidity) allow insights on the weather-related driver of the mean forward premium. Several criteria could be identified with a significant impact on mean deviations of the forward premium. A general positive forward premium effect can be associated with southwest wind, anticyclonic weather patterns on 950 hPa, or dry weather. In contrast to this, a negative effect on forward premiums is estimated for no prevailing wind direction, cyclonic weather patterns on 950 hPa, or wet weather. However, even if these effects are significant, they do not necessarily lead to higher/lower forward premiums in each hour. Based on this analysis, the impact of weather type criteria on forward premiums can only be used as a rule of thumb. The dominating effect by a combination of sub-groups is ex-ante not clear (e.g. what is the mean forward premium effect under positive-expected anticyclonic and negative-expected wet weather?). The detailed information on each combination (i.e. each weather type) with its criteria is estimated in Table 3.2. In these results, the different effects of each weather type on the mean forward premiums become obvious. Several weather types have significant positive and negative implications to the mean of the forward premiums. The results can be applied by market participants such as traders to approximate the mean level of forward premiums additional to typical effects by production deltas. To derive statements for price forecasting, further investigations are necessary which could require applications in price forecasting models. However, this is not the scope of this paper and remains for further research.

The different forward premium effects by the weather types motivate the subsequent uncertainty categorization as basis for the empirical analysis in Section 3.4.4.

3.4.3 Weather classifications as a distinction of wind and solar forecast uncertainty

This subsection provides information about the wind and solar uncertainty categorization which is applied to examine Hypothesis B (forward premium increase by wind and solar uncertainty) in Section 3.4.4.

Wind and solar production levels are no sufficiently distinguishable indicators for uncertainty

For the subsequent regression analysis, the uncertainty should properly be considered. An intuitive classification could be the production level of wind and solar power. A classification based on the production level underlies the assumption of heteroscedastic errors with respect to the production level. However, the production level classification indicates low differentiation possibility. This is discussed in 3.6.4. Thus, the production level classification seems not to be suitable for an adequate forecast error distinction.

Weather classes have deviating statistical characteristics

A potential classification scheme could be defined on weather types. This is motivated by the aforementioned analysis that weather types have distinguishable effects on forward premiums. Thus, the DWD objective weather type classifications are analyzed for potential uncertainty categorization. Details as to the weather type definitions can be found in Table 3.8 whereas statistical numbers are listed in Table 3.9 in the Appendix.

Certain weather types correlate with specific wind and solar forecast situations. As an example, assume anticyclonic weather constellations which are also known as high-pressure situations. Such high-pressure situations are more likely to have fewer clouds. Solar production is thus better predictable compared to changeable weather types. Therefore, solar production uncertainty should be lower.

Figure 3.4 compares the 40 objective weather type classifications with respect to the aggregated wind and solar production deviations. The production deviations are defined as the realized value minus the forecast normalized by the monthly capacity. The normalization ensures comparability of the forecast errors over the time horizon. The delta is positive if more electricity is produced than expected. It becomes obvious

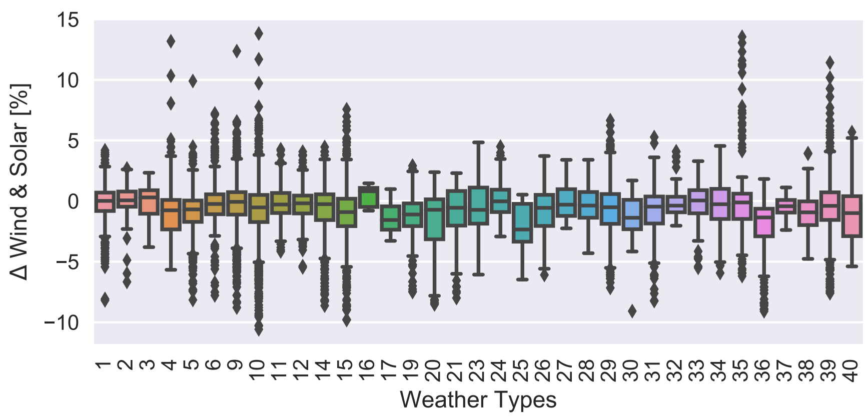

Figure 3.4: Aggregated wind and solar forecast errors (realization minus forecast) of each objective weather class. Production deltas are relative to the monthly installed capacity. Data covers July 2015 to December 2016.

that the median, quartiles and outliers might deviate strongly between the individual classes. The distinction possibility is also true for the standard deviation as one indicator for the spread of the forecast errors. Additionally, note that weather classes have different frequencies.

Focus on the weather type's standard deviations

Based on the weather type classifications, the standard deviation can be calculated per weather type and be used as an indicator for expected uncertainty. Several weather types have a lower standard deviation than the average whereas some have remarkable higher standard deviations. A higher standard deviation of wind and solar forecast errors indicates that exact wind and solar production is harder to predict. Figure 3.5 compares the relative standard deviations of capacity-normalized wind and solar deltas for each weather type (ascending ordered). The standard deviations per weather type are relative to the grand standard deviation, i.e. of all observations. Several weather classes show a relative standard deviation below the

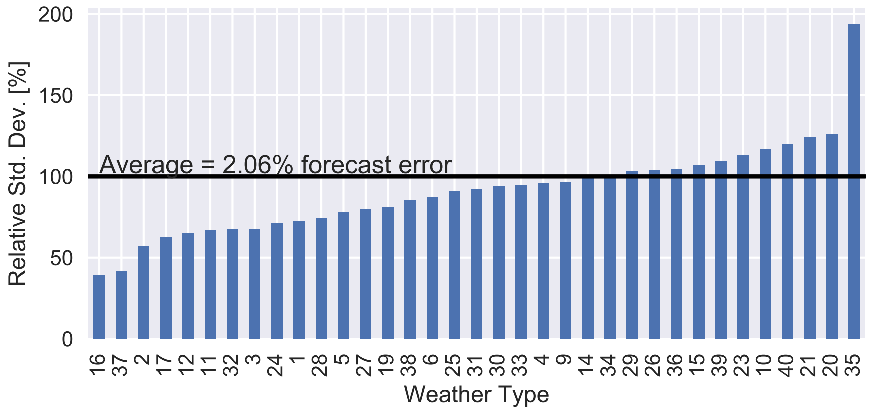

Figure 3.5: Relative standard deviations of the wind and solar forecast errors per weather type. The wind and solar forecasts errors are normalized by the monthly capacity. The standard deviation per weather class is relative to the standard deviation over all data (which is a forecast error of 2.06 %). Data covers July 2015 to December 2016.

average down to a minimum of 40% (i.e. absolute standard deviation of 0.82% forecast error[4]). On the other hand, weather class #35 has an exceptional high standard deviation of approximately 200% compared to the average. Class #35 defines dry cyclonic northwest wind situations which has an almost average number of occurrences. Most standard deviations are in the range between 60% and 130%. It is expected, that a higher uncertainty of the wind and solar production leads to an higher uncertainty of the forward premiums. This hypothesis is examined and supported in Appendix 3.6.6. The subsequent analysis goes one step beyond. The focus is on the increasing forward price level by uncertainty instead of a solely increased

[4]Note that the wind and solar forecast error is the difference between realization and forecast normalized by the monthly capacity, which results as a percentage.

(obvious) price uncertainty.

3.4.4 Forward price premiums rise with wind and solar production uncertainty (Hypothesis B)

This section examines empirically the Hypothesis B that an increased wind and solar production uncertainty leads to an increase in forward price premiums. Thus, empirical support is given for the price increasing effect shown analytical in Section 3.3. To identify the effects, three OLS regression analyses are performed denoted by *Model B1*, *Model B2* and *Model B3*. The dependent variable is the forward price premium defined as the delta between the day-ahead price to the intraday price. The results allow detecting the overall forward premium effect. An increase in the forward premium can result by either an increased day-ahead price, a decreased intraday price or both effects simultaneously. The analysis is not suitable to determine which effect influences the forward premium. A discussion of this is provided in the latter.

Model description

The estimated models can be expressed as

$$\begin{aligned}\text{Model B1: } ForwardPremium_h &= \alpha + \beta_1 \Delta(Wind\&Solar)_h \\ &\quad + \beta_2 StdDev(Wind\&Solar)_h + \epsilon_h \end{aligned} \tag{3.6}$$

$$\begin{aligned}\text{Model B2: } ForwardPremium_h &= \alpha + \beta_1 \Delta Load_h + \beta_2 StdDev(Load)_h \\ &\quad + \beta_3 \Delta(Wind\&Solar)_h \\ &\quad + \beta_4 StdDev(Wind\&Solar)_h + \epsilon_h \end{aligned} \tag{3.7}$$

$$\begin{aligned}\text{Model B3: } ForwardPremium_h &= \alpha + \beta_1 \Delta Wind_h + \beta_2 StdDev(\Delta Wind)_h \\ &\quad + \mathbb{1}_{solar,h}(\alpha_{Solar} + \beta_3 \Delta Solar_h \\ &\quad + \beta_4 StdDev(\Delta Solar)_h) + \epsilon_h \end{aligned} \tag{3.8}$$

where h denotes the hourly observations for the investigated timeframe from July 2015 to December 2016. Model B1 (Equation (3.6)) is the basic model. It estimates the price deviations dependent on the wind and solar production delta as well as the wind and solar uncertainty. The production delta is defined as *realization minus forecast*. Note that the uncertainty is defined as the standard deviation of the observations that belong to the same weather type. Since each weather type last for a complete day, the values are matched to the hourly observations. Model B2 (Equation (3.7)) extends the basic model by the consideration of the load deltas and the load uncertainty. An impact of load deltas to the forward price deviation can be expected (cf. Bessembinder and Lemmon (2002)). Model B3 (Equation (3.8)) is similar to the Basic Model B1 except that wind and solar are independent regressors. Since hours at night with 0 MWh solar forecast and solar production would bias the estimates for solar, a dummy variable is applied. The dummy variable (or indicator function) is denoted as $\mathbb{1}$ and equals 1 if not both solar forecast and production are equal to 0 MWh.

The models estimate timeseries data. Thus, it is relevant to test for stationarity, homoscedasticity and non-autocorrelation. Additionally, multi-collinearity between the variables is helpful to verify the model specification.

Requirements check

Low multicollinearity No relevant high correlation occurs within the regressor variables of each analysis. The relevant correlation values between the regressors are in the range between -0.06 and 0.11. Higher correlation could occur between variables which are not simultaneously used in the same regression (e.g. a correlation of 0.86 between wind deltas as well as wind and solar deltas). The dependent variable *forward premiums* could have higher correlation to the regressors which is not critical (e.g. 0.43 to wind and solar deltas). Correlation values can be found in Appendix 3.6.7.

Stationarity: Unit root test via Augmented Dickey-Fuller test An Augmented Dickey Fuller test is performed as a unit root test to check for stationarity. Detailed numbers are listed in the Appendix 3.6.7. The test statistics show that the null hypothesis of unit roots can be rejected. Thus, the timeseries is stationary or, in other words, does not have a time-dependent trend.

Heteroscedasticity and autocorrelation White's Lagrange Multiplier Test for Heteroscedasticity rejects the null hypothesis of homoscedasticity. Additionally, the Durbin-Watson test with a value of 0.45 rejects the null hypothesis of no autocorrelation.[5] To address heteroscedasticity and autocorrelation, heteroscedastic and

[5] No autocorrelation would require a Durbin-Watson test statistic approximately at the value of 2. Values of 0 or 4 denote perfect positive or negative auto-correlation.

autocorrelation robust Newey-West standard errors are applied (Newey and West (1987)).

Regression results

Table 3.6 shows the estimated coefficients for Model B1, Model B2 and Model B3. For Model B1, both regressors are significant. The capacity-normalized delta in wind and solar production is significant at the 1% level whereas the standard deviation for wind and solar deltas per weather type is significant at the 5% level. The high significance of the wind and solar delta is expected since a lower wind and solar production than expected should lead to higher prices. This effect is also stated in other literature as for instance Kiesel and Paraschiv (2017), Sensfuß et al. (2008) or Hirth (2013). The interesting finding is the significant effect of wind and solar uncertainty on forward prices. A higher standard deviation of the wind and solar production delta per weather type leads to higher forward premiums. That indicates, in general, that the ex-ante known uncertainty is hedged to forward premiums.

Model B2 shows significant coefficients for the three regressors (a) load delta, (b) the capacity-normalized wind and solar delta and (c) the standard deviation of the capacity-normalized wind and solar delta. The standard deviation of the load delta is not significant. The non-significance of the load uncertainty is not surprising since the weather types are defined on meteorological conditions and do not necessarily reflect relevant load characteristics. Note that this does not imply, that the standard deviations of load deltas are not relevant in general. Another aggregation (e.g. load deltas dependent on season, hour or load level) may lead to significant load results, as mentioned by Bessembinder and Lemmon (2002) or Longstaff and Wang (2004). However, the load uncertainty is not the focus of this investigation and an investigation of different load uncertainty aggregations is thus neglected. The findings of the Model B2 are the following:

- An increase in the load delta (i.e. more realized load than expected) decreases the forward premium. Per GWh increased load, the price delta is estimated to decrease by 0.19 EUR/MWh.
- An increase in the capacity-normalized wind and solar delta (i.e. more realized volatile renewable production than expected) increases the forward premium. Each percent-point increased utilization of wind and solar production increases the forward price delta by 1.22 EUR/MWh. Note that the production delta is normalized by the installed capacity to account for capacity extensions.

Table 3.6: Regression results on the dependent variable *Forward Premium* with hourly observations. The standard deviations are calculated for each weather types and then matched to the corresponding hours. Model B1 is the basic model which considers capacity-normalized wind and solar production deltas and uncertainty. Model B2 extents Model B1 by consideration of load deltas and the load uncertainty. Model B3 separates the wind and solar data. $\mathbb{1}_{solar,h}$ is a dummy variable for solar production. Wind and solar production as well as the standard deviations are calculated with production deltas which are normalized by the monthly installed capacity to account for capacity extensions over time. Data covers July 2015 to December 2016. Standard Errors are heteroscedasticity and autocorrelation robust (HAC). Standard errors in parentheses. * p<.1, ** p<.05, ***p<.01

$FowardPremium_h$	Model B1	Model B2	Model B3
Intercept	−0.132	−0.357	−0.075
	(0.305)	(0.377)	(0.255)
$\Delta Load_h$		−0.193***	
		(0.032)	
Std.Dev($\Delta Load)_h$		0.177	
		(0.134)	
$\Delta Wind\&Solar_h$	1.220***	1.208***	
	(0.037)	(0.036)	
Std.Dev($\Delta Wind\&Solar)_h$	0.393**	0.376**	
	(0.158)	(0.158)	
$\Delta Wind_h$			0.542***
			(0.020)
Std.Dev($\Delta Wind)_h$			0.124*
			(0.070)
$\mathbb{1}_{solar,h}$			0.110
			(0.441)
$\Delta Solar_h$			0.937***
			(0.041)
Std.Dev($\Delta Solar)_h$			0.170
			(0.221)
N	13040	13040	13038
Adj. R^2	0.166	0.171	0.174
F-statistic	557	290	269

- A higher standard deviation of the delta in wind and solar production (i.e. more uncertainty of the wind and solar forecast error) has a significant positive effect on the forward premium. It is significant at the 5% level. An increased standard deviation by 1 percent-point leads to a 0.39 EUR/MWh increase in forward premiums.

For Model B3, the combined regressors for wind and solar are disentangled. The general results of Model B1 hold true for Model B3. The separation allows additional insights on the origin of the price premium effects. A difference between the normalized wind and the solar deltas can be observed. The capacity-normalized solar deltas have a higher coefficient. This means that forward premiums are stronger increased by an unexpected additional percent-point of solar production than wind production. This finding is in line with common research for European and especially the German electricity markets. The high correlation of peak-load at noon with general high solar feed-in has a strong price reducing potential. See for instance Hirth (2013), Jägemann (2015) and Cludius et al. (2014). As to the uncertainty, only the standard deviation of wind deltas are significant (at a 10% level). The solar uncertainty is not significant at all. The positive effect of the disentangled wind uncertainty on the forward premium is 0.30 EUR/MWh. A schematic plot how uncertainty affects the forward premiums is visualized in Figure 3.6.

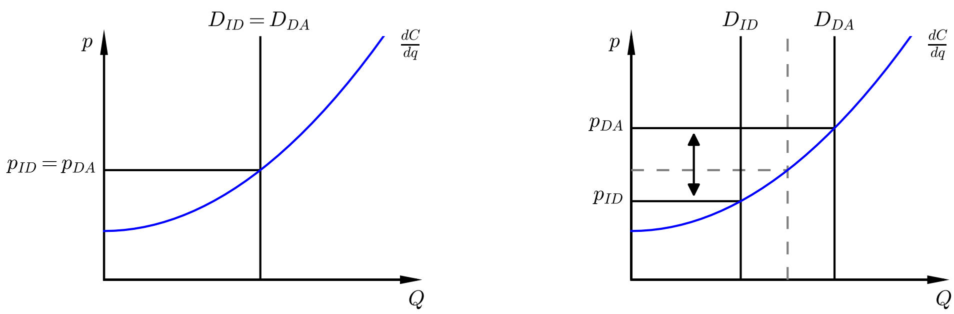

(i) Schematic day-ahead and intrady prices without uncertainty

(ii) Schematic day-ahead and intrady prices with uncertainty

Figure 3.6: Schematic effect of uncertainty on the forward premium. The left figure (a) visualizes a situation without uncertainty (perfect foresight). Day-ahead and intraday prices are equal. Figure (b) shows the schematic impact of wind and solar production uncertainty. The forward premium is in general increased under uncertainty. p denotes prices and D denotes the demand for the day-ahead (DA) and intraday (ID) market.

The regression analysis explains effects on the forward premium whereas the forward premium is defined as the price delta. Thus, for an (absolute) increased forward premium, it is not clear whether the day-ahead price is increased, the intraday price is decreased or both effects occur. Following seems rational (even if the analysis is not suitable to provide statistical evidence): The deviations in load or wind and solar production can be assumed to be ex-ante unknown random processes in the short-run. All available ex-ante information is incorporated in the day-ahead price. Thus, short-term deviations are traded in the intraday-market which has no price effect on the earlier closed day-ahead market. These deviations should therefore influence only the intraday prices. On the other hand, the degree of uncertainty could be known ex-ante. A higher ex-ante known uncertainty level could be incorporated in the day-ahead market as well as in the intraday-market. The market selection is based on the traders' decision at which time they internalize the uncertainty. Internalization of the uncertainty in the day-ahead market would be rational in the sense of risk hedging. However, a final determination is not possible solely on these regression results. The theoretical results in Section 3.3 suggest to internalize uncertainty in the day-ahead forward markets. Note that these results are not differentiated as to seasons or hours. This differentiation remains for further research.

Overall, *Hypothesis B* of an increasing forward premium effect by increased production volatility can thus be confirmed based on the regression results. These findings give new insights and contribute to existing literature on forward premiums. It supports the analytic finding in Section 3.3 that weather-dependent production uncertainty increases the forward premium. Thus, it extends the fundamental literature which focuses on forward premium effects by demand uncertainty (e.g. Bessembinder and Lemmon (2002), Longstaff and Wang (2004)) and which identifies forward premiums with respect to different temporal resolutions (Viehmann (2011), Kiesel and Paraschiv (2017) or Furió and Meneu (2010)). The novel aspect in this research is that the weather types are almost fully decoupled of the current observation due to the long time horizon. Classical literature (e.g. Contreras et al. (2003),Conejo et al. (2005),Weron (2007)) often apply autoregressive timeseries models which predict uncertainty-based price forecasts on limited past observations. Thus, the forward premium prediction is derived out of the current situation. The analysis within this paper applies a long-lasting time horizon to classify uncertainty. Hence, it can be interpreted as a classification which does not rely on the current situation. Additionally, the analysis shows that weather types are a suitable clustering method to consider wind and solar uncertainty. The effects on the forward premium are expected to increase under a higher merit order convexity as well as under a higher wind and solar production standard deviation.

Approximation of the economic implications

The economic implication for Germany suggests a relevant reduction in total costs if the forward premium due to wind an solar uncertainty could be reduced by 1%-point. Costs savings can be derived based on a rough approximation. For 2016, the total costs for electricity production on the day-ahead market amounts to EUR 6.625bn. This is the summation of the hourly day-ahead prices multiplied with its corresponding day-ahead volumes. The source is the EPEX Spot Market. Based on the Model B2 results, a 1%-point decrease in the wind and solar uncertainty translates to 0.376 EUR/MWh reduced forward premiums. The overall costs for 2016 with a 1%-points improved wind and solar standard deviation are EUR 6.536 bn. Therefore, the potential cost saving estimates to EUR 88m per year. The slightly higher forward premium reduction effect of Model B1 with a value of 0.393 EUR/MWh would result in total cost savings of EUR 92 million. The approximation indicates the high relevance of an forecast quality increase to reduces total system costs. Under the assumption of an inelastic consumer demand function, this represents the welfare gain of an improved forecast quality. Note that the rough approximation neglects rebound effects or interdependencies between markets (effects on intraday-markets or long-run forward markets). Additionally, the approximation assumes an equal forward premium reduction effect for each hour, which is on average true but could be higher or lower in certain situations.

3.5 Conclusion

Weather-dependent wind and solar production are facing an increasing share in electricity systems. This increasing share induces higher production uncertainty due to volatile characteristics by wind and solar production. This essay contributes to closing the research gap how wind and solar production uncertainty affects forward price premiums. First, theoretical evidence of an increasing forward price effect by increased uncertainty is identified. The theoretical findings show an increase in forward prices dependent on the merit order convexity and the production's standard deviation. In a second step, the theoretical findings are connected to weather type definitions and supported by empirical evidence for the German day-ahead and intraday market. The weather types have relevant impact to the forward premium levels. Additionally, the production uncertainty per weather type has an increasing effect on the forward premiums. Thus, this research contributes to understand short-term forward price premiums within electricity markets. As to the best of my knowledge, this is the first work on weather-dependent price premiums. Results support that weather types are a suitable measure for wind and solar production uncertainty. Thus, weather types should be incorporated in price forecasting methods to increase quality. An improved wind and solar forecast quality by 1%-point could additionally result in welfare gains of approximately EUR 88 million for Germany. Therefore, emphasize should be put on further weather forecast quality improvements.

3.6 Appendix

3.6.1 On the order of the German electricity supply curve

Bessembinder and Lemmon (2002) performs his theoretical analysis with different orders of the supply curve. Note that the order reflects the highest exponent and that the supply curve is synonym with the merit order. Note additionally, that the supply curve is the first derivative of the total production costs function. Dependent on the supply curve order, the influence of the mean and skewness of the price distributions might have different effects. For instance, for higher orders (i.e. >2) of the supply curve, the forward price premium might become negative with very high standard deviations. In contrast, for linear or quadratic supply curves, the forward premium is always positive. Within the empirical evaluation, Bessembinder and Lemmon (2002) estimates the order of the supply curve via

$$Price_t = a\,(Demand_t)^{\tilde{c}} \tag{3.9}$$

$$\Leftrightarrow \qquad ln(Price_t) = a + \tilde{c}\ln(Demand_t) + \varepsilon_t, \tag{3.10}$$

where $Price_t$, is the daily average on-peak spot price, $Demand_t$ is the daily average load and a and $\tilde{c}$ the parameters to be estimated. The analysis is performed with data from PJM and CALPX electricity markets for approximately 1998 to 2000. They find empirical evidence for an average merit order convexity with a coefficient $\tilde{c} = 3.8$ for PJM and $\tilde{c} = 4.81$ for CALPX. This shows a high convexity of the merit order function. Note that Bessembinder and Lemmon (2002) estimates the order c of the Total Costs Function which first derivative reflects the order of the Marginal Cost Function $\tilde{c}$.

The estimated function in this section is similar to Equation (3.10) but with data for the German electricity market on hourly data from July 2015 to December 2016.

The residual demand is applied, which is defined as total demand subtracted by wind and solar production. The estimated value for $\tilde{c}$ is 1.32 and statistical significant at a 1% level with an $Adj.R^2$ of 0.49. Different months suggest a slight deviation of the merit order function. The convexity is highest in January and December with a significant $\tilde{c}$ of 1.45 or 1.6, respectively. This effect can be explained by -in general- higher demand which utilizes power plants in the steeper right sight of the merit order. However, the estimated $\tilde{c}$ suggest a convexity between the linear and quadratic merit order function for the German electricity market for 2015 and 2016. This supports the assumption that the theoretical investigation in Section 3.3 is limited to the quadratic merit order function.

However, situations might occur which have higher merit order convexities, e.g. under high residual load and scarcity situations. The identification and analysis of these situations remain to further research.

3.6.2 Proof of Proposition 3.1

Proof. Assume the model definition as to Section 3.3. Assume that the expected production μ is smaller than the total demand.[6] Because all renewable producers are symmetric, the total traded renewable production of all players in stage 1 can be denoted by $q_{r1} := q_{ir1} + (N-1)q_{jr1}$ (where q_{jr1} is another symmetric renewable producer). Additionally, denote the realized production in stage 2 by $Q := NQ_i$, the expected quantity by $\mu := N\mu_{iq}$ and the standard deviation by $\sigma := N\sigma_i$.

The basic profit function of a renewable producer i in the present theoretical model framework is described in Equation (3.1). The following expected profit function is

[6] If $\mu > D$, then the total demand can be fulfilled by renewable production such that prices close to zero or below are expected and renewable production curtailment could occur.

derived by plugging in the above formulas:

$$
\begin{aligned}
\mathbb{E}[\Pi_{ir}(q_{ir1},(N-1)q_{jr1})] = & -D^2 a q_{ir1} \int f(Q_i)\,dQ_i + D^2 a \int Q_i f(Q_i)\,dQ_i \\
& + 2DNa q_{ir1} \int Q_i f(Q_i)\,dQ_i - 2DNa \int Q_i^2 f(Q_i)\,dQ_i \\
& - Db q_{ir1} \int f(Q_i)\,dQ_i + Db \int Q_i f(Q_i)\,dQ_i \\
& - N^2 a q_{ir1} \int Q_i^2 f(Q_i)\,dQ_i + N^2 a \int Q_i^3 f(Q_i)\,dQ_i \\
& + Nb q_{ir1} \int Q_i f(Q_i)\,dQ_i - Nb \int Q_i^2 f(Q_i)\,dQ_i \\
& - c q_{ir1} \int f(Q_i)\,dQ_i + c \int Q_i f(Q_i)\,dQ_i + q_{ir1} \Big(a \big(D \\
& - q_{ir1} - q_{jr1}(N-1) \big)^2 + b \big(D - q_{ir1} - q_{jr1}(N-1) \big) + c \Big).
\end{aligned}
\tag{3.11}
$$

The first derivative with respect to q_{ir1} is

$$
\begin{aligned}
\frac{\mathrm{d}}{\mathrm{d}q_{ir1}} \mathbb{E}[\Pi_{ir}(q_{ir1},(N-1)q_{jr1})] = & -D^2 a \int f(Q_i)\,dQ_i + 2DNa \int Q_i f(Q_i)\,dQ_i \\
& - Db \int f(Q_i)\,dQ_i - N^2 a \int Q_i^2 f(Q_i)\,dQ_i \\
& + Nb \int Q_i f(Q_i)\,dQ_i + a \big(D - q_{ir1} - q_{jr1}(N - \\
& 1) \big)^2 + b \big(D - q_{ir1} \\
& - q_{jr1}(N-1) \big) - c \int f(Q_i)\,dQ_i + c + q_{ir1} \big(a \\
& \big(-2D + 2q_{ir1} + 2q_{jr1}(N-1) \big) - b \big).
\end{aligned}
\tag{3.12}
$$

This can be simplified by the following substitutes for the probability density function

$f(Q)$:

$$\text{Distribution function has a total probability of 1:} \quad \int f(Q_i)\,dQ_i = 1 \tag{3.13}$$

$$\text{Expected value for } Q_i\text{:} \quad \int Q_i f(Q_i)\,dQ_i = \mu_i \tag{3.14}$$

$$\text{The second moment (re-ordered):} \quad \int Q_i^2 f(Q_i)\,dQ_i = \mu_i^2 + \sigma_i^2 \tag{3.15}$$

This leads to the simplified necessary condition for the profit maximizing quantity q_{ir1}^* as

$$\begin{aligned}\frac{d}{dq_{ir1}}\mathbb{E}[\Pi_{ir}(q_{ir1},(N-1)q_{jr1})] = &-D^2a+2DNa\mu_i-Db-N^2a\left(\mu_i^2+\sigma_i^2\right)+Nb\mu_i+a\Big(D\\ &-q_{ir1}-q_{jr1}(N-1)\Big)^2+b\left(D-q_{ir1}-q_{jr1}(N-\right.\\ &\left.1)\right)+q_{ir1}\left(a\left(-2D+2q_{ir1}+2q_{jr1}(N-1)\right)-b\right)\\ &\overset{!}{=}0.\end{aligned} \tag{3.16}$$

Now this equation can be solved for q_{ir1} which results in the profit maximizing quantity

$$\begin{aligned}q_{ir1}^* = \frac{1}{3a}\Big(&2Da-2Naq_{jr1}+2aq_{jr1}+b+\Big[4D^2a^2\\ &-6DNa^2\mu_i-2DNa^2q_{jr1}+2Da^2q_{jr1}+4Dab+3N^2a^2\mu_i^2+N^2a^2q_{jr1}^2+\\ &3N^2a^2\sigma_i^2-2Na^2q_{jr1}^2-3Nab\mu_i-Nabq_{jr1}+a^2q_{jr1}^2+abq_{jr1}+b^2\Big]^{1/2}\Big)\end{aligned} \tag{3.17}$$

for producers $i=1,...,N$. Note the square root for the square brackets. The second derivative becomes zero if and only if $q_{ir1} = \frac{1}{2N+1}(2D+\frac{b}{a})$ which can only be the case for $q_{ir1}=0$ for perfect competition (whereas the case of perfect competition is the investigation focus).

In an equilibrium of identical players, the solutions q_{ir1} are identical as well. Thus,

$q_{ir1} = q_{jr1}$ holds and can be replaced. Following is derived:

$$q_{ir1} = \frac{1}{3a}\Big(2Da - 2Naq_{ir1} + 2aq_{ir1} + b \pm \big[4D^2a^2 \\ - 6DNa^2\mu_i - 2DNa^2q_{ir1} + 2Da^2q_{ir1} + 4Dab + 3N^2a^2\mu_i^2 + N^2a^2q_{ir1}^2 + \\ 3N^2a^2\sigma_i^2 - 2Na^2q_{ir1}^2 - 3Nab\mu_i - Nabq_{ir1} + a^2q_{ir1}^2 + abq_{ir1} + b^2\big]^{1/2}\Big) \tag{3.18}$$

This can be solved with respect to q_{ir1} which gives

$$q_{ir1}^* = \frac{1}{2Na(N+2)}\Big((N+1)(2Da+b) + \big[4D^2N^2a^2 + 8D^2Na^2 + 4D^2a^2 - 8DN^3a^2\mu_i \\ - 16DN^2a^2\mu_i + 4DN^2ab + 8DNab + 4Dab + 4N^4a^2\mu_i^2 + 4N^4a^2\sigma_i^2 \\ + 8N^3a^2\mu_i^2 + 8N^3a^2\sigma_i^2 - 4N^3ab\mu_i - 8N^2ab\mu_i + N^2b^2 + 2Nb^2 + b^2\big]^{1/2}\Big) \tag{3.19}$$

Note that another possible profit optimal solution exists. This solution would have a negative bid. Thus, it is not in the feasible range of solutions and neglected. Equation (3.18) is the profit maximizing quantity q_{ir1}^* of one symmetric player i in a price-competitive oligopoly.

The optimal joint bid of all renewable producers' becomes

$$\begin{aligned} q_{r1}^* &= \sum_{i=1}^{N} q_{ir1}^* \\ &= Nq_{ir1}^* \\ &= \frac{1}{2a(N+2)}\Big((N+1)(2Da+b) - \big[4D^2N^2a^2 + 8D^2Na^2 + 4D^2a^2 - 8DN^2a^2\mu \\ &\quad + 4DN^2ab - 16DNa^2\mu + 8DNab + 4Dab + 4N^2a^2\mu^2 + 4N^2a^2\sigma^2 - \\ &\quad 4N^2ab\mu + N^2b^2 + 8Na^2\mu^2 + 8Na^2\sigma^2 - 8Nab\mu + 2Nb^2 + b^2\big]^{1/2}\Big), \end{aligned} \tag{3.20}$$

where $\mu = N\mu_i$ and $\sigma = N\sigma_i$ since all renewable producers are assumed to be symmetric.

The focus lies on the solution under perfect competition. This is reflected via $N \to \infty$. For $N \to \infty$, Equation (3.20) becomes

$$q_{r1}^* = D + \frac{1}{2}\frac{b}{a} - \sqrt{\left[\left(\left(D + \frac{1}{2}\frac{b}{a}\right) - \mu\right)^2 + \sigma^2\right]} \tag{3.21}$$

To derive Equation (3.21) from Equation (3.20), terms with N in the denominator goes to 0 for $N \to \infty$. Additionally, if there are multiple exponents for N in one term, only the highest exponent of N is dominant for $N \to \infty$. Equation (3.21) is the optimal first stage total renewables' bid under uncertainty and the solution of the proposition. $\square$

3.6.3 Statistics on the data

Statistics on the wind, solar, price forecasts

Table 3.7 shows statistics for the price, wind and solar deviation dataset.

Table 3.7: Statistics on the price and wind/solar deviation dataset. Data covers July 2015 to December 2016.

	Mean	Std.dev.	Min	Max
Price forecast deviation [EUR/MWh]	0.5	12.4	-138.8	253.4
Wind forecast error [GWh]	-0.4	1.5	-8.4	11.5
Solar forecast error [GWh]	-0.1	0.9	-5.8	4.7

A structural deviation of the mean value for the wind and solar forecast erros can be observed. A reason for the structural deviations could be the extrapolation methods of the TSOs (cf. 50Hertz (2017), Amprion (2017), Tennet (2017), TransnetBW (2017) and APG (2017)). Additionally, structural forecast overestimation could exist due to reduced efficiency (old PV modules/wind turbines), surface roughness, aerosols and air pollution and similar effects. The standard deviation of wind forecast errors is higher than for solar forecast errors.

Objective Weather Type Classification

Table 3.8 shows characteristics for the forty DWD *Objective Weather Type Classifications*. Each combination of wind speed, cyclonality on 950 hPA, cyclonality on 500 hPa and humidity exists. Additionally, the frequency is shown. Table 3.9 gives statistical numbers for combined wind and solar forecast errors per weather type.

Table 3.8: Objective Weather Type Classification by the German Weather Service (DWD) defined by Bissolli and Dittmann (2001). Frequency counted by daily occurrences from 1979 to 2016.

No.	Wind direction	Cyclonalitity in 950 hPa	Cyclonalitity in 500 hPa	Humidity	Frequency (from 1979 to 2016)
1	no direction	anticyclonic	anticyclonic	dry	751
2	northeast	anticyclonic	anticyclonic	dry	498
3	southeast	anticyclonic	anticyclonic	dry	120
4	southwest	anticyclonic	anticyclonic	dry	640
5	northwest	anticyclonic	anticyclonic	dry	1204
6	no direction	anticyclonic	anticyclonic	wet	401
7	northeast	anticyclonic	anticyclonic	wet	80
8	southeast	anticyclonic	anticyclonic	wet	45
9	southwest	anticyclonic	anticyclonic	wet	1262
10	northwest	anticyclonic	anticyclonic	wet	1058
11	no direction	anticyclonic	cyclonic	dry	331
12	northeast	anticyclonic	cyclonic	dry	351
13	southeast	anticyclonic	cyclonic	dry	48
14	southwest	anticyclonic	cyclonic	dry	582
15	northwest	anticyclonic	cyclonic	dry	1241
16	no direction	anticyclonic	cyclonic	wet	103
17	northeast	anticyclonic	cyclonic	wet	20
18	southeast	anticyclonic	cyclonic	wet	9
19	southwest	anticyclonic	cyclonic	wet	439
20	northwest	anticyclonic	cyclonic	wet	178
21	no direction	cyclonic	anticyclonic	dry	148
22	northeast	cyclonic	anticyclonic	dry	16
23	southeast	cyclonic	anticyclonic	dry	128
24	southwest	cyclonic	anticyclonic	dry	159
25	northwest	cyclonic	anticyclonic	dry	32
26	no direction	cyclonic	anticyclonic	wet	223
27	northeast	cyclonic	anticyclonic	wet	9
28	southeast	cyclonic	anticyclonic	wet	207
29	southwest	cyclonic	anticyclonic	wet	975
30	northwest	cyclonic	anticyclonic	wet	109
31	no direction	cyclonic	cyclonic	dry	372
32	northeast	cyclonic	cyclonic	dry	55
33	southeast	cyclonic	cyclonic	dry	111
34	southwest	cyclonic	cyclonic	dry	276
35	northwest	cyclonic	cyclonic	dry	304
36	no direction	cyclonic	cyclonic	wet	251
37	northeast	cyclonic	cyclonic	wet	22
38	southeast	cyclonic	cyclonic	wet	143
39	southwest	cyclonic	cyclonic	wet	745
40	northwest	cyclonic	cyclonic	wet	173

Table 3.9: Statistics on the (combined) wind & solar forecast errors for the objective weather type classifications. Observations cover July 2015 to December 2016 in hourly resolution. Units are in GWh (except for count). *std* denotes the standard deviation which is incorporated as the uncertainty measure for the empirical analysis. The standard deviations deviate between 0.66 and 3.35.

Weather type	count	mean	std	min	25%	50%	75%	max	RMSE	MAE
1	623	-0.09	1.21	-6.48	-0.68	0.01	0.58	3.45	1.22	0.88
2	264	0.09	0.96	-5.25	-0.39	0.05	0.65	2.13	0.96	0.69
3	96	0.00	1.13	-3.06	-0.84	0.24	0.74	1.92	1.12	0.90
4	648	-0.83	1.59	-4.57	-1.94	-0.63	0.08	10.62	1.79	1.31
5	1248	-0.74	1.31	-6.70	-1.41	-0.57	0.04	7.97	1.50	1.09
6	480	-0.16	1.46	-6.16	-0.88	-0.20	0.45	5.96	1.47	1.00
9	1176	-0.18	1.62	-7.00	-0.91	-0.05	0.61	9.96	1.62	1.12
10	1296	-0.61	1.94	-8.43	-1.44	-0.43	0.42	11.13	2.03	1.40
11	336	-0.13	1.12	-3.38	-0.82	-0.24	0.54	3.38	1.13	0.88
12	360	-0.22	1.07	-4.31	-0.81	-0.15	0.37	3.19	1.09	0.81
14	576	-0.52	1.66	-7.09	-1.26	-0.20	0.45	3.73	1.74	1.19
15	1008	-0.81	1.79	-7.82	-1.71	-0.74	0.15	6.54	1.97	1.47
16	24	0.33	0.66	-0.66	-0.40	0.67	0.89	1.21	0.73	0.67
17	24	-1.19	1.06	-2.68	-1.93	-1.28	-0.36	0.81	1.58	1.35
19	336	-1.02	1.33	-5.91	-1.70	-0.91	-0.16	2.35	1.67	1.30
20	216	-1.42	2.09	-6.79	-2.58	-0.60	0.12	1.94	2.52	1.71
21	120	-0.92	2.08	-6.48	-1.63	-0.45	0.66	1.87	2.27	1.61
23	144	-0.47	1.89	-4.80	-1.49	-0.60	0.93	3.99	1.94	1.56
24	168	0.15	1.19	-2.39	-0.72	-0.02	0.78	3.68	1.20	0.93
25	48	-1.67	1.53	-5.30	-2.74	-1.87	-0.18	0.41	2.25	1.76
26	168	-0.77	1.74	-4.94	-1.61	-0.45	0.42	3.10	1.89	1.39
27	24	0.04	1.36	-1.86	-1.01	-0.25	0.81	2.80	1.33	1.08
28	168	-0.30	1.27	-3.55	-1.14	-0.31	0.63	2.87	1.31	1.06
29	960	-0.49	1.70	-5.81	-1.52	-0.42	0.47	5.18	1.77	1.35
30	48	-1.04	1.56	-7.23	-1.85	-1.12	0.08	1.41	1.86	1.38
31	528	-0.65	1.52	-6.52	-1.48	-0.38	0.32	4.13	1.65	1.20
32	72	-0.06	1.17	-1.65	-0.77	-0.32	0.29	3.48	1.17	0.85
33	96	-0.19	1.62	-4.67	-0.86	0.04	0.72	2.69	1.63	1.17
34	312	-0.34	1.67	-4.81	-1.19	-0.21	0.82	3.58	1.70	1.30
35	144	0.42	3.35	-4.93	-1.21	-0.09	0.50	11.55	3.36	2.13
36	312	-1.68	1.74	-7.37	-2.34	-1.11	-0.53	1.51	2.41	1.73
37	48	-0.44	0.72	-1.98	-0.80	-0.36	0.08	0.93	0.84	0.65
38	120	-0.74	1.42	-3.93	-1.62	-0.77	-0.02	3.26	1.60	1.27
39	912	-0.33	1.84	-6.16	-1.28	-0.33	0.59	9.28	1.87	1.35
40	96	-0.87	2.01	-4.29	-2.33	-0.82	0.34	4.75	2.18	1.75
Total Data	13199	-0.52	1.67	-8.43	-1.33	-0.37	0.38	11.55	1.75	1.24

3.6.4 The wind and solar production level gives insufficient information on forecast errors

Figure 3.7 addresses the question whether the wind and solar production level would be a suitable classification for forecast errors. One would expect that higher renewable production results in higher renewable forecast errors. The both upper plots of Figure 3.7 show the forecast errors per hourly observation. The observations do not indicate a sufficient heteroscedastic behavior. That means, the forecast errors are not sufficiently increasing with the production level. The lower plots show the standard deviations per production level aggregated to 1 GWh clusters. It is obvious, that in a broad range of the production levels, the standard deviations have only minor gradients. The small gradients mean, that these observations have only slight differences to the surrounding classes and thus limited distinction possibility. Thus, the level of wind or solar production can be expected as no adequate estimator for forecast errors. Note that a longer dataset time period would smooth the error but incorporates a bias effect due to different capacity levels. Lange and Heinemann (2002) report a similar finding that the production level has only limited distinction possibility.

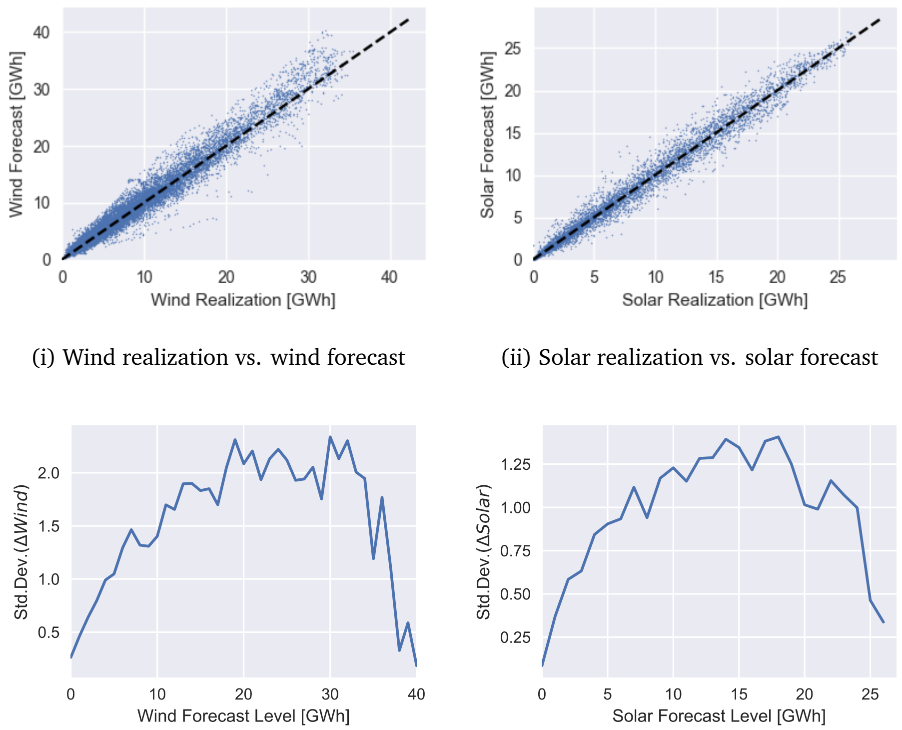

(i) Wind realization vs. wind forecast

(ii) Solar realization vs. solar forecast

(iii) Standard deviation of wind production clustered as to wind forecast level (1 GWh each)

(iv) Standard deviation of solar production clustered as to solar forecast level (1 GWh each)

Figure 3.7: Forecast errors for wind and solar dependent on forecast levels. The black dotted lines in the upper plots displays the diagonal line. Data covers July 2015 to December 2016.

3.6.5 Effect coding results for cyclonality at 500 hPa

Table 3.10 reports the results of the effect coding with respect to cyclonality on 500 hPa. The effect coding estimates the deviation in the group means to the grand means. The groups are cyclonic and anticyclonic weather patterns at 500 hPa. The estimates are not significant which means, that they do not significantly deviate from the overall mean forward premium.

Table 3.10: Results of the effects coding approach for the weather types' criteria *cyclonality on 500 hPa* for the model $ForwardPremium_h = Intercept + \sum_i \beta_i Cyclonality500hPa_{i,h} + \epsilon_h$. The estimated values indicate the difference of the criterias' mean value to the grand mean. Number of observations is 13040 hourly values from July 2015 to December 2016. Significance levels denoted by * p<.1, ** p<.05, ***p<.01. Significance and estimations of the grand mean indicates the difference to a zero mean value. Note that five weather classes are omitted due to too less observations in the investigated time horizon.

Cyclonality on 500 hPa	Difference to grand mean
Grand mean	-0.140***
Anticyclonic	-0.057
Cyclonic	0.078

3.6.6 Wind and solar uncertainty translates to price uncertainty

General price decreasing effect of positive production deviations

Several studies analyze the effect of an increase in renewable production on the day-ahead to intraday price differences. In general, more renewable production than forecasted would decrease the realized prices (compared to the price forecast). This is in line with the expectation (cf. Hirth (2013)). A similar trend can be observed within this dataset. It is not the focus of this research, but the dataset used shows a typical decreasing trend. The trend can be observed in Figure 3.8.

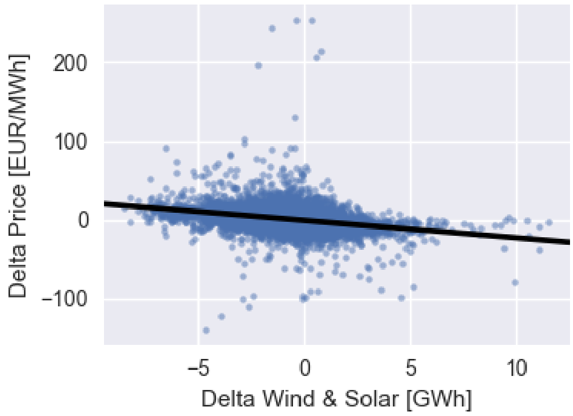

Figure 3.8: Price effect of an increase in renewable production compared to forecasts (delta = realization - forecast). Price realizations are the volume weighted prices of the last three hours (ID3-prices). Observations cover July 2015 to December 2016.

An increase in wind and solar production delta (*realization minus forecast*) tend to an decrease in price delta (*intraday minus day-ahead*). A linear regression shows a price decrease of 2.22 EUR/MWh per additional GWh wind or solar production in the intraday-market. Former years (back to 2010) have higher price reduction effects than latter years. This trend can be explained by adjustment processes, learning and saturation effects.

However, in this simple linear OLS regression, several drivers are not considered. For instance, one relevant factor is the shape of the merit order, which covers e.g. information about the actual power plant fleet and outages. Another relevant factor is the residual demand level, which determines the intersection on the merit order shape and serves e.g. as an indicator for scarcity situations. Thus, the fit of the linear regression is strongly limited and has an Adj. R-squared value of 0.09.

Weather type production volatility implies forward price volatility

In this supplementary section, the hypothesis is stated that an increased production uncertainty leads to an increase in the price uncertainty. The price uncertainty is the standard deviation of the forward premiums within each weather type. The uncertainty of wind production, solar production and load is defined analogous. Note that wind and solar production are capacity-normalized to account for capacity extension over the time horizon.

Figure 3.9 compares the standard deviations of the capacity-normalized wind and solar deltas (wind and solar uncertainty) to the standard deviations of the forward premiums (price uncertainty); categorized as to the weather types.

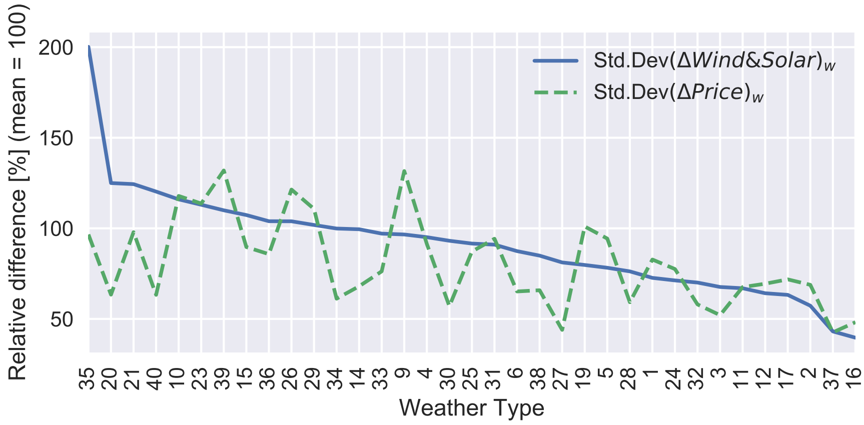

Figure 3.9: Relative standard deviations of capacity-normalized wind and solar deviations as well as price deviations per weather type w. Descending sorted w.r.t. weather types' standard deviation of wind and solar deviation. Data is additionally normalized to the sample mean. Observations cover July 2015 to December 2016. The Forward premium is calculated as the delta between the day-ahead price and the volume weighted intraday price of the last three hours (ID3).

Both standard deviations have a Pearson correlation factor of 0.48, which indicates a medium correlation. Since the wind and solar uncertainty should be independent of the price forecasts, the relationship can be interpreted as a causality. Thus, it indicates that a reduction in weather uncertainty leads in general to a certain reduction in price uncertainty.

To examine the impact of load, wind and solar uncertainty on the the forward premium uncertainty, two regression estimations are performed. In *Model C1*, the standard deviations of the forward premiums are explained by the standard deviations of the load deviation and the standard deviation of the combined wind and solar deviations (per weather type). *Model C1* can be expressed as Equation (3.22). In *Model C2* the standard deviations of the forward premiums are explained by the separated standard deviations of the (capacity-normalized) wind and the solar deltas as denoted in Equation (3.23):

$$\text{Model C1:} \quad Std.Dev(FP)_w = \alpha + \beta_1 Std.Dev(\Delta Load)_w + \beta_2 Std.Dev(\Delta Wind\&Solar)_w + \epsilon_w \tag{3.22}$$

$$\text{Model C2:} \quad Std.Dev(FP)_w = \alpha + \beta_1 Std.Dev(\Delta Wind)_w + \beta_2 Std.Dev(\Delta Solar)_w + \epsilon_w \tag{3.23}$$

where w states the weather type. Due to low observations (limited amount of weather types), the number of regressors need to be restricted. Thus, in Model A1, the general effect of load and volatile renewable production (i.e. combined wind and solar) are estimated. Whereas Model A2 disentangles the effect within wind and solar production and neglects load.

Table 3.11 shows the regression results of the Weighted Least Squares estimation. The estimation weights are the corresponding number of observation per weather type. Note that not every weather type is represented due to occurrence in the estimated time range.

Table 3.11: Weighted Least Squares estimation. Hourly data is aggregated to weather types. Weights are the number of observations per weather type. Note that not every weather type is represented due to occurrence in the estimated time range. Standard errors in parentheses. * p<.1, ** p<.05, ***p<.01

Std.Dev$(FP)_w$	Model C1	Model C2
Intercept	2.190**	3.043***
	(0.873)	(1.033)
$\Delta Load_h$	0.749**	
	(0.301)	
$\Delta Wind\&Solar_h$	1.132***	
	(0.343)	
$\Delta Wind_h$		0.556***
		(0.167)
$\Delta Solar_h$		0.468
		(0.413)
N	32	32
Adj. R^2	0.357	0.247

The estimation of Model C1 shows significant coefficients for both regressors.

However, the coefficient of the standard deviation for wind and solar deviations is significant at a 1% level whereas the standard deviation of the load deviations has a broader significance level of 5%. The lowered significance level is somehow expected, since the classification is based on weather data which has limited influence on load data. The coefficient for the standard deviation of the capacity-normalized wind and solar deviations is 1.1%; the coefficient for the standard deviation of load is 0.75 GWh. Among the wind and solar deviations, the wind deviations have a significant effect whereas the solar deviations have not. This becomes obvious by the results of Model C2. Overall, the stronger the deviations with respect to wind and solar or load, the stronger fluctuates the forward premium, i.e. the day-ahead to intraday price delta. The hypothesis of an increased price volatility by increased production volatility can thus be confirmed.

3.6.7 Requirement checks for the regression analysis

No relevant correlation of regression variables

Figure 3.10 shows the correlation matrix within a heatmap. No relevant high correlation occurs. The relevant correlation values between the regressors are in the range between −0.06 and 0.11. Higher correlation could occur between variables which are not simultaneously used in the same regression (e.g. a correlation of 0.86 between wind deltas as well as wind and solar deltas). The dependent variable *forward premiums* could have higher correlation to the regressors which is not critical (e.g. 0.43 to wind and solar deltas).

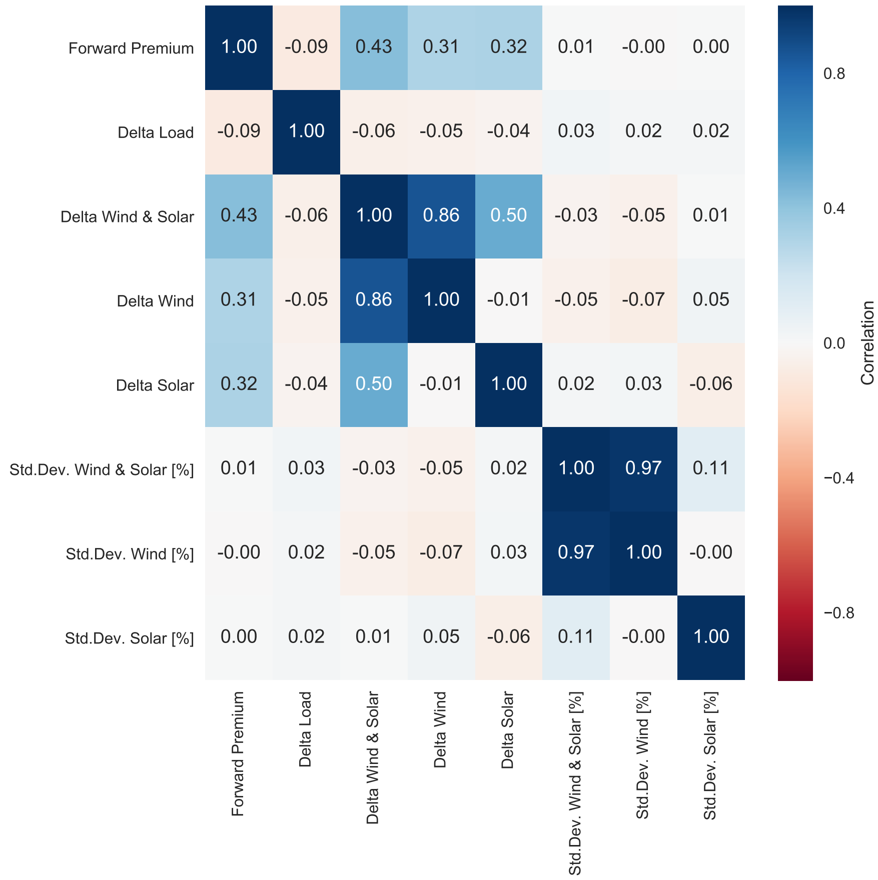

Figure 3.10: Pearson correlation of the regression variables. Data covers July 2015 to December 2016.

Time series data is stationary

Table 3.12 shows the statistics of the Augmented Dickey Fuller test. The null hypothesis of non-stationarity can be rejected. Thus, the data have no statistical significant time-dependent structure like a trend or seasonal effect. The time series OLS prerequisite of stationarity is fulfilled.

Table 3.12: Test statistics for the Augmented Dickey Fuller test for unit roots (cf. Dickey and Fuller (1979)). The null hypothesis of a unit root in the respective period of observation is rejected. The test uses the Akaike Information Criterion (AIC) in order to determine the optimal lag lengths. Additional to the standard Augmented Dickey Fuller test which controls for a constant effect, the Augmented Dickey Fuller test is performed with a linear trend as well as with a linear and quadratic trend (trend and drift). Both additional tests indicate the same result, i.e. to reject the non-stationarity hypothesis at a 1% significance threshold. The *model residuals* refer to the estimation results for Equation (3.8).

	Test Statistic	p-value	# lags
$\Delta Prices$	-22.96	0.00	14
$\Delta Load$	-13.71	0.00	37
$\Delta Wind$	-10.02	0.00	41
$\Delta Solar$	-12.84	0.00	27
$\Delta Wind\&Solar$	-10.50	0.00	41
StdDev($\Delta Wind$)	-11.82	0.00	24
StdDev($\Delta Solar$)	-12.22	0.00	24
Model residuals	-18.88	0.00	17

4 Tender Frequency and Market Concentration in Balancing Power Markets

Balancing power markets ensure the short-term balance of supply and demand in electricity markets and their importance may increase with a higher share of fluctuating renewable electricity production. While it is clear that shorter tender frequencies, e.g. daily or hourly, are able to increase the efficiency compared to a weekly procurement, it remains unclear in which respect market concentration will be affected. Against this background, we develop a numerical electricity market model for Germany to quantify the possible effects of shorter tender frequencies on costs and market concentration. We find that shorter time spans of procurement are able to lower the costs by up to 15%. While market concentration decreases in many markets, we – surprisingly – identify cases in which shorter time spans lead to higher concentration.

4.1 Introduction

In electricity markets supply and demand need to be equal at all times and commonly transmission system operators (TSOs) are in charge of balancing supply and demand. Due to unbundling policies TSOs are not allowed to own generation assets and need to procure short-term flexibility from operators of power plants. These power plants need to be able to adjust their production on short notice to balance supply and demand. In Germany, balancing power (which is one kind of ancillary services) is currently procured on a weekly basis for the fastest two load balancing services of primary and secondary balancing power.[1] Operators that offer for example positive balancing power therefore need to withhold production capacities over the time span of a whole week and cannot sell their full capacity into the spot market. The costs that arise from balancing power provision are thus based on the opportunity costs with respect to selling the capacity in the spot market, namely the foregone profits from spot market operation.

[1]The ancillary services primary and secondary balancing power are also known as Frequency Control Reserve (FCR) and automated Frequency Restoration Reserve (aFRR), respectively.

In this paper, we take a closer look at the German balancing power markets with a special focus on two problems that may arise from the current (weekly) market design. First, the weekly procurement leads to inefficiencies as operators need to withhold capacities for a whole week and cannot fully participate in the hourly spot market. There is a missing market for hourly balancing power products that could be solved by an hourly procurement of balancing power. Secondly, we observe that large players with a broad portfolio of power plants are able to provide balancing power at lower costs, especially in a weekly auction. These economies of scale for large players may lead to highly concentrated markets and the possible abuse of market power.

Whereas in theory it is well understood that shorter time spans lower costs and might change market concentration, the magnitude of a change in market design towards shorter time spans remains unclear. In order to assess the possible impact, we develop a numerical model that accounts for the operator structure in the balancing power market and considers different time spans for balancing power procurement. Based on the model we are able to quantify the effects of different market designs (weekly, daily, hourly) on system costs and market concentration.

The modeling of balancing power markets is complex, as it is driven by the opportunity costs of operators. Just and Weber (2008) started to write down this problem analytically and solved the simplified model numerically. Later the methodology was again applied by Just (2011) to analyze the implications of different tender frequency on the procurement costs but without considering the operator structure. Richter (2012) bases his analysis on the model developed by Just and Weber (2008) and is able to show the existence of a competitive simultaneous equilibrium in spot and balancing power markets that is unique and efficient. He finds out that the bids of the capacity providers form a u-shaped bidding function around the spot demand. This work shows that the integrated modeling of spot and balancing power markets in a fundamental model as it is done in the analysis at hand yields meaningful results. In addition, the equilibrium of the spot and balancing power market was further analyzed by Müsgens et al. (2014) in the context of the German market design. They present an analytical expression of the balancing opportunity costs as well, which is used in our latter analysis. The procurement of balancing power is commonly organized via auctions. A special characteristic of the balancing power procurement process is that the cost structure of participants can be divided into two parts. One part is fixed for a period and stems from withholding capacity for balancing purposes. The second part are variable costs for the supply of energy in the case of being called during operation. Bushnell and Oren (1994) were the first to analyze the auction design of balancing power markets. Their work was later extended by Chao and Wilson (2002) in order to design incentive compatible scoring and settlement rules. They found that incentive compatible auctions can be designed by considering only the capacity bid for scoring in a uniform price auction. Nevertheless many of the implemented auction designs in Europe differ from their proposals.

The auction design of balancing markets was also studied by Müsgens et al., who analyzed the importance of timing and feedback (Müsgens and Ockenfels, 2011, Müsgens et al., 2012). The development in the tertiary reserve market and the change in rules was analyzed by Haucap et al. (2012). They find that the cooperation of the four TSOs in Germany decreased costs for the procurement of tertiary reserve.

Whereas previous literature focuses on the efficient design, high market concentrations are an additional issue in balancing power markets with few big operators. In 2010, Growitsch et al. (2010) analyzed the operator structure in the tertiary balancing power market. They find high market concentration in certain situations of the tertiary balancing power market. Heim and Götz (2013) looked at the market outcomes in the German secondary reserve market based on exclusive data provided by the BNetzA and find that the price increase in 2010 can be traced back to the bidding behavior of the two largest firms.

While the general effects of a design change towards shorter spans is well understood, the empirical importance is less clear. To contribute to filling this gap, we simulate one design change for the German balancing market. We compare simulation results for the current market design to simulation results for shorter time spans. Besides the changed provision duration, all other assumptions are held constant to focus solely on the effect of a shortened provision duration. From the comparison of the results, we derive a difference of 15% balancing cost in favor of shorter time spans. With respect to concentration, our model results indicate that an hourly market design for balancing power leads to certain periods with higher market concentration. This means that in some hours market concentration could increase by a change of market design from weekly to hourly and policy makers should be aware of this. The regulatory implication of this finding is a trade-off between a moderate level of market power over a weekly provision or a potentially high market power in certain periods of shorter provision durations. To the best of our knowledge, there are no sufficient regulatory mechanisms to mitigate market concentration or market power in occasional situations with high mark-ups. A potential price-sensitive demand function might decrease market power but with the drawback of a reduced security of supply (which would need to consider the value of lost load as well as statistical probabilities). These designs are not considered in the current European balancing market harmonization approach (cf. European Commission (2017)). Whereas the analysis at hand is limited to market concentration, it is left for further research to determine the mark-ups that can be realized in concentrated situations and to establish a regulatory mechanism that is able to mitigate this potential market power.

The paper is organized as follows: In Section 4.2 we focus on the background information which include, among others, the general electricity market structure, bidding behavior for balancing power and the concepts of market concentration indices. Section 4.3 introduces the methodology, namely a unit-commitment model for electricity markets and the model specifications to account for the balancing power markets. Section 4.4 presents the modeling results as to the system costs and the market concentration indices. Section 4.5 concludes.

4.2 Background

4.2.1 On the Functioning of the Balancing Power Market

The balancing power market is an additional market for electricity generators, besides the classic spot markets like the day-ahead and intraday market. In the balancing power market, system operators procure spare production capacity that is called upon in case of imbalances. It is usually divided into products depending on the urgency and the direction of power provision. In Germany, the markets are divided into primary, secondary and tertiary balancing power provision which differ mainly in reaction time. In the primary balancing power market, power plants need to be able to adjust their output in both directions (upward and downward). Secondary and tertiary balancing power markets are divided into products for positive and negative balancing power. The secondary balancing power market is further divided into a peak and off-peak product. Additional information on the current German market design can also be found in Hirth and Ziegenhagen (2015).

An ongoing harmonization process of European energy and balancing markets leads to similar designs for instance in the International Grid Control Cooperation

(IGCC).[2] Typical design characteristics are an inelastic demand as well as a day-ahead or week-ahead procurement of balancing power. An up to date comparison of European balancing markets is given in Ocker et al. (2016). The European Commission gives suggestions on an EU-wide balancing market, which aims at a harmonization of regulations as it is done already within the IGCC (European Commission, 2017). In contrast to the European *day-ahead* or *week-ahead* balancing markets, *real-time* balancing markets are implemented for instance by the regional transmission operators of PJM, MISO (formerly Midwest ISO) and ISO New England in the US (Vlachos and Biskas (2013), PJM (2017), MISO (2016), ISO New England (2011)). Here, the balancing amount and corresponding prices are calculated in real-time, e.g. 5 minutes before delivery. In the subsequent paper, we focus on the implications of shorter tender frequencies in the German balancing power market for two reasons. First, the German market is the largest balancing market within Europe with similar characteristics as in other European countries. Second, shortening of the week-ahead provision duration to an hourly provision duration could be considered as a reasonable step towards real-time balancing markets. Depending on the market design, this could have impacts on efficiency and market concentration. However, the scope of the paper is not to find an optimal market design for balancing markets (i.e. with consideration of the value of lost load and optimal demand response), but to isolate the possible economic effects of a regulatory change by a shortened provision duration.[3]

Because the balancing of imbalances has to occur in very short time periods before physical delivery, providers of balancing power have to reserve capacity for balancing purposes. This means for example that an operator for positive balancing power cannot sell all her production capacity into the spot market and needs to operate power plants below the maximum capacity level. When being called for the supply of balancing power, the power plant needs to increase its output. For the case of negative balancing power provision, operators need to run their plants above their minimum production capacity and when negative balancing power is called, these plants have to be able to decrease their electricity production.

The cost structure of participants in the balancing power market is thus different compared to the spot market. The marginal costs of generation and the opportunity costs for balancing power provision are exemplary shown for positive balancing

[2] IGCC aims for an increased cooperation of balancing power procurement and utilization. Participating countries in 2017 are AT, BE, CH, CZ, DE, DK, FR, NL.

[3] For analyses of the optimal design of balancing market see for instance Chao and Wilson (2002) or Vandezande et al. (2010).

power in Figure 4.1. If no balancing power is procured it would be optimal that all power plants sell their full generation capacity in the spot market based on their marginal generation costs (blue dashed curve) until demand is satisfied. In the case that positive balancing power is procured, power plants need to withhold production capacity from the spot market for being able to satisfy the demand for balancing capacity. Since power plants need to operate at a minimum production level and can only offer a fraction of their generation for balancing purposes, some power plants could face a trade-off between not running and running at minimum production to offer balancing power. Two different types of opportunity costs are therefore possible, which can either be inframarginal or extramarginal. Based on Müsgens et al. (2014), they can be expressed for positive balancing power as

$$CapacityCosts_{reserve} = \begin{cases} (VC - price_{DA}) & \text{, if } VC \leq price_{DA} \\ (VC - price_{DA})\frac{Cap_{min}}{Cap_{reserve}} & \text{, if } VC > price_{DA}. \end{cases} \tag{4.1}$$

Here, VC are the variable costs of generation, $Cap_{reserve}$ and Cap_{min} are the reserve capacity provision and the minimal load capacity, respectively. Inframarginal power plants have generation costs lower than the spot price and would be running in the spot market also without the existence of a balancing power market. The opportunity costs therefore just result in the difference between the spot price and their variable costs. Extramarginal power plants have generation costs higher than the spot price, but are nevertheless selling their electricity in the spot market if the loss is compensated by a high balancing price.

For example, a power plant that has marginal generation costs a bit lower than the spot market price, has very low opportunity costs for positive balancing power provision (red dash-dotted curve). If this power plant decreases its spot market production in order to offer positive balancing power, the income from the spot market is only slightly lowered. The opportunity costs for the provision of positive balancing power are thus close to zero, as can be seen for power plants close to the spot market demand of 60 GW in Figure 4.1. In contrast to this, if the power plant has very low marginal costs of production compared to the spot price, the opportunity costs for positive balancing power provision are very high, as the forgone spot market profits are very high. Opportunity costs are even higher for extramarginal power plants with high variable costs that would incur a large loss when selling electricity in the spot market.

The spot demand of electricity depends mainly on the time of consumption and

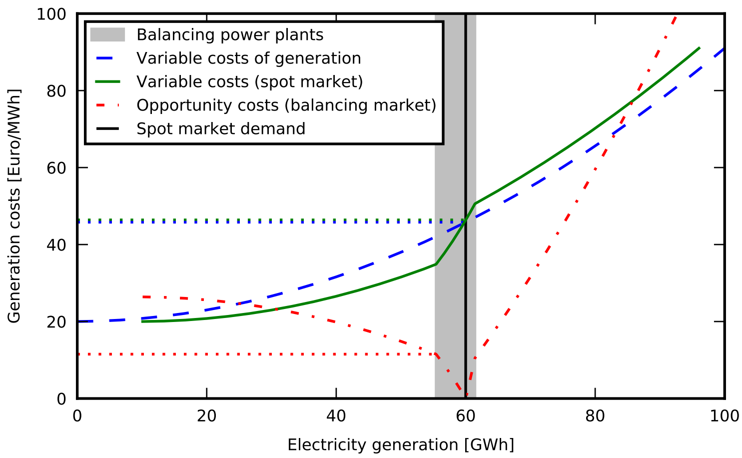

Figure 4.1: Capacity bidding behavior for balancing power markets is theoretically based on an opportunity cost strategy to the spot market (here: positive balancing power)

fluctuates throughout the day. Therefore prices fluctuate as well. This means opportunity costs of single power plants are constantly changing and providers of balancing power need to take this into account. For the case of operators owning multiple power plants with a well-diversified portfolio this effect is not as severe because in the best case they are always operating a power plant with marginal costs close to the spot price that has very low opportunity costs. This makes it obvious that bigger power plant portfolios may have significant cost advantages compared to small players.

In order to illustrate the effect of the portfolio on the opportunity costs, we consider the following example which is visualized schematically in Figure 4.2: Let us assume that there are three power plants A, B, and C with the same capacity but different marginal costs of 10, 20 and 30 EUR/MWh. With an ordering according to the marginal costs, we derive the simplified spot market merit order. The spot market clearing price is thus the intersection of the demand function with the merit order. We calculate the opportunity costs based on Equation (4.1) above. Note that, for this stylized example, we assume the minimum load capacity and the balancing capacity provision to be equally sized (e.g. both 50% of the total capacity). Then, both terms cancel out each other for the extramarginal case in Equation (4.1) which simplifies the example. In the modeling approach, detailed technical characteristics as to minimum load as well as capacity provision are considered.

Now, let us consider two demand situations: A low and a high spot market demand situation. In the low demand situation, the demand is lower than the total capacity of plant A. Hence, the cheapest power plant A can satisfy the total spot market demand resulting in a spot market clearing price of 10 EUR/MWh. This leads to opportunity costs of 0, 10 and 20 EUR/MWh for A, B and C respectively[4] (shown in Figure 4.2 on the lower y-axis part). In the high demand situation, the demand exceeds the joint capacity of plant A and B. Therefore, plant C determines the spot price of 30 EUR/MWh, which results in opportunity costs of 20, 10 and 0 EUR/MWh for A, B and C respectively. If we assume that power plants need to provide the

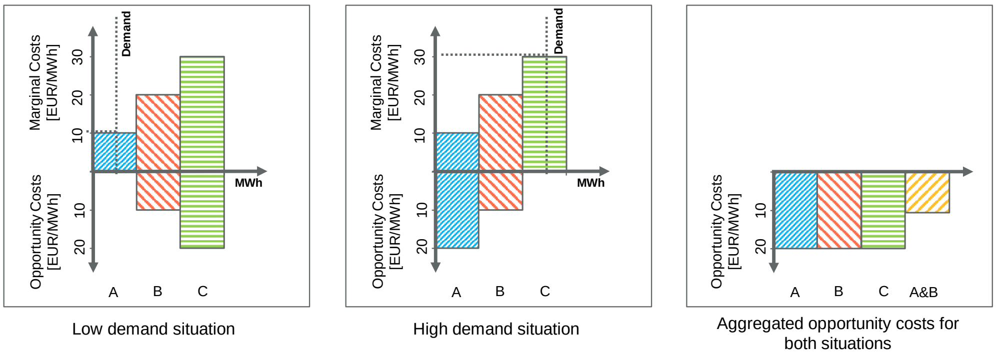

Figure 4.2: Schematic situation of the portfolio effect

positive balancing power for both situations, the opportunity costs in each situation sum up for each power plant:

$$TotalOpportunityCosts(p) = \sum_{i=low,high} OpportunityCosts_i(p) \qquad , \forall p \in \{A, B, C\} \tag{4.2}$$

This results in total opportunity costs of 20 EUR/MWh for each power plant. A coalition of two power plants could reduce the joint opportunity costs. Power plants A and B could cooperate, e.g. belong to the same operator. Then, in each situation the operator can provide balancing power by her power plant with the lowest opportunity costs. She would use plant A in the low demand situation, and plant B in the high demand situation. The joint opportunity costs for power plant A and B for both situations is 10 EUR/MWh, which is lower than the individuals' 20 EUR/MWh. For the negative balancing power, this portfolio effect does not hold in general. The opportunity costs are 0 for inframarginal power plants and usually monotonically increasing for extramarginal power plants. This leads to monotonically increasing

[4]We assume that power plants need to run in order to provide positive balancing power (e.g. due to minimum load or ramping constraints). If plants B and C would not need to run, their opportunity costs would be 0 EUR/MWh.

opportunity costs in each demand situation. The sum of monotonically increasing functions is still monotonically increasing. Thus, the cheapest power plants to provide negative balancing power are always in the left segment of the merit order and there is no possibility to get better off in a portfolio.

Note that we made some simplifying assumptions in this stylized example, e.g. we neglected part load efficiency decreases and attrition costs. We assumed the capacity provision and the minimum load capacity to be equal such that it cancels out for the calculation of the extramarginal opportunity costs. Furthermore, we assumed the balancing power demand to be comparably small such that the marginal power plant can fully provide the balancing power demand. All simplifying assumptions are relaxed and accounted for in the detailed optimization model.

The portfolio effect only occurs if balancing power is procured over a long time horizon that differs from the hourly spot market tender frequency. Here, large players may have significant cost advantages because they can provide balancing power at lower costs from their portfolio. For shorter time periods of balancing power procurement, the portfolio effect is reduced.

In Figure 4.3, an exemplary merit-order for Germany divided into the main operators is shown. Power plants that do not belong to the largest five companies are considered as power plants of a fringe.[5]

As previously explained, opportunity costs in the balancing power market do strongly depend on the intersection of supply and demand in the spot market. Therefore, to investigate market concentration, we need to consider the power plant portfolio of all operators in the merit order (cf. Figure 4.3). Fuel costs as well as capacities are based on the year 2014. Detailed numbers can be found in Table 4.4 in the appendix. We can see that several ranges are covered by only a few operators. Especially, in the left part of the merit order, there are only two to three operators covering a range of up to several Gigawatts. These are operators owning nuclear and lignite power plants with high investment costs and low marginal costs.[6] Those ranges with few operators tend to favor market concentration. By incorporating the operators and their power plant portfolio into our modeling, we are able to show the effect of different provision duration on market concentration.

[5]Throughout the paper we use the following abbreviation for the operators: RWE (RWE), E.ON (EON), Vattenfall (VAT), STEAG (STE), EnBW (ENB), fringe (FRI).

[6]Note that the fringe at the right of the merit order does not cause higher market concentration, because those plants do not belong to a single firm.

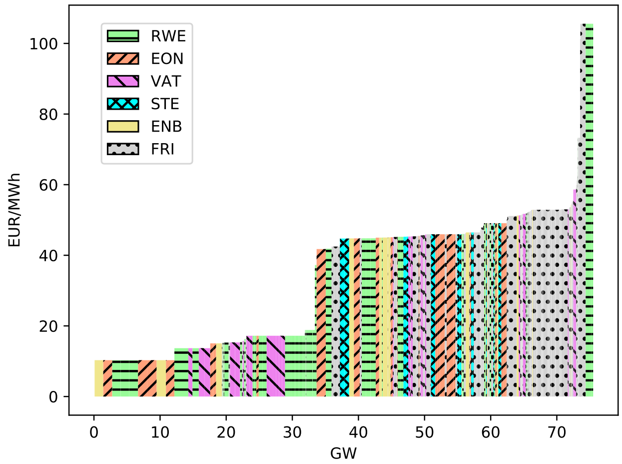

Figure 4.3: Merit Order in Germany colored as to the operators (capacity and cost data corresponds to the year 2014 and can be found in Appendix 4.6.1)

4.2.2 Market Concentration

In order to compare different levels of market concentration, we apply typical market concentration indices from the economic literature. Those indices are the Herfindahl-Hirschmann-Index (HHI, Hirschman (1964)) and the residual supplier index (RSI).[7]

The HHI uses the market shares of operators as an indicator for market concentration. It is defined as

$$HHI := \sum_{i=1}^{n} {MS_i}^2 \tag{4.3}$$

where MS_i is the market share of operator i in % and n the total number of operators.[8] Note, that we use the decimal representation of the market shares (50% = 0.5). Therefore, our HHI index is in the range between 0 and 1. Comparable high market shares have a higher impact to the HHI due to the squared functional representation. If we would have only five operators in the electricity market, the

[7] We do not focus on the pivotal supplier index (PSI), since the non-binary RSI is a refinement of the binary PSI. Furthermore, we do not investigate market concentration indices which involve prices, e.g. Lerner-Index (Elzinga and Mills, 2011). Since we apply a mixed-integer model, prices cannot be easily derived from the results due to the convexity problem (cf. (Bjørndal and Jörnsten, 2008, Ruiz et al., 2012)). Technical restrictions like minimum load or start-up costs in mixed-integer problems lead to non-convexities. Therefore, the marginal of the supply-demand-equilibrium cannot directly be interpreted as an estimator for electricity prices. Power plant specific variable costs can be above the system marginal costs of mixed-integer problems.

[8] The HHI is broadly applied in energy economics, see for instance Hogan (1997) and Twomey et al. (2006). A general discussion on concentration indices can be found in Green et al. (2006).

HHI could not be lower than 0.2 which would be the case of equally shared capacity. Since we also consider a fringe in our numerical analysis, these lower bounds are not necessarily holding. Based on the described indices we are able to compare the effects of different market designs on market concentration.

The RSI for operator x measures the remaining capacity without supplier x's capacity to fulfill the demand. It is defined as

$$RSI(x) := \frac{\text{TotalCapacity} - \text{Capacity}_x}{\text{demand}}, \tag{4.4}$$

where Capacity_x is the capacity of operator x (cf. Twomey et al. (2006)). In our analysis, we account only for active capacity which means capacity that is already operating. Non-operating capacities cannot provide balancing power in time or have additional start-up costs which make the opportunity costs not competitive. That means, if a power plant provides balancing power, it has to be operating (such that the production adjustment can be achieved) during the total provision duration. If pooling is allowed, this constraint is relaxed. In this case, the operator may shift the capacity within her power plant portfolio and hence is not dependent on the operation of a single power plant. The capacity of the operator in a weekly balancing power provision is defined by the minimum capacity of the operator's portfolio in the hours of the week. Note that HT and NT differentiation may apply. For comparison reasons, we focus on the inverse value, i.e. RSI^{-1}. Thus, similar to HHI, a higher value indicates higher market concentration

The HHI represents a market concentration index based on the market share while the RSI represents a market concentration index based on the residual supply (remaining capacity). Both measures therefore give different insights on the level of market concentration.

4.3 Methodology

In this section, details of the basic modeling approach as well as data and assumptions are presented.

4.3.1 Modeling Approach

The analysis is performed with a unit-commitment model for the German power market.[9] The basic model formulation is based on the work by Ostrowski et al. (2012) and Morales-España et al. (2013) and is extended for the modeling of balancing power provision.

In this article, we explain the general modeling approach for unit-commitment models but abstract from the detailed formulation that can be found in the literature on unit-commitment models (e.g. Ostrowski et al. (2012) and Morales-España et al. (2013)). The focus is set on the introduction of additional equations that account for the characteristics of balancing power markets.

The overall goal of the unit-commitment model is to derive the cost minimal production schedule of power plants to satisfy the demand for electricity. Power plants are modeled blockwise on an hourly time resolution. Power plant blocks are denoted by index p and hourly timesteps by index t. The objective function of the unit-commitment model is to minimize the total costs of electricity production and can be expressed as

$$\min TotalCosts = \sum_{t,p} (VarCosts(t,p) + StartUpCosts(t,p)). \tag{4.5}$$

StartUpCosts arise if a power plant is not producing in time step t but produces electricity in time step $t+1$. The actual *StartUpCosts* are dependent on the power plant p as well as on the non-production duration (time steps since last time operating). Power plants produce electricity to satisfy the demand. This essential constraint is represented as

$$\forall sm: \qquad \sum_{p_{sm}} production(p_{sm}) + import(sm) - export(sm) = demand(sm) \tag{4.6}$$

and holds for every time step t and every spot market sm. Here, p_{sm} are the power plants in spot market sm, *import* considers the electricity flow from other countries (spot markets) to the respective one and vice versa for *exports*.[10] The exogenous

[9] The model builds on the modelling framework **MORE** (**M**arket **O**ptimization for Electricity with **R**edispatch in **E**urope) that was developed at *ewi Energy Research and Scenarios gGmbH* and is written in GAMS (further information can be found at http://www.ewi.research-scenarios.de/en/models/more/).

[10] In the analysis at hand, only the German spot market is considered. Imports and exports are given exogenously as explained later.

demand is assumed to be perfectly inelastic.[11]

Technical characteristics of power plants are modeled via different constraints. An important modeling aspect of unit-commitment models is that it accounts for different states of power plants that can be incorporated by using binary variables. This makes the model a mixed-integer model. For example, each power plant has a range of feasible production which can be described by

$$production(p) = 0 \qquad \text{or} \tag{4.7}$$
$$minload(p) \leq production(p) \leq capacity(p). \tag{4.8}$$

Additional technical constraints of power plant blocks are also incorporated, such as part load efficiency losses, load change rates, combined heat and power operation and start up times. Part load efficiency is modeled via a convex function between the minimum load level and the full load level (according to Swider and Weber (2007)). This increases relative costs at reduced load levels due to part load losses compared to operation at full load operation. Load change rates determine technology specific ramping constraints which only allow for a certain adjustment of the power plants' production from one timestep to the next. Those constraints apply for ramp-up and ramp-down operations. We assume that the minimum load level corresponds to the grid synchronization. Thus, as soon as the power plant operates at the minimum load level, it feeds the production into the grid. This approach includes no-load costs implicitly.

The basic model is extended to account for the unique characteristics of balancing power markets. These characteristics are essentially given by (i) different provision intervals and (ii) operator structures. We therefore need to map the hourly timesteps to the balancing provision intervals as well as the different power plant blocks to operators.

Table 4.1 gives an overview of the sets, parameters and variables used for the modeling of balancing power. In the following, the equations of the model will be discussed.

The total demand for balancing power during a provision interval must be satisfied

[11] If this assumption would be relaxed, we expect a similar outcome with respect to balancing power provision, since the intersection point of demand and supply curve at the spot market, and hence the relevant opportunity costs would not change.

Table 4.1: Overview of sets, parameters and variables

Set	
BPi	interval for balancing power provision, e.g. week, day or hour
op	operator
t	hour
p	powerplant
t_BPi	set of hours in the balancing power provision interval
p_OP	set of plants that belong to respective operator
FRI	Fringe operators
Parameters	
D(BPi)	balancing power demand in interval
Variables	
BP_O(BPi, op)	balancing power provision by operator in interval
BP(t, p)	balancing power provision by plant and hour
BP_F(BPi, p)	balancing power provided by fringe operators in the interval

by the sum of the provision of all operators:

$$\forall \quad BPi: \sum_{op} BP\_O(BPi, op) = D(BPi). \tag{4.9}$$

The balancing power provision of all operators during a provision interval is constituted by the provision of the plants of the operators in each hour:

$$\forall \quad BPi, \quad t \in t\_BPi, \quad op: \sum_{p \in p\_OP} BP(t,p) = BP\_O(BPi, op). \tag{4.10}$$

The balancing power provision of the fringe during the provision interval is constituted by the fringe power plants without the option to pool:

$$\forall \quad BPi: \sum_{p \in p\_OP(\text{“}FRI\text{”})} BP_F(BPi, p) = BP\_O(BPi, \text{“}FRI\text{”}). \tag{4.11}$$

The power plant specific balancing power provision of fringe power plants is fixed in each hour of the provision interval:

$$\forall \quad BPi, \quad t \in t\_BPi, \quad p \in p\_OP(\text{“}FRI\text{”}): \quad BP_F(BPi, p) = BP(t,p). \tag{4.12}$$

Thus, the model allows the fundamental modeling of power plants that provide balancing power accounting for the operator structure. However, calls of balancing power are not modeled. Model outputs are the hourly production per power plant, as well as, balancing power provision by operator and power plant. In combination with the operator structure, we can evaluate market concentration indices in an ex-post analysis.

4.3.2 Input Data and Assumptions

We model two representative weeks in 2014, i.e. a winter week and a summer week. Figure 4.4i shows the demand, residual demand, solar feed-in and wind feed-in during the winter week. This winter week represents a typical situation of high demand in the early evening hours combined with no or very few solar radiation during the day. Especially at the beginning of the week, the wind production is low as well. As a result, there are situations with a residual demand of up to 71.2 GW in which the conventional power plant fleet (nuclear and fossil power plants, pumped storage plants) is utilized up to 69.3%. In the last three days of the week, the residual demand is low due to low demand during the weekend and high wind feed-in. In such a situation of low residual demand, the base load power plants supply a large share of the spot market demand. Since the base load plants are owned by the large operators, situations with low demand may show a high market concentration in the spot market. This has implications for the market concentration on the balancing power markets as well.

Figure 4.4ii shows the demand, residual demand and renewable feed-in in the summer week. It can be seen that there is a contrast to the conditions of the winter week. The demand in summer is typically low and there is high solar radiation during the day. This combination leads to a reduced utilization of the power plant fleet and therefore to lower prices. Here, even base load and mid load German power plants (lignite and hard coal power plants) reduce their production. Wind feed-in is on a relatively low level (below 10 GW in every hour), but increases during the weekend when the demand is already especially low. This leads to a low residual demand of only 24.3 GW on the Sunday.

Typical weeks during spring and autumn can be interpreted as a combination of the situations in those weeks. The varying demand and renewable feed-in in every single hour of those weeks cover a broad range of situations and therefore reflect also average situation with medium demand and/or renewable feed-in.

The assumptions on power plant capacities are based on Bundesnetzagentur (2014).

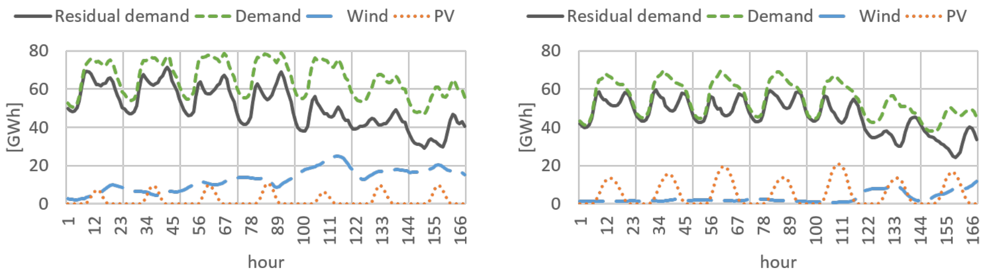

(i) Winter Week (Monday-Sunday)

(ii) Summer Week (Monday-Sunday)

Figure 4.4: Demand, Residual Demand, Solar Feed-In and Wind Feed-In

Only German power plants are modeled. Imports and exports are exogenously given based on ENTSO-E data. Fuel costs and CO_2 prices are based on historical data. Installed capacities, fuel costs and techno-economic parameters of power plants can be found in the Appendix.

Power plants are also constrained in their balancing power provision. We consider primary and secondary balancing power in our model, but abstract from tertiary balancing power provision.[12]

We assume that all running plants can provide a certain share of their capacity as balancing power. For the fossil and nuclear power plants, this share is derived by information about the ramping speeds multiplied by the time duration until the power adjustment needs to be realized. The ramping speed deviates by the year of construction of the technology. Furthermore, we assume that the capacity (share) for positive balancing power is the same as for negative balancing power. Table 4.2 shows the maximum allowed share of the capacity to provide balancing power for different power plant technologies.[13] We assume that power plants that are not running have high starting costs, e.g. due to attrition and fuel consumption, and thus are

[12]We do not consider tertiary balancing power since (i) technical restrictions are lower for the tertiary market and it tends to be compensated by the intraday-market (30 min before physical delivery), (ii) the current market design of tertiary balancing power has already a high tender frequency (provision duration of four hours), and (iii) there are many competitors in the tertiary market which reduces the risk of market power. Therefore, primary and secondary balancing power are in the focus of our analysis.

[13]Pumped storage plants have a high ramping speed. Therefore, they have a high technical potential to provide balancing power (up to 30 % of the capacity for the primary balancing power, and up to 45% for the secondary balancing power for a single plant). However, due to multiple bidding strategies and prequalification requirements, we assume that not all pumped storage plants are bidding their total technical potential into the balancing power markets.

Table 4.2: Share of total capacity that can be used for balancing power provision

	primary balancing power	secondary balancing power
CCGT	2.5 - 4%	25 - 40%
Coal	1 - 2.5%	5 - 12.5%
Lignite	1 - 2.5%	5 - 12.5%
Nuclear	2 - 2.5%	10%
OCGT	5 - 12.5%	50 - 60%
Oil	2%	20%
Pumped Storage	10%	15%

not competitive in offering balancing power.[14] We do not consider balancing power provision by renewables and demand side management, because those technologies were not important for the balancing power market in 2014 (Dena, 2014).

There is only one product that is procured for primary balancing power. However, in the case of secondary balancing power, we consider a positive and negative product for peak and off-peak times, respectively. Additionally we investigate the cases of shorter tendering times, namely daily and hourly. In the case of a weekly provision, the peak time are working days between 8 am and 8 pm. All other hours (night and weekends) are off-peak time. In the case of a daily provision, the peak time is the time between 8 am and 8 pm on every day (including weekends). In an hourly auction, the distinction between of peak and off-peak products disappears.

We map the information about the ownership to each power plant. We consider the German power plant operators E.ON, RWE, EnBW, Vattenfall and STEAG in our model. All other power plants are mapped to the fringe. We obtain information about ownership of plants from a list of the German regulator Bundesnetzagentur.[15]

E.ON, RWE, EnBW, Vattenfall and STEAG can use pooling to provide balancing power over a time period, e.g. they can offer a certain volume of balancing power during the provision period and use different power plants within their pool to fulfill their commitment. The fringe is not allowed to pool meaning that each power plant of the fringe has to provide the balancing power of the whole provision period. This is the most restrictive assumption for the pooling of the fringe. Indeed, there are sev-

[14]Start-up costs for a cold start can be up to 60.000 Euro for e.g. a 500 MW CCGT or OCGT power plant with 2010 cost data (Schill, 2016). These costs would have to be reimbursed by the revenue in the balancing power markets. Additionally, a faster start-up than usually increases the attrition and has a higher consumption of equivalent operating hours (EOH).

[15]Each power plant is mapped to only one owner. This corresponds to the assumption that even if several owners have shares in one plant, only one owner is responsible for marketing balancing power.

eral pooling companies which aggregate smaller producers to a virtual power plant and therefore allow for pooling for subsets of the fringe. However, if we allow that the whole fringe may use pooling effects, the fringe would operate as an additional big producer. Therefore, we expect that the general results for market concentration hold and only the absolute level of market concentration deviates.[16]

4.4 Results

In this section, we present the model results for a weekly, daily and hourly provision duration. The weekly provision duration represents the status quo which is currently in operation in Germany. Daily and hourly provision duration are currently discussed as alternative market designs for the German balancing power market. We analyze the balancing power provision in three dimensions. First, we focus on the efficiency gains by a shortened provision duration which are captured in the total system costs. Second, we analyze the balancing power provision by technology and operator which enables us to shed light onto the level of market concentration for the different provision duration using the indices HHI and RSI^{-1}.[17]

4.4.1 System Costs

Power system costs of different model configurations are a benchmark for the efficiency of the market design. In order to assess the costs of balancing power provision, we additionally model the electricity system without balancing power provision. The difference between this baseline run and the model runs with balancing power provision can thus be considered as the extra costs of balancing power provision.[18]

Table 4.3 gives an overview of the total system costs in the simulated summer and winter week with different designs of the balancing power markets. Irrespective of if and how balancing power is provided, it can be seen that the system cost in the winter is more than EUR 50m higher than in the summer.

As outlined above, the major power plant operators are allowed to pool their port-

[16]Furthermore, fringe power plants are typically gas fired power plants. Therefore, the effect on market concentration affects only situation with high residual demand as to the opportunity cost bidding strategy and the merit order.

[17]Note that we use RSI^{-1} instead of RSI. Thus, a higher value of RSI^{-1} indicates higher market concentration, similar to the interpretation of HHI.

[18]When referred to balancing power in this section, primary and secondary balancing power is meant.

Table 4.3: Total System Cost in Reference Scenario in Million Euros

in mio. Euro	no provision	hourly	daily	weekly	weekly (no pooling)
Winter	175.6	176.7	176.8	177.0	178.0
Summer	124.6	125.1	125.2	125.2	125.6

folio in order to provide balancing power. In order to quantify the efficiency gain resulting from pooling, a sensitivity with weekly balancing power provision in which pooling is not allowed is simulated additionally to a weekly configuration with pooling and hence included in Table 4.3.

The difference between the system costs without balancing power provision and the system costs of a configuration with hourly / daily / weekly balancing power provision can be understood as the respective costs of balancing power provision. Figure 4.5 illustrates those costs. It can be seen that not only the total modeled system costs are higher in winter, but also the costs of balancing power provision. This is expected given the higher residual demand levels in the winter.

If pooling would not be allowed, the cost of balancing power provision would be EUR 2.361m in the winter week and EUR 0.995m in the summer week. The modeled costs of the current weekly market design (with pooling of major operators) amount to EUR 1.328m in the winter week, and EUR 0.677m in the summer week. The cost difference between the weekly configuration with pooling and without pooling, that can be interpreted as the efficiency gain of pooling, is EUR 1.033m in the winter and EUR 0.319m in the summer.[19]

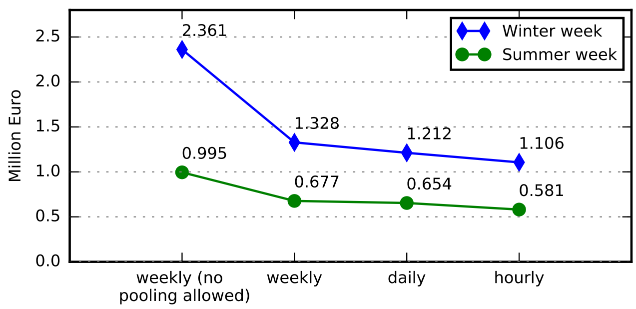

Figure 4.5: Costs of primary and secondary balancing power (compared to no provision)

The difference between the system costs of a configuration with weekly balancing

[19]An additional sensitivity analysis not included in figure 4.5 in which pooling of all fringe operators in one common fringe pool would be allowed shows no significant further efficiency gain.

power provision and a configuration with hourly balancing power provision (from now on we only consider configurations with pooling) can be interpreted as the maximum efficiency gain from shortening the provision duration. This cost difference is EUR 222k in the winter week, and EUR 96k in the summer week.[20] The system costs of the daily balancing power provision are between the system costs for the hourly and weekly balancing power provision. Compared to the efficiency gain from pooling, this further efficiency gain by a shortened provision duration is small.

The level of renewable feed-in can influence those results. Therefore, we consider a sensitivity in which we double the values of the historically observed renewable feed-in in the simulated weeks. The detailed results are shown in Appendix 4.6.2. A higher renewable feed-in leads to higher costs of balancing power provision especially in the summer week compared to the configuration with less renewables. For instance, in the case of weekly provision in the summer, the balancing power costs increase by EUR 559k if the renewable feed-in doubles. Due to the lower residual demand, more power plants have to be operational only in order to provide balancing power. The order of magnitude of the efficiency gain from pooling, however, remains unchanged by doubling the renewable feed-in.

The German expenses for the provision of primary and secondary balancing power was EUR 331m in 2014 (Bundesnetzagentur, 2016) corresponding to average expenses of EUR 6.37m per week.[21] This means that the average real expenses were higher than the simulated costs for the balancing power market with the weekly market design (EUR 1.328m in the winter and EUR 0.677m in the summer). Our model calculates *total costs* for power plants to provide balancing power under perfect competition and foresight. Those can be interpreted as a lower bound for producers' costs for the balancing power provision. The Bundesnetzagentur publishes the *total expenditures* for the balancing power provision. These expenditures also include producers' surplus. If every operator would bid their real costs in the pay-as-bid auction (under perfect foresight and perfect information), both results should be the same. However, since it is profit maximizing for the operators to estimate and bid the system marginal costs instead of own marginal costs (see for instance Müsgens et al. (2014)), the real expenditures are higher than the modeled costs for provision. Furthermore, the exercise of market power (e.g. withholding of volumes) could even lead to higher system marginal costs and hence higher producers' surplus. Effects

[20] Due to solver inaccuracies (difference between current best integer solution and optimal value of LP relaxation), we cannot resolve the exact effect. However, we can be sure about the order of magnitude of the effect.

[21] This figure is calculated based on capacity bids, not energy bids. This is consistent with our modeling approach in which we consider only provision and not calling of balancing power.

like strategic bidding between capacity and electricity bid or sub-optimal behavior due to information asymmetries could further increase the cost difference between real expenditures and the model results. Additionally, uncertainty for e.g. residual demand, prices, and power plant shortages of the next week are included in the bids which increase costs. These aspects are not considered by the cost minimizing model under perfect foresight. Therefore, we would expect our results to be a lower bound for the possible cost reductions.

4.4.2 Provision of Balancing Power

Balancing power is provided by different types of power plants within the portfolio of operators. Depending on the portfolio of operators and the pooling within the portfolio, the balancing power provision by technology changes from hour to hour. This effect can be observed in the graphs in Figure 4.6i for different provision durations at the example of positive secondary balancing power in the winter week.

For the weekly provision, we see a strong hourly fluctuation within the technologies although operators are restricted to a weekly provision duration. This indicates that the operators make significant use of the pooling option. The operators can freely select the power plants that shall provide balancing power in certain hours of the week. Therefore, the operators choose those power plants in their portfolio which have the lowest opportunity costs with respect to the spot market. Here, obviously, operators with a large portfolio have an advantage compared to small operators. For primary balancing power as well as for the case of the summer week, the fluctuation of balancing power providing technologies are similar to the Figure 4.6i.

If we take a look at the provision by technology for daily or hourly provision duration, we find a surprisingly similar structure to the weekly provision duration. However, small differences in the diagrams can be identified. CCGT, for instance, have a more important role in peak hours with the hourly provision compared to the outcomes with longer provision duration. In the daily configuration, coal power plants provide more often balancing power compared to the other configurations. The hourly provision duration can be expected to be the efficient benchmark where the owner structure of power plants does not matter. This means that the most cost efficient power plants in each hour provide balancing power. Since the capacity provision by technology of the weekly and daily cases are similar to the hourly benchmark, we conclude that the pooling possibilities allow a provision pattern that is close to the most efficient outcome. Even with a weekly provision duration, almost the same cost efficient technologies provide balancing power as in the case with an hourly provision. Except from the shown technology classes in Figure 4.6i, no other modeled technologies provide balancing power.[22] This interpretation is in line with the results presented in Section 4.4.1 where the efficiency gain from pooling was quantified to be EUR 1.382m in the winter week whereas the respective efficiency gain from shortening the provision duration from a weekly to an hourly market design was found to be EUR 0.222m.

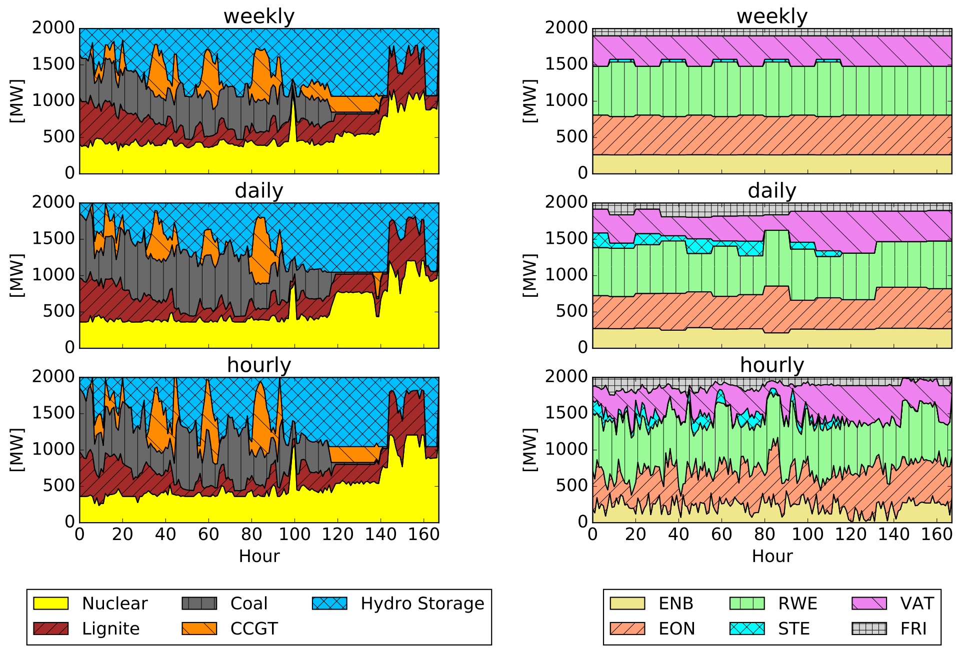

(i) Provision by technology

(ii) Provision by operator

Figure 4.6: Comparison of the technologies (left) and operators (right) providing positive secondary balancing power for the weekly, daily and hourly provision duration in the winter week (model results)

Figure 4.6ii shows the modeled capacity provision by operator for positive secondary balancing power for a weekly, daily and hourly provision duration. Compared to the modeled provision by technology, the modeled provision by operators differs more significantly for the three market designs. The fluctuation of market shares becomes higher with a shorter provision duration.

The capacity provision by operator can be considered as a first indicator for the market concentration indices. Therefore, we expect stronger fluctuation of the mar-

[22]This result does not only hold for the case of positive secondary balancing power, but also for the other investigated products.

ket concentration indices for shorter provision duration. Drivers for this are:

- the absolute residual demand level at a given time point in the time frame,
- the volatility of the residual demand level in the provided time frame,
- the steepness of the marginal cost function of the power plants and therefore the steepness of the opportunity cost function,
- the operator structure of the opportunity cost function, i.e. whether operators' capacities are in blocks or spread in the opportunity costs merit order.

Thus, the capacity provision by operator is typically dependent on the specific market circumstances, e.g. the product definition, the annual season, and the provision duration. Hence, we investigate the different market designs based on market concentration indices in detail to derive further insights.

4.4.3 Market Concentration

Based on the balancing power provision by operator observed in Figure 4.6ii we compute market indices for the three balancing power products, primary, secondary positive and secondary negative balancing power. The indices vary depending on the market design and provision duration. In order to assess the different ranges of market concentration indices, we analyze the model results in histograms for the HHI (cf. Figures 4.7, 4.9 and 4.10). Those diagrams show the HHI values in the weekly market design as a red line. In the case of secondary balancing power, two red lines are present due to the two contract durations (HT and NT, as described in Section 4.2). For the hourly provision duration, 168 different products are defined and hence 168 HHI values. The histograms show the distribution of those hourly HHI values. Similar histograms for the RSI^{-1} are evaluated (cf. Figures 4.8, 4.12 and 4.13).[23]

For the interpretation of the results, we also add dotted lines into the histograms which indicate threshold values for high market concentration. For the HHI, a strong market concentration exists at a value of 25% according to US Department of Justice, Federal Trade Commission (2010, §5.3) and at 20 % (with further restrictions) as to EUR-lex (2004, 19. and 20.). In the case of the RSI^{-1} we consider a threshold

[23] Additionally, an analysis for the concentration ratio CR1 and CR3 was conducted. The CR for m firms is defined as $CR(m) := \sum_{i=1}^{m} MS_i$ where MS_i is the market share of operator i in % for the m largest firms. The analysis for CR1 and CR3 did not lead to different conclusions compared to the analysis based on HHI and RSI^{-1}. Furthermore, the CR as an market share concentration index is similar to the HHI and thus to some extent redundant.

value of 1.11 (which corresponds to a threshold value of 0.9 for the original RSI definition).

The indices are no absolute measures in which one index would be sufficient to indicate market concentration. Nevertheless, high market concentration is more likely if both discussed indices point to a critical level.

Market Concentration for Primary Balancing Power Provision

For the modeled provision of primary balancing power, the HHI values are displayed in Figure 4.7. We observe that the summer seems to be slightly more concentrated in balancing power provision than the winter. The reason for this lies in the different demand profiles and the increasing production of solar generation (cf. Figure 4.4i). In the summer, a lower electricity demand and higher solar generation lead to less demand of generation from conventional power plants and therefore there are less power plants available (i.e. running) that are able to provide primary balancing power. This is also indicated by high values of the RSI^{-1} that can be seen in figure 4.8.

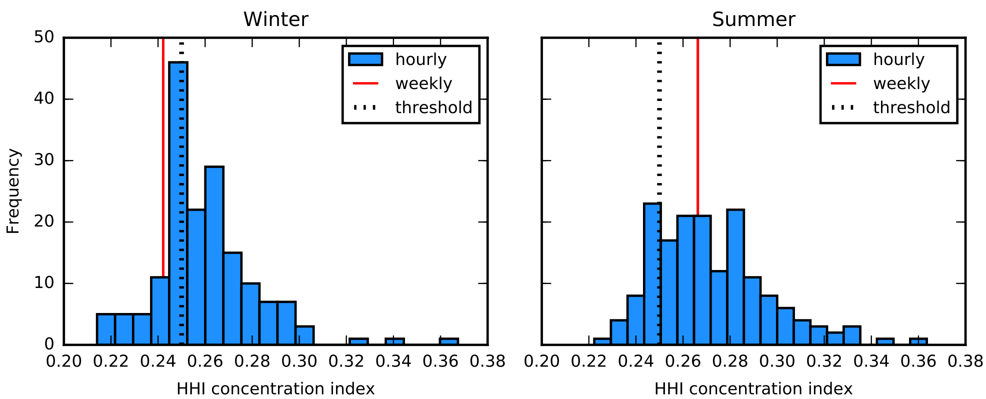

Figure 4.7: Histogram of the hourly HHI values for primary balancing power in winter week (left) and summer week (right)

Based on the model results we can infer that the primary balancing power market is prone to high market concentration. When the market design is changed from weekly provision to hourly provision we observe that the indices take on a broader range of values. This means there are hours in which market concentration is increased and hours when market concentration is lowered. An increase in market concentration may occur if the level of demand is at a level where only few operators are close to the marginal production level. As previously explained in Section 4.2 and shown in Figure 4.3, there are intervals in the merit order where only some operators own power plants. This is for example the case for lignite power plants that are owned by Vattenfall and RWE. When demand is low and lignite power plants are marginal in their production, they can provide balancing power at lowest cost. Since this effect only depends on one single demand period in the hourly provision case instead of multiple demand periods in the weekly design, the modeled market concentration increases in some hours. In addition, market concentration is higher in the summer because of lower demand levels and therefore less conventional power plants that are operating. These baseload power plants which are still operating are owned by fewer operators, which increases market concentration.

There is no clear trend observable to conclude whether shorter provision duration structurally mitigates or favors market concentration. The RSI^{-1}, however, that can be seen in Figure 4.8, decreases in average with shorter provision duration especially in the winter week. This means that the average market concentration is reduced because there is more active capacity that could provide balancing power. Nevertheless, there are some hours when the RSI^{-1} indicates a slightly higher concentration compared to the weekly provision. The number of hours with critically high values can be significantly reduced if the market design is changed to an hourly balancing power provision. In the winter this leads to RSI^{-1} values below the threshold. In the summer, however, the RSI^{-1} can only be decreased below the threshold in some hours. Based on the model results, the primary balancing power market seems to be highly concentrated such that even in the case with an hourly balancing power provision the average market concentration in the summer is still modeled as critically high.

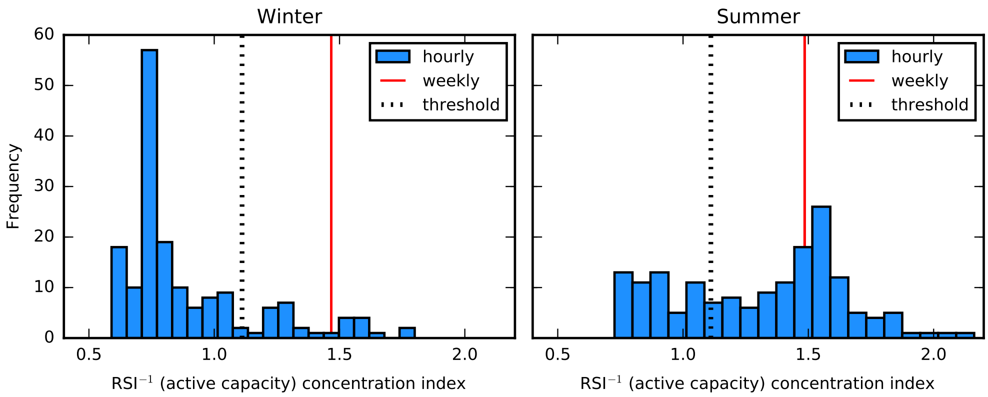

Figure 4.8: Histogram of the hourly concentration index RSI^{-1} for primary balancing power in winter week (left) and summer week (right)

Market Concentration for Positive Secondary Balancing Power Provision

Whereas primary balancing power is mostly provided by baseload power plants that are able to increase and decrease their generation, secondary balancing power is divided into positive and negative balancing power. In the case of positive balancing power, power plants provide the ability to increase their generation when being called. For the winter we see the respective technology and operator mix in Figure 4.6. The result for the summer week is similar, which is the reason why it is not shown additionally. The main difference is that more lignite power plants are providing balancing power instead of CCGTs than in the winter week. Especially the high provision of balancing power from lignite power plants leads to a high market share by RWE and Vattenfall.

The market concentration indices in Figure 4.9 show a high market concentration based on the HHI. Here, again, concentration seems to be higher in the summer compared to the winter. Nevertheless, the story is a bit different compared to the provision of primary balancing power because in the case of positive secondary balancing power there is a larger proportion of active power plants that could potentially provide balancing power. The respective RSI^{-1} indicates that the market is not too concentrated because the providing power plants could be replaced by the provision from power plants that are currently not delivering balancing power (the histogram for the RSI^{-1} can be found in the Appendix). Therefore the market can be considered as not as concentrated compared to the primary balancing power market. When the provision duration is lowered to an hourly level, the average modeled market concentration based on the RSI^{-1} is further reduced. In the case of the HHI, there is, however, no clear evidence for a reduction in average market concentration by reducing provision durations. There are single hours with very high modeled market concentrations in the hourly case.

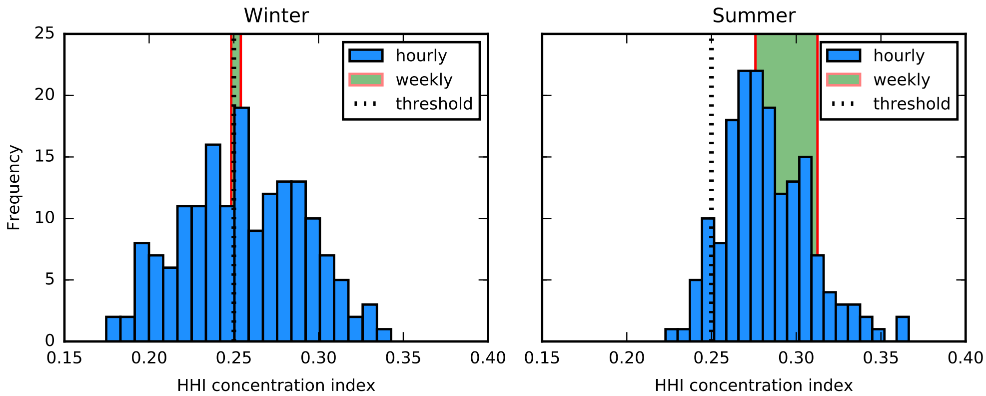

Figure 4.9: Histogram of the hourly HHI values for positive secondary balancing power in winter week (left) and summer week (right)

Market Concentration for Secondary Negative Balancing Power Provision

The HHI values for secondary negative balancing power that can be seen in Figure 4.10 have similar characteristics as the values for the positive secondary balancing power. Nevertheless, in the negative secondary balancing power market, we would expect no abuse of market power even with a high market concentration. The rationale for this is as follows: As to Section 4.2, the costs for capacity bids for balancing power are driven by opportunity cost compared to the spot market. Thus, for one hour, all operating power plants have zero costs for offering negative balancing power. For a longer provision duration, the costs would increase if the power plant would not be inframarginal all the time. However, due to pooling effects, operators can choose power plants which are operating in a specific situation. Therefore, the opportunity costs for each provider can be assumed to be (almost) zero. Many fringe operators can potentially participate in the auction, since e.g. wind producers could also provide negative balancing power. This means that the resulting supply curve for negative balancing power is very flat. If operators would try to withhold quantities in an attempt to increase prices, fringe operators with similar small costs would provide the balancing power. Hence, prices of (almost) zero for negative balancing power should be the consequence. Note that in reality, there is uncertainty (e.g. power plant outages) which leads to slightly positive capacity bids. With our model, we can find the cost minimal provision of balancing power but we would expect fierce competition. Therefore, even high shares of market concentration that can be observed in the model results should not lead to the abuse of market power because all providers face the same low level of opportunity costs. This argumentation is supported by the results on the RSI concentration index for negative balancing power (cf. Appendix 4.6.3, Figure 4.13), where most situations point to sufficient available active capacities to mitigate market concentration.

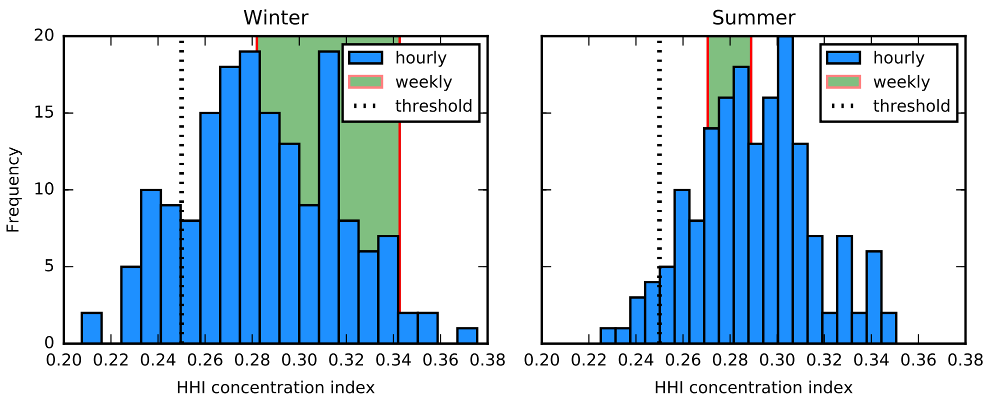

Figure 4.10: Histogram of the hourly HHI values for negative secondary balancing power in winter week (left) and summer week (right)

4.4.4 Influence of additional Demand Response on the Market Concentration

A shortened provision duration relaxes the provision duration constraint and potentially leads to dynamic market entries, e.g. by demand response technologies. The participation of demand response in US real-time balancing markets is well investigated, see for instance Heffner (2008), Vlachos and Biskas (2013) or Wang et al. (2015). In order to gain insights into the role of additional demand response technologies in our case, we model a sensitivity with additional 2.000 MW of pump storage. In the model rationale, pump storage capacity has the same features as flexible demand response processes or local storage applications. We model the capacity belonging to the fringe operators which reflects the assumption of competitively acting small operators. As expected, the average market concentration in the hourly market design is reduced in the sensitivity compared to the corresponding case without the additional capacity. However, the main observation of the market concentration analysis is found in the sensitivity as well, i.e. that there are hours with higher market concentration in the hourly market design compared to the weekly market design. This holds true for primary balancing power as well as for secondary balancing power.

4.5 Conclusion

Currently, the German primary and secondary balancing power markets have a weekly tender frequency. In a weekly market design, large power plant operators make use of pooling within their portfolio in order to provide balancing power. Fringe operators, however, do not have pooling options and need to withhold the capacity of their plants from the spot market for a whole week to provide balancing power which can lead to inefficiencies. Hence, fringe operators could potentially benefit from a shortened provision duration. The analysis at hand focuses on (1) efficiency gains from a shorter provision duration in primary and secondary balancing power markets, and (2) market concentration in market designs with different provision duration. Since it is known from the literature that simultaneous equilibria in spot and balancing power markets are efficient and unique (Richter, 2012), our methodology is based on a cost minimizing unit-commitment model for the electricity market in which we account for the ownership of power plants.

We quantify the efficiency gain from allowing pooling in a weekly market design to be EUR 1.033m in a winter week and EUR 0.139m in a summer week. Compared to this, the further efficiency gains that can be realized by shortening the provision duration from a week to an hour are small. An hourly market design would lower the costs of balancing power provision by EUR 222k in a winter week and EUR 96k in a summer week. Relative to the total simulated cost of balancing power provision in the weekly market design with pooling, the efficiency gain is 17% in the winter week, and 14% in the summer week.

Besides the efficiency gains, we identify effects on the market concentration. Here, we investigate the HHI and RSI^{-1} indices which are based on the market share and the residual supply, respectively. According to the model results, we see the potential for high market concentration in the primary balancing power market due to the technical requirements power plants need to fulfill in order to participate in this market. In the market for positive secondary balancing power, the model results indicate less concentration because there is more available capacity that could potentially replace the providing power plants. For the negative secondary balancing power, our results are quantitatively similar to the other products. However, we consider concentration in the market for negative balancing power not to be an issue due to the low opportunity costs for providing negative balancing power. Based on the model results, we find a higher market concentration in the summer than in the winter in all considered markets. The higher market concentration in the summer is driven by a lower level of demand, which reduces the number of active power plants and also the number of operators that are providing balancing power.

Our results reveal a tendency towards decreasing average market concentration by shortening the provision duration. However, the market concentration indices take on a broader range of values in the case of a shorter provision duration depending on the residual demand level and its volatility. There are single provision periods with a very high market concentration in the hourly and daily market design that could favor the potential for market power abuse.

Although market concentration can be an indicator for market power, it does not necessarily identify market power. The characteristics of the supply curve for balancing power determine the potential for market power abuse. If high market concentration is found in a flat segment of the supply curve, prices cannot be raised significantly. The goal of further research should be to comprehensively understand market imperfections in balancing power markets which is a prerequisite for conducting a comprehensive cost-benefit analysis for changes in market design like shortening of provision periods. Besides market concentration, aspects like e.g. strategic bidding between capacity and energy bid and uncertainty about the renewable feed-in or demand should be considered.

As a policy implication, we recommend to monitor market concentration and price levels carefully after a change of the market design in the balancing power market. In specific situations, single operators may have a cost advantage compared to their competitors.

4.6 Appendix

4.6.1 Input Data for Modeling

Since we model the year 2014, we are able to use realistic data according to publicly available sources. Assumptions that are made are in line with typical assumptions for modeling the electricity generation sector in Germany. The installed power plant capacities of different fuel types are shown in Table 4.4 and are based on Bundesnetzagentur (2014).[24] Additionally, Table 4.4 shows the assumed fuel costs and the CO_2 emission coefficients by fuel. We assume those costs to be static over the whole year. The CO_2 emission certificates are assumed to be 6.2 EUR/t CO_2. The fuel costs of pumped storage are based on opportunity costs.

Table 4.4: Model Inputs: Installed capacity in Germany for 2014, fuel costs, costs for CO_2 emissions certificates, and CO_2 emission coefficients

	Capacity [GW]	Fuel Costs [EUR/MWh_{therm}]	CO2 Emission Coefficient [EUR/t CO_2]
Nuclear	12.1	3.6	0
Lignite	21.3	1.5	0.404
Coal	25.5	13.2	0.399
Gas	26.9	22.8	0.202
Oil	2.4	49.4	0.281
Pumped Storage	6.4	(opportunity costs)	0
Others	1	22.8	0.202
PV	32.7	0	0
Wind onshore	31.4	0	0
Wind offshore	0.4	0	0
Biomasse	7.5	31.8	0
Hydro	4.4	0	0

Table 4.5 shows the assumed technical power plant parameters (particularly dependent on the year of construction).

[24]The actual input of installed capacities is further separated as to the year of construction: This gives further technical characteristics and parameters like full load and part load efficiency. The newer a power plant, the better are its technical parameters.

Table 4.5: Techno-economic parameters for conventional power plants

	Net efficiency full-load [%]	FOM-costs [EUR/kW/a]	Availability [%]	Start-up time [h]	Minimum part-load [%]
Coal	37 - 46	36 - 54	84	4 - 7	27 -40
Lignite	32 - 47	43 - 65	86	7 - 11	30 - 60
CCGT	40 - 60	28	86	2 - 3	40 - 70
OCGT	28 - 40	17	86	0.25	40 - 50
Nuclear	33	97	92	24	45
Biomass	30	165	85	1	30

4.6.2 Robustness Checks

As a robustness check, a model run is considered in which the values of renewable feed-in is doubled. Table 4.6 gives an overview of the total system costs, and Figure 4.11 illustrated the costs for providing primary and secondary balancing power compared to a model run without balancing power provision.

Table 4.6: Total system cost in scenario with doubled renewable feed-in in million Euros

in mio. Euro	no provision	hourly	daily	weekly	weekly (no pooling)
Winter	131.6	132.8	132.9	133.0	134.1
Summer	102.4	103.5	103.5	103.6	104.3

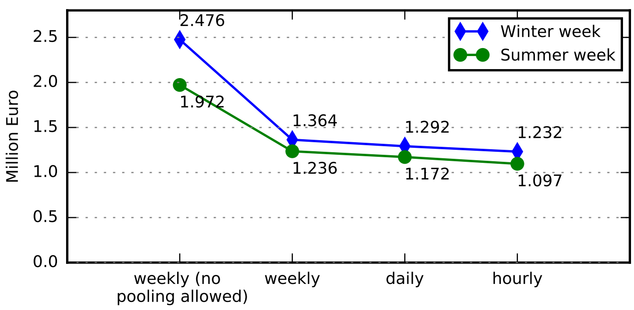

Figure 4.11: Costs of primary and secondary balancing power (compared to no provision) in scenario with doubled renewable feed-in

4.6.3 RSI concentration index for secondary balancing power

Figure 4.12 and 4.13 show the RSI^{-1} market concentration indices for secondary balancing power (positive and negative, respectively). Values above the threshold of 1.1 point to high market concentration situations in which one supplier might be pivotal. It becomes obvious that in most situations, enough (active) capacity is available. The situation is more critical in the modeled summer than winter week.

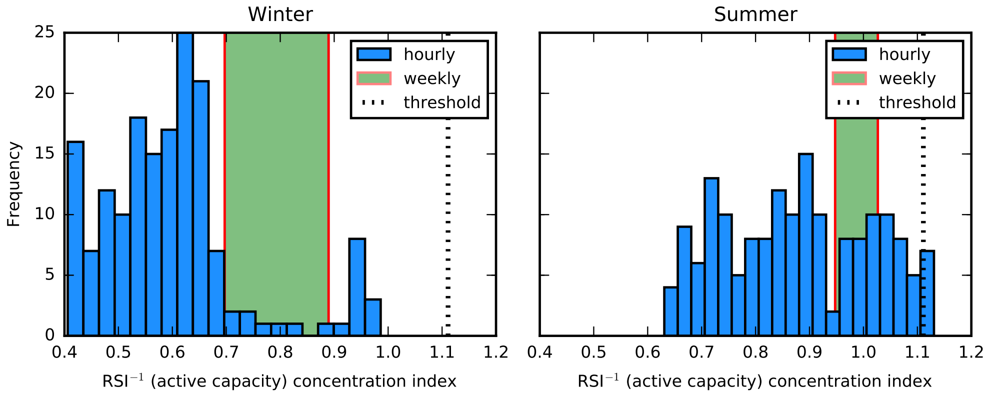

Figure 4.12: Histogram of the hourly concentration index RSI^{-1} for positive secondary balancing power in winter week (left) and summer week (right)

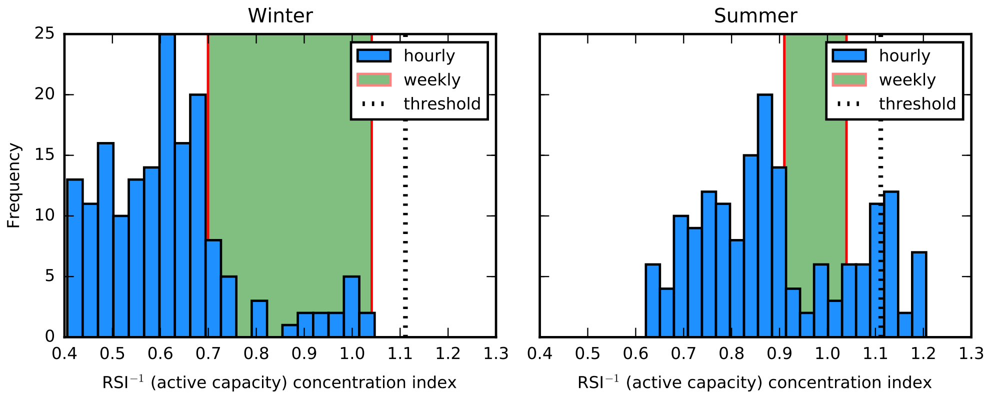

Figure 4.13: Histogram of the hourly concentration index RSI^{-1} for negative secondary balancing power in winter week (left) and summer week (right)

5 The Benefit of Long-term High Resolution Wind Data for Electricity System Analysis

Future energy systems rely increasingly on the wind power supply. Understanding its characteristics is essential for the functioning of future electricity systems. Critical low wind situations may endanger the security of supply. So far, historical observations of wind power production are limited to few recent historical years and may not suffice to quantify the expected overall wind contribution, its variability, and its regional balancing effects for future electricity systems. With a novel long-term high-resolution wind power production dataset (hourly on a 6x6 km grid for 20 years) we derive new insights. First, we find advantages of our high-resolution dataset compared to previous studies. Second, we find a strong variation in annual wind production (variation of up to 14% for Germany). And third, we find a potential benefit from electricity exchange with neighboring countries in low wind conditions (for Germany in 81% of the low wind situations). The results are highly relevant for further investigation on the level of secured capacity or to identify optimal power transmission capacities within energy market modeling.

5.1 Introduction

Weather dependent renewable energies, in particular wind energy, has recently gained an increasing importance for energy systems all over the world. For instance, the European wind capacity share raised from 6% (41 GW) in 2005 to 16.7% (154 GW) in 2016 (WindEurope, 2017). Thus, for understanding future energy systems, the overall wind power contribution, its short- and long-term variability as well as its regional balancing effects are crucial. Especially regarding energy system reliability the unique characteristics of wind power production, such as low wind situations, play an important role.

This encounters at least two major challenges. First, available historical wind power production data is insufficient for future predictions. Due to the rapid expansion of wind employment, extensive long-term observations are scarce. Therefore, simulations of wind power time series using current and expected future wind park fleets are required. However, this is leading to the second issue - the lack of meteorological observations with sufficiently high spatio-temporal resolution at the long-term scale, matching with operation sites to perform such simulations.

Recently a number of studies are making use of wind datasets from various reanalysis products in order to deal with these issues (Cosseron et al., 2013, Gunturu and Schlosser, 2012, Hallgren et al., 2014, Ritter and Deckert, 2017, Staffell and Pfenninger, 2016). However, most of these studies are limited in the sense of spatial coverage (single countries), coarse spatial resolutions or the level of details concerning the conversion from wind energy to electricity generation. For instance, Staffell and Pfenninger (2016) apply NASA's Modern-Era Retrospective Analysis (MERRA) in combination with a country based calibration to European wind parks calculating long-term wind power time series. Although the temporal resolution (hourly) of the MERRA reanalysis is sufficient for most energy related applications, the accuracy of the wind dataset might suffer from its coarse horizontal grid spacing (approximately 50 km in Europe) since important local effects happen at sub-grid scales.

In this article, we face these challenges by applying a novel wind power model to a unique high resolution wind dataset. The hourly and 0.055°x0.055° (approximately 6x6 km in Germany) resolution dataset is obtained from the brand-new reanalysis product of the Consortium for Small-scale Modeling (COSMO-REA6). In combination with a location specific European wind park portfolio of 2014, we generate a high resolution wind power database on an advanced level of details. Since the COSMO reanalysis contains long-term time series of 20 years, we are able to capture the broad range of variations, in particular the long-term variability of wind speed and hence electricity generation. In addition we apply a country based calibration to our model results using bias corrections triggered by historical time series.

We focus on three main insights from this approach. First, we have a closer look at advantages of our higher spatial resolution compared to other previous studies which rely on coarser reanalysis products. Second, by using long-term data we are able to analyze the variability and occurrence frequency of extreme events in the wind power sector. This leads to the question whether it is reasonable to define representative years as it is common in many energy studies. Third, we investigate regional balancing effects induced by wind power generation, on a European scale, as well as on a national scale (Germany). This highlights once more the advantages from extending electricity grids to reap the benefits from balancing effects. The dataset can be applied in further high-detailed energy market models and cost-benefit analyses.

The paper is structured as follows: In Section 5.2 we develop and apply the model to simulate wind power time series. The modeling results are further analyzed in Section 5.3 with respect to annual variation and balancing effects. We finally conclude in Section 5.4.

5.2 Methodology

In this section, the methodology is presented. Due to the high-resolution in time and space, the model has the potential to outperform existing wind datasets with a coarser resolution. Since wind speeds are highly dependent on regional effects (surface roughness, landmass, etc.) a high resolution is crucial to derive detailed data which is necessary for follow-up analysis in e.g. electricity dispatch and investment models, transmission grid expansions, as well as security of supply analysis.

5.2.1 A model for high resolution wind power production

We develop a method to accurately estimate spatially and temporally high resolution wind power production time series for given installed wind park capacities in a certain domain. The method is implemented in the Renewable Energy Output Model (REOM). To calculate the power output P_{out} of a single wind turbine at a known location for given instantaneous wind speeds at hub height v_{hub} the following equation, also called power curve, is used:

$$P_{out} = \begin{cases} 0 & v_{hub} < v_{in} \\ \frac{1}{2}\pi R^2 c_p \rho_{hub} \cdot v_{hub}^3 & v_{in} <= v_{hub} < v_r \\ C & v_r <= v_{hub} < v_{out} \\ 0 & v_{hub} => v_{out} \end{cases} \tag{5.1}$$

The rotor diameter R, efficiency c_p, capacity C, cut-in wind speed v_{in}, cut-out wind speed v_{out} as well as rated wind speed v_r are determined by the specific turbine type. The cut-in wind speed is the speed, where a turbine starts to generate power output. At rated wind speeds it produces at maximum (capacity) level and for wind speeds above the cut-out it stops due to technical limitations and security issues. The wind speed v_{hub} and air density ρ_{hub} from equation (5.1) need to be known at the turbine's hub height, since both quantities vary substantially with height.

Due to the cubic dependency of the power output by the wind speed at hub height in equation (5.1), it is crucial to have highly accurate wind input data. The wind input data is obtained from reanalysis data on a pre-defined grid. Two steps are necessary to get the wind speed at the specific turbine location and hub height. First of all, wind speeds are horizontally interpolated from adjacent grid points to the exact specific wind park location using the inverse distance weighting method. Second, wind speeds need to be vertically interpolated, respectively extrapolated to the adjacent hub height. Reproducing the vertical wind profile is a challenging task due to the complexity of atmospheric stability conditions (Kaimal and Finnigan, 1994, Motta et al., 2005, Stull, 1988). In this paper, we use a vertical interpolation between the first six model layers obtained from the reanalysis data by a 3rd order fit.

5.2.2 Application of REOM: A European long-term dataset

A wind park dataset is necessary to provide information about geographical coordinates, commission dates (production start dates), hub height, rotor diameter as well as the specific power curve characteristics (cut-in, cut-out, rated speed and capacity) for every single wind park in Europe. We use an extract of the worldwide database for wind turbines and power parks from *The Wind Power*[1] The Wind Power (2016), last updated in April 2016. In order to be able to compare different years of weather and hence wind power production, we use the European wind power park fleet of the end of 2014 as the basis for our long-term wind power production simulations. After filtering out parks without a detailed location, production status or commission date information, 15 400 European parks contributing to an overall installed capacity of 119.85 GW for 2014 are left. However, some parameters are still lacking to different extents. For instance, for more than half of all parks in Europe the rotor diameter is unknown and for roughly 40% the exact hub height is lacking. In these cases default values are set, obtained by the mean of the particular parameter and country. In the appendix, Figure 5.7 and Figure 5.8 show the distribution of installed capacity in Europe for 2014 and Table 5.3 summarizes the parameter availability.

Imprecise wind input, due to the cubic dependency in equation (5.1), results in highly inaccurate wind energy outputs. Since wind speed is highly variable in time and space it is desired to use temporal and spatially high resolution wind input data. Reanalysis products are an approach to solve the lack of high resolution and homo-

[1]www.thewindpower.net

geneously distributed data. They are systematic approaches to generate long-term datasets on a defined homogeneous grid for climate research by combining an assimilation scheme for historical observations with a certain atmospheric circulation model. Several reanalysis datasets are available for different historical periods, spatial domains and resolutions. However most of these products have a coarse horizontal resolution (Staffell and Pfenninger, 2016), e.g. ERA-Interim with approximately 80 km in Europe, due to their global coverage and computational limits. This might be a problem especially in mountainous regions, where the meteorological model is not able to reproduce the underlying terrain and capture wind speed variations adequately (Kaiser-Weiss et al., 2015). To reduce these inaccuracies we use the novel high resolution reanalysis dataset COSMO-REA6 from the Climate Monitoring Branch of the Hans Ertel Centre for Weather Research (HErZ-TB4) funded by the German Weather Service (DWD). It provides hourly wind data between 1995 and 2014 in Europe on a 0.055° (approximately 6 km) horizontal grid spacing with 40 different vertical layers. For more details about the reanalysis model and dataset see Bollmeyer et al. (2015).

Staffell and Pfenninger (2016) point out that a key factor for previous wind power production studies using reanalysis products is "the need for calibration, or bias correction, to bring simulated capacity factors in line with reality". They find significantly varying bias correction factors for different European countries showing the site dependency of such corrections. We follow the simple and promising bias correction method of Staffell and Pfenninger (2016) by using the bias of the simulated wind power output instead of directly taking reanalysis wind speeds.

To correct our new simulated time series by the capacity factor bias in every country we use the wind power production database from the European Network of Transmission System Operators for Electricity (ENTSO-E) as a basis for comparison. The database contains monthly wind power capacity factors (CF) between 2010 and 2014 for all European countries. Similar to Staffell and Pfenninger (2016) the resulting bias factors show significant regional dependencies. Country-wise correction factors can then be applied to calculate new wind speeds at the specific hub heights yielding bias corrected wind power production time series for all European wind power parks. We need to mention here, that specific single wind park sites might face significant errors due to the usage of country averaged production data from ENTSO-E.

With the wind park and reanalysis dataset we are able to calculate hourly time series for all wind turbine locations in 30 countries, including 28 countries of the

European Union (EU-28) complemented by Norway and Switzerland (from now on defined as Europe), for a time period of 20 years between 1995 and 2014.

This dataset is very useful in the field of energy meteorology and energy economics because of two distinct characteristics. First, we derive hourly wind production time series for each wind turbine location. Our high-resolution data (hourly time-resolution on 6x6 km) provides superior accuracy compared to classical European-scale wind datasets (e.g. 6-hourly temporal resolution for ERA-Interim and 50x50 km horizontal grid as for MERRA-2). Second, we can gain additional insights on long term energy output of wind turbines over a time span of 20 years that could not have been measured historically. By providing these insights, we can especially contribute to energy systems planning. Here, time series over a time span of 20 years lead to much more robust results and insights compared to the historical measurements.

5.3 Results

5.3.1 Evaluation of the underlying reanalysis dataset

First of all we have a closer look at the reanalysis wind speed input dataset. Yet there are only few studies dealing with the performance of the COSMO reanalysis product due to the recency of the dataset. Kaiser-Weiss et al. (2015) compare statistical properties of wind speeds observed at 210 meteorological stations over Germany with near-surface fields of the COSMO-REA6, ERA-Interim and ERA-20C reanalysis products for recent years. With respect to monthly correlations, they find for 96% of all stations a correlation coefficient $R \geq 0.8$ and for 80% of the stations $R \geq 0.9$ in the case of COMSO-REA6, in contrast to 82% and 47% for ERA-20C as well as 89% and 66% for ERA-Interim. They state that the improved correlation of COSMO-REA6 is "valid for daily, monthly and seasonal scale" and add that regional reanalysis "improves monthly correlations [...] in areas with more complex topography".

To further assess the wind speed quality of data produced by reanalysis we compare COSMO-REA6 (6 km grid), ERA-Interim (80 km grid) and MERRA-2 (50 km grid) wind speeds to observations. The data used here are the synoptical observations (SYNOP) provided by the DWD with a temporal resolution of 10 minutes (averages). In order to compare only with independent observations, SYNOP stations lower than 100 m above sea surface are omitted since these observations are used for the COSMO assimilation procedure. The observations are compared to the nearest grid point of the respective reanalysis. As the observations are compared to 10 m wind reanalysis data only observations with measurement height between 8 and 12 m are taken into account. The DWD provides for every SYNOP observation site a spatial representativeness value. To avoid comparisons with observations influenced by local obstacles, sites with representative values greater than 500 m are considered only. Thus, 59 different SYNOP stations remain with 10 minute observations. Table 5.1 shows the bias, standard deviation and Pearson correlation coefficient of COSMO-REA6, MERRA-2 and ERA-Interim compared to SYNOP observations.

Table 5.1: Bias, standard deviation (STD) and Pearson correlation coefficient (R) of COSMO-REA6, MERRA-2 and ERA-Interim compared to 59 SYNOP observation sites in Germany for 2014.

	Bias $[ms^{-1}]$	STD $[ms^{-1}]$	R
REA6	-0.14	1.44	0.74
MERRA	0.53	1.76	0.67
ERA-I	0.17	1.65	0.67

The time period of investigation are hourly values in the year 2014. COSMO-REA6 represents the mean absolute wind speeds best with a slight underestimation of -0.14 ms^{-1}. The other two reanalysis slightly overestimate the wind speeds. In addition to the smallest systematic error, COSMO-REA6 shows the lowest standard deviation and highest linear correlation coefficient. Thus, COSMO-REA6 performs best in representing absolute values of observations.

There are various processes on different spatiotemporal scales determining the atmospheric wind field. To get an insight on how well the processes at the different temporal scales are simulated (and therefore produce realistic spatial wind variability) a method suggested by Cannon et al. (2015) is used. We compare the observed (OBS) and reanalyzed (R) wind speed differences (δv) between different observation sites i, j:

$$\delta v_R = v_{R,i} - v_{R,j} \tag{5.2}$$

$$\delta v_{OBS} = v_{OBS,i} - v_{OBS,j} \tag{5.3}$$

Figure 5.1 shows the linear correlation coefficients between the observed and synthetic wind speed differences for COSMO-REA6, MERRA-2 and ERA-Interim. The correlations increase from small to large distances, because large scale processes are in general better represented than small scale processes. COSMO-REA6 shows significant higher correlations to observations, followed by MERRA-2 and ERA-Interim. As COSMO-REA6 shows highest correlations for all distances, COSMO-REA6 outperforms the other two reanalysis not only in representing small scales processes but also large scales processes.

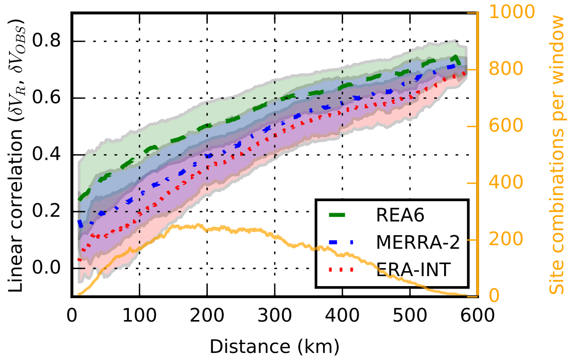

Figure 5.1: Linear correlation of observed wind speed differences (site to site) and reanalyzed wind speed differences as a function of site distance. Solid lines show the moving average in a window of ±25 km. The standard deviation of the moving average is shadowed.

5.3.2 Evaluation of the REOM model

As a next step we compare the ENTSO-E time series on a monthly basis to bias corrected control data containing REOM wind power simulations between 2010 and 2014. To estimate the performance of the REOM model only countries with reliable installed capacity data in the considered time span are taken into account, leaving 21 European countries. The average European CF of 22.85% in ENTSO-E is slightly underestimated by our model (22.01%), yielding a difference of 3.6%. The good fit throughout the time period can be seen in Figure 5.2i.

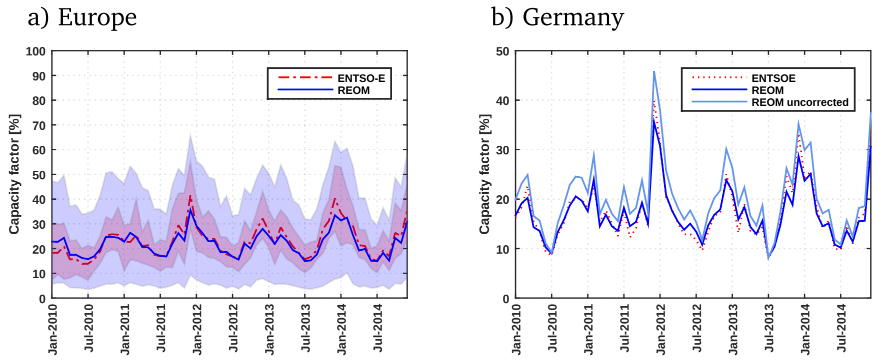

Figure 5.2: Monthly means of capacity factors between 2010 and 2014. In a) for REOM (blue, solid) and ENTSO-E (red, dashed) averaged over all European countries. In addition the 10 and 90% percentiles are shaded. In b) only for Germany. In addition the uncorrected REOM (blue, dashed) is shown.

However, it is evident that the spreads between the 10 and 90% percentiles vary significantly between REOM and ENTSO-E due to over- and underestimations in certain countries. The same can be observed on an intra-annual scale - the monthly averaged CF across Europe are showing very good agreement in spring and summer months but also some bias in autumn and winter (cf. Figure 5.2ii).

Considering output reductions of 5% in all ENTSO-E data due to transmission and distribution losses, as suggested by Staffell and Pfenninger (2016), would result in an even closer match. The simulations show high correlations for almost all countries in Europe. They range between 0.98 for Germany and 0.71 for Bulgaria leading to an average correlation coefficient of 0.88 for entire Europe. As an example, Figure 5.2ii illustrates the German CF between 2010 and 2014 for the historical data, the bias corrected and uncorrected REOM data. It is evident that the model is able to capture the general trends. The bias correction shifts the data towards the ENTSO-E values, yielding comparable capacity factors. Looking at errors, the model shows root mean square errors between 1.45% (Germany) and 6.78% (Bulgaria), while 3.97% are estimated in average for Europe.

To evaluate the performance of the REOM model in combination with the COSMO-REA6 dataset on an hourly basis, the modelled wind production is compared to published hourly means of wind production data by EEX for the reference years between 2010 and 2014 in Germany. The hourly time series are as well highly correlated ($R = 0.97$) and the German average CF is underestimated by 3.9%, with 17.08% CF for REOM and 17.88% CF for EEX. An investigation of the diurnal cycle averaged over the 5 years shows that REOM is in good agreement with EEX and only slightly underestimates the CF during night times and vice versa during midday (cf. Figure 5.9 in Appendix 5.5.3). The occurrence frequencies of capacity factors (cf. Figure 5.10, Appendix 5.5.3) show that the REOM underestimates the lowest range of CF (<10%) and slightly overestimates CF between 10 and 30% compared to EEX.

Besides these minor differences between our simulation results, ENTSO-E and EEX our model performs well on annual, seasonal, daily as well as hourly time scales. It is able to reproduce the general trend in wind power generation as well as its magnitude on the European and country based scale. However a country based bias correction is applied to our simulations, the performance quality still differs between countries significantly.

5.3.3 Long-term variability of wind power production

By making use of 20 historical weather years, we are able to simulate the wind power production over a comparably long time span with high resolution. We model the wind power generation in Europe for the installed capacities that existed in 2014. With this approach we are able to analyze the variation of wind power generation over a long time span which enables us to compare the characteristics of different weather years regarding annual average generation, high and low wind conditions. Note that the research focus is on the analysis of the wind variability and its characteristics. We explicitly do not perform a cost-benefit analysis of wind production sites nor an economic viability analysis. Thus, economic characteristics as renewable subsidies, electricity demand and supply, or market values are not relevant for this investigation. However, the underlying high resolution dataset can be applied to improve existing research as for instance applied in the high resolution market value estimation of Obermüller (2017a).

The distribution of hourly simulated wind generation over the time span of 20 years is plotted for Europe and Germany in Figure 5.3i and 5.3ii. In Europe, the capacity factor takes on values between 0% and 68%. For Germany, higher CF can also be observed that take on values as high as 88%. Generally, we find that the German distribution of CF inhibits more extreme conditions with high or low capacity factors. In Europe as a whole these extreme low and high values cannot be observed because there are balancing effects between countries.

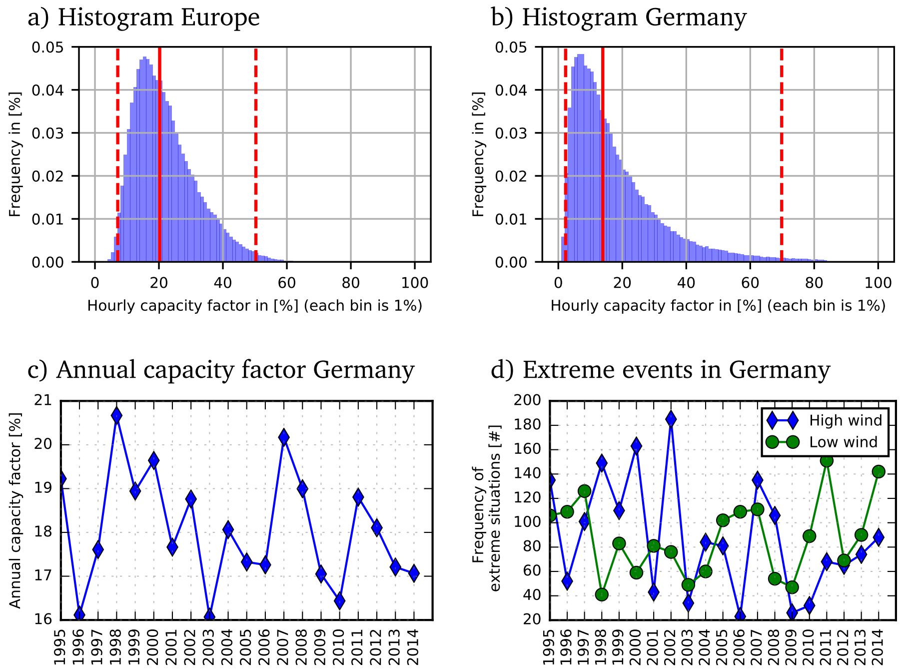

Figure 5.3: Distribution of the hourly capacity factors in Europe (a) and Germany (b) between 1995 and 2014, red dashed lines illustrate the 1% and 99% percentiles and red solid lines the median. The annual moving average (c) and occurrence of extreme events (d) in Germany are shown for the same period.

This leads on the one hand to a low probability of very low CF and on the other hand to a very low probability of very high CF. In this paper, we define low wind situations as situations below the 1% percentile threshold of the wind production distributions and, vice versa, high wind situations above the 99% percentile of the wind production distributions (exemplary plotted for Europe and Germany in Figure 5.3i and 5.3ii as red dotted lines). These are relative thresholds with respect to the different capacity and production levels. This means the absolute threshold for a German low wind condition is different from the European absolute threshold. The absolute threshold for the German low wind situations is at a CF of 2.27% or a production level of 0.8 h, whereas the European threshold is a CF of 7.13% or 8.54 GWh (high wind in Germany 69.83% or 24.57 GWh, Europe 50.31% or 60.29 GWh).

Figures 5.3iii and 5.3iv show the average annual CF for Germany and the occurrences of low and high wind situations for the whole time period. We see that the average CF can have huge variations between different historical years. For example between 1996 and 1998 the difference amounts to 4.6%-points in CF which means that in 1998 wind was able to generate 14.04 TWh more compared to 1996. In relative terms, the wind power production in 1996 would have been only 78% of the wind power production in 1998. The maximum deviation to the 20-year-average annual CF is 14.4% (see Table 5.2).

Table 5.2: Statistics of the simulated annual capacity factors for Germany between 1995 and 2014.

	Capacity Factor [%]	Deviation to mean [%]
min	16.1	-11.0
25%	17.2	-4.9
mean	18.1	-
75%	19.0	5.0
max	20.7	14.4

One relevant point is wind degradation, i. e. the wind power adjustment process which could occur due to climate change. By Figure 3c no annual degradation process is obvious. A corresponding OLS estimation shows no significant trend in annual wind capacity factor degradation. Small-scale regional effects could occur but have limited relevance for our national-level investigation focus.

The variation between different years is not only large in average terms but also with respect to the extreme high and low wind conditions. In Figure 5.3iv we can see that there is a large variation in the occurrence of low and high wind conditions in Germany. Based on the observations there is no clear link between the frequency of extreme wind conditions and the annual wind power production. For instance, 2011 was an average year in terms of annual wind power production with an exceptionally high number of low wind conditions and a comparably low number of high wind conditions. It is therefore not sufficient to define a representative year which covers characteristics of the whole time horizon that can, for example, be used for energy system modeling purposes. Especially in order to capture extreme events that may determine the reliability of future electricity systems, it is essential to consider observations from a long historical time span.

5.3.4 Balancing potentials in Europe and Germany

Balancing effects between different European countries can occur as long as there is enough transmission capacity available between countries. In this paper we will abstract from the limitations of transmission capacity and shed light on the theoretical potential of balancing effects assuming sufficient availability of transmission capacity. We are aware of the fact, that the underlying data by itself has limited potential to quantify the correct amount of transmission extensions. To quantify this, a dynamic energy dispatch and investment model would be necessary which accounts for physical power flows. However, the underlying data can serve as high-detailed input for further investigations in energy market models (e.g. Bertsch et al. (2016)) and is thus highly relevant. The work of Hagspiel et al. (2017) applies our wind dataset to evaluate the regional cooperation benefits on firm capacity under security of supply aspects.

For the analysis of balancing effects we distinguish two situations that are relevant with respect to the electricity system. First, balancing effects are beneficial when electricity generation of two locations are uncorrelated. We will refer to this case as average balancing effects. In this case both countries can benefit from the exchange of electricity because generation may be higher in one country when generation is low in the other. Second, we will analyze the case of balancing effects during low wind conditions in Germany. For both balancing effects, average and low wind, we will focus on Germany within the European electricity system.

Figure 5.4 shows the correlation of wind power production for each country to the German power production over the whole time span from 1995 to 2014.

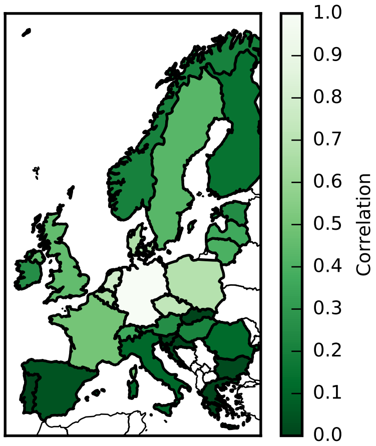

Figure 5.4: Correlation of German and European wind power production between 1995 and 2014.

All countries are positively correlated with the German wind power production and as expected more distant countries are less correlated by trend. This is in line with the results of Monforti et al. (2016), although they focus on the correlation compared to Europe instead of Germany (based on a time span 1961-2050 in daily resolution from a data ensemble of 12 regional climate models). For Germany, it is beneficial to be connected to countries with low correlations with their national wind power supply. This may for example be the case for Norway or Austria, which are close by but rather uncorrelated in terms of wind power production. Whereas Germany has already very high transmission capacity to Austria, the connection towards Norway is so far only able via Denmark and a direct connection is currently being built (NORD.LINK). By trading electricity with countries of low correlation, Germany and the respective counter party are both able to benefit during average conditions. When we take a closer look at low wind conditions, this may not necessarily be the case.

During low wind conditions, balancing effects may be lifted when there is still power production available within Europe and especially in neighboring countries. As previously defined, we use a threshold of 2.27% CF which identifies the lower 1% percentile. Figure 5.5 shows the histogram of the production in Europe and neighboring countries, when Germany is experiencing low wind conditions.

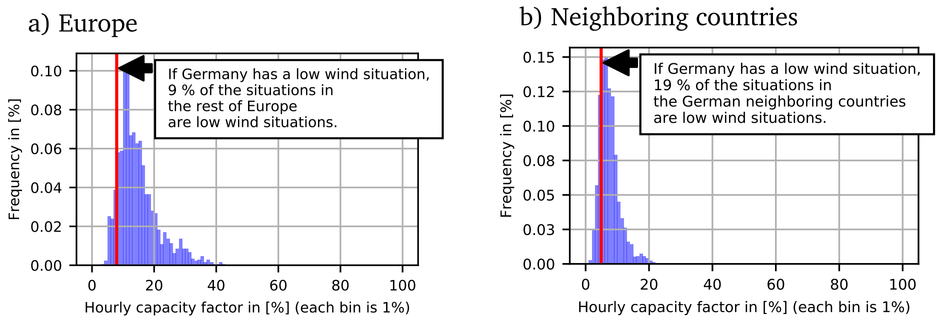

Figure 5.5: Hourly capacity factor distribution for Europe (a) and neighboring countries (b) during low wind conditions in Germany between 1995 and 2014.

In most cases, the production in Europe and the neighboring countries are also low compared to their 20-year median production (cf. Figure 5.3). Nevertheless, the power production is only in some cases a critically low wind situation as to the 1%-percentile threshold for the CF. Within Europe, the capacity factor in 9% of the cases is also below the 1% percentile. For neighboring countries, this probability increases to 19%, which would occur with a joint probability of 0.19%. In all other low wind cases we can expect balancing between countries to take place. This means not all countries are experiencing extreme low wind conditions at the same time.

5.3.5 Balancing potentials within Germany

Balancing effects can also occur on geographical scopes within countries. Due to the high spatial data resolution of our dataset, the above methodology can easily be extended to analyze inner-country effects. The subsequent focus is Germany. High Northern (i.e. coastal) wind speeds and a corresponding subsidy scheme have caused higher installed wind capacities to be located in the Northern regions. The North German plain is located in this area, which shows low surface roughness enhancing the occurrence of strong winds in near-surface layers. South-German topography consists of mid- and highlands with a higher surface roughness. This leads to significant differences in regional wind locations within the country.

Figure 5.6 shows the distribution of capacities (5.6i), average CF (5.6ii) and correlations of CF time series to the total German wind production time series (5.6iii) in Germany.

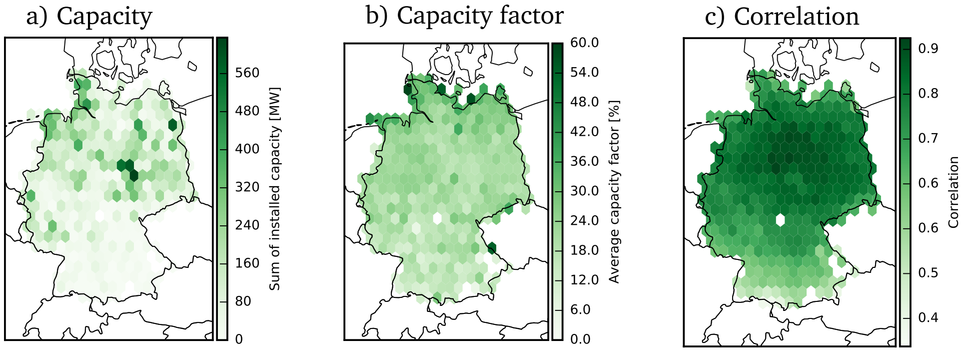

Figure 5.6: Wind production in Germany a) sum of installed capacity within each hexagon, b) average capacity factor of wind turbines in each hexagon, and c) correlation of energy production in each hexagon with the total German wind energy production

The value of each hexagon is obtained by an aggregation of the individual wind turbine values in that area. The capacity is the sum over all capacities within the area. The CF is defined as the average total wind production divided by the total capacity. The correlation is calculated based on the production in each hexagon compared to the total German wind power production. Darker colors point to higher capacities, capacity factors or correlation values.

Wind power capacities are mainly located in the northern part of Germany. The highest concentration of capacities can be found in the north-eastern part. Higher CF are located at the Northern coast. The main reasons are higher wind speeds which evolve over the sea and the North German plain due to more northwest wind situations in central Europe.

The highest correlations of wind power production can be found in the North German plain. Here, high installed wind capacities lead to an implicit weighting of the correlation time series. The aggregated correlations of the hexagons are up to 0.9 in this area compared to the total German wind production. Wind locations (i.e. the corresponding aggregated values per hexagon) in the Southern regions can be weakly correlated as 0.3. This difference is driven by different wind speeds (e.g. due to the alps and the country-side) as well as less installed wind capacities.

With the same motivation as of the European analysis, which stated that favorable wind locations should have high capacity factors but should be less correlated, we find the following: to achieve highest wind production per installed MW wind capacity, wind locations are favorable in Northern windy areas. However, due to the high correlation in the North German plain, coastal regions would be more favorable compared to areas in the center of the North German plain. Lowest correlation values can be achieved in the Southern regions, i.e. close to the Alps. In this region, however, capacity factors are very low.

5.4 Conclusions and implications

In this paper, we present a temporal (hourly) and spatial (wind park level) high-resolution wind production model. We apply the model to the 20-year high resolution COSMO-REA6 reanalysis dataset for the EU-28 region (plus Norway and Switzerland). The focus is on the characteristics and the variability of wind power production over 20 years. This dataset and the corresponding analysis allow us to contribute to existing research in three aspects.

First, we show that our wind input dataset, the COSMO reanalysis product, outperforms the widely used ERA-Interim and MERRA time series. Taking this as a basis, we create a novel time series dataset for wind production with our new model and the unique COSMO-REA6 wind speed data. It covers a time span from 1995-2014 with an hourly resolution for each European wind park. Our model can easily account for higher temporal or spatial resolution and is only restricted by available input data.

Secondly, we identify the annual variability as well as the frequency of high and low wind situations in Germany for the 20 years of simulation. This analysis indicates that there is no single representative wind year which inhibits characteristics of average production as well as extreme situations. Thus, input weather years need to be carefully chosen and a longer time span could lead to more robust results in energy system modeling.

Thirdly, we find that Germany and European countries have significant balancing effects and can benefit from electricity transmission. On the one hand, we find evidence for average balancing effects based on correlation values. On the other hand, we identify that only a share of low wind situations in Germany are facing low wind situations in neighboring countries or in entire Europe at the same time.

Finally, the scalable REOM as well as the derived new wind production dataset allow further detailed analyses due to their high resolution applicability. The results should be considered in transmission extension analyses as this is strongly dependent on statistical balancing effects of wind production. Our 20-year time-horizon can be assumed to incorporate all relevant occurrences of wind situations. The general investigation can be extended to analyze local balancing effects which has a high relevance for countries with strong regional concentration of wind parks at windy locations, e. g. Germany. The high resolution wind production dataset can increase the accuracy of electricity system modeling to evaluate security of supply under balancing effects as well as the regional market value of wind in a nodal pricing model. Further improvements of the input wind park dataset would contribute to a higher accuracy of the wind energy model.

5.5 Appendix

5.5.1 Distribution of installed wind capacity

The underlying wind park dataset (i.e. installed capacities) varies across Europe. The regional distribution is shown in Figure 5.7, which indicates an accumulation at coastal areas: Northern Germany, coasts of Spain as well as Italy.

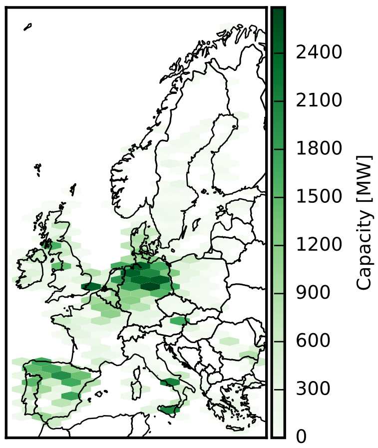

Figure 5.7: Distribution of the regional wind capacity [MW] within Europe (aggregated to local hexagons)

The absolute installed capacity of wind power per country (cf. Figure 5.8), which is used for simulations, shows a highest installed capacities in Germany, Spain and Great Britain, followed by France and Italy.

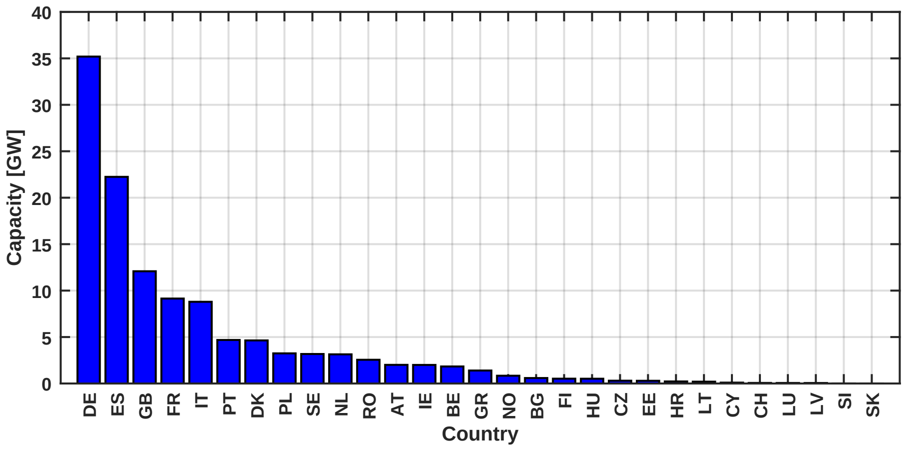

Figure 5.8: Installed wind power capacities [GW] in European countries.

The installed capacity (in combination with the regional wind speeds has influence on the correlation, capacity factors as well as balancing effects.

5.5.2 Completeness of the wind park dataset

The underlying wind park dataset contains relevant information for the technical characteristics of the installed European wind parks. However, not all information are contained for each wind park or turbine. Table 5.3 provides statistics as to the completeness of each technical characteristic as well as the used default parameter, in the case of missing values.

Table 5.3: Parameter availability for all wind parks in Europe for the database of *The Wind Power* and their default value averaged over all countries.

Parameter	Availability (%)	Default value
Location	100	-
Commission date	100	-
Number of turbines	100	-
Hub height	60.6	90 m
Rotor diameter	37.5	66.7 m
Cut-in	66.8	3.5 ms^{-1}
Cut-out	66.8	25 ms^{-1}
Rated speed	66.8	12 ms^{-1}

5.5.3 Evaluation

Subsequently, we evaluate the modeled wind production data and data provided by the EEX transparency platform. The model is not calibrated to this data since the EEX data is an approximation itself. In addition the EEX dataset only covers Germany and similar informations are scarce concerning all European countries.

Figure 5.9 compares the diurnal cycle of both time series. Our simulations show only slight differences with higher values during daytime and lower values in the night.

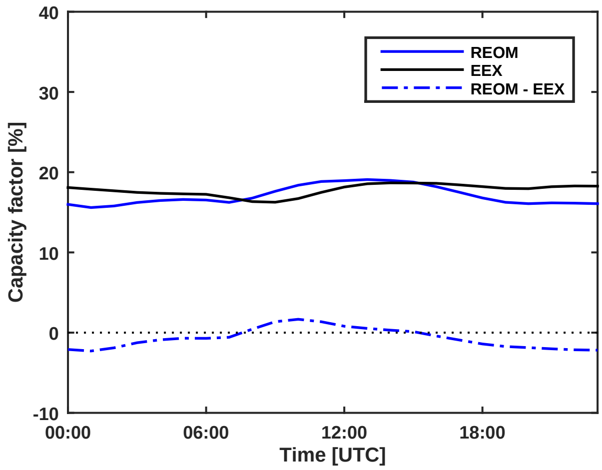

Figure 5.9: Moving average of the diurnal cycle of capacity factors between 2010 and 2014 in Germany for REOM (blue, solid), EEX (black, solid) and their residual (blue, dashed).

Figure 5.10 shows the high correlation of the modeled CF to the calculated factor based on the EEX data. For very low CF, our simulations are higher than for EEX while this behavior turns around for CF ranging between 10% and 30%.

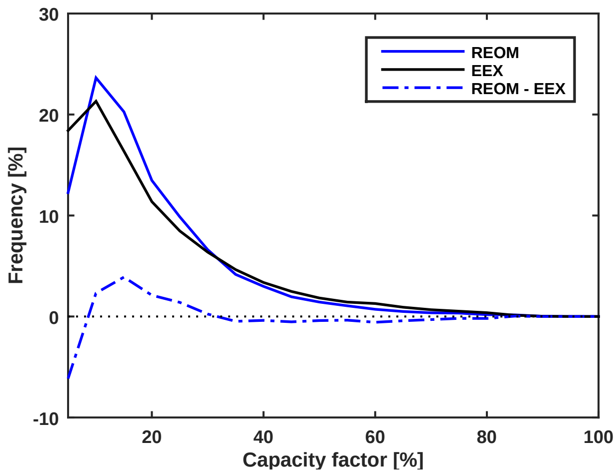

Figure 5.10: Occurrence frequency of hourly capacity factors for REOM (blue, solid), EEX (black, solid) and their residual (blue, dashed) in Germany between 2010 and 2014

6 Build Wind Capacities at Windy Locations? Assessment of System Optimal Wind Locations

In recent years, the installed capacities of renewable energies have steadily been increasing. This raises the question for optimal locations of renewables. Ideally, the market prices induce efficient locations. Distorting effects, i.e. non incorporation of the physical grid situations, could lead to sub-optimal regional incentives compared to a system optimal perspective. In this paper, the wind production revenues under nodal and zonal pricing are investigated. The analysis is extended to the widely used wind value factor. The analysis identifies the zonal pricing wind revenues as inefficient location signals. Location signals need to consider the grid situations. Wind revenues could face an average increase of 21% and more than 200% for certain locations. This is highly relevant to design efficient subsidy schemes or to identify regional grid and capacity extension necessities.

6.1 Introduction

The energy transition promotes huge extensions of renewable capacities. This was mainly achieved by subsidy schemes. Several common subsidy schemes are (to some extent) decoupled from market price signals as for instance the fixed feed-in tariff (see Couture and Gagnon (2010)). The IEA strongly encourages the market integration of renewable energies (IEA, 2016) in the long-run. This transfers market incentives to the renewable operators and should increase efficient locational investments and production decisions. Especially volatile renewables need to consider regional simultaneity effects in production (also known as regional correlation or self-cannibalization effects (Hirth and Müller, 2016, Kreuz and Müsgens, 2017)). Thus, the market situations with their timely varying electricity prices (dependent mainly on demand, supply and nowadays weather) have an increased importance to choose optimal renewable locations. From an operator's perspective, optimal locations aim for a maximization of the renewables' profits which transfers to a maximization of revenues due to almost zero marginal costs of wind production.

However, the market revenues under zonal pricing might incentivize sub-optimal system locations. In markets with zonal pricing, physical grid situations and congestion are not necessarily internalized in the market prices within the bidding zones. This holds true for instance for the European electricity markets. Thus, a discrepancy could occur between the optimal locations under *zonal pricing* (i.e. without internalized transmission situations) and the optimal locations under *nodal pricing* (i.e. with internalized transmission situation). Despite the revenues, the market value factor is widely used as an indicator to assess the contribution to the electricity market especially for renewables. The market value factor is the relation between the production-weighted revenues per MWh and the average market price. Based on regional market value analyses, insights on beneficial locations could be derived as well. However, the market value as an aggregated indicator is lacking essential information like total production levels and the corresponding time structures. Therefore, it is questionable if the market value factor is suitable to assess regional production signals.

In this paper, two relevant questions are answered to identify optimal renewable locations: (1) Are the *revenues under nodal pricing* the preferable indicator to assess optimal renewable locations compared to the *revenues under zonal pricing*? And (2), are the value factors of renewables sufficient to evaluate optimal locations? Both findings are highly relevant for the design of subsidy schemes as well as capacity and grid extension processes and of course for the adequate evaluation of wind production.

The analysis is performed on the case of wind production in Germany due to several reasons. Wind capacities contribute significantly to the German electricity production. As to AG Energiebilanzen (2017), wind production has a share of 12.1% of the total German gross electricity production in 2016. Wind production is a main technology to achieve the energy transition to a highly renewable-based energy system in the long run. Germany has built a dominant share of its wind capacities at northern windy locations favored by an implemented feed-in tariff.[1] This implies challenges to the transmission grid in some situations. Primarily in situations with strong wind (and low demand), the grid is not capable to transfer the wind production to the load centers (Kunz, 2013). Therefore, strong deviations between the optimal wind locations under zonal or nodal pricing can be expected.

[1]An early version of the renewable feed-in tariff was implemented in 1991 (see Bundesregierung (1991) which was adjusted in between and lasts until 2012. In 2012, the feed-in tariff was changed to a feed-in premium (Bundesregierung, 2012) and adjusted in 2014 (Bundesregierung, 2014) and 2017 (Bundesregierung, 2017). However, the design of the feed-in premium is still very similar to a feed-in tariff and might favor the similar locations.

The underlying research is based on two literature fields: The optimal wind locations from an operator's perspective as well as the market value factor. Existing research on optimal wind locations cover mainly the electricity systems (or markets) perspective in order to reduce integration costs or smooth the production profiles. This is the case for instance in Roques et al. (2010) who identify risk-minimal or volatility-minimal wind locations on a country level (DE, AT, FR, DK, ES) under co-operation. In contrast to this, the operators' potential revenues are identified since this should be the economical main objective for new wind capacities. Additionally, the focus lies on inner-country effects as in Grothe and Schnieders (2011). In contrast to the underlying research, they aim at smoothed production instead of operators' optimal locations. Burke and O'Malley (2008) and Burke and O'Malley (2011) focus on optimal wind locations under a revenue maximizing perspective. They identify optimal locations in nodal pricing test networks with consideration of physical transmission characteristics. However, they do not consider high-resolution real world data (as it is done for Germany) and they do not compare the the nodal pricing revenues to the typical zonal pricing revenues. Pechan (2015) is very close to the underlying research in that way that she compares (among others) the spatial distribution effects on wind capacity under a nodal and under a zonal market premium subsidy scheme. In contrast to the present research, she uses a strongly simplified model with six nodes and eight lines. Furthermore, she assumes additional subsidy schemes (fixed feed-in tariff or market premium under nodal and under uniform) instead of a pure market integration. The subsidy schemes may distort the optimal wind locations by its additional income stream (cf. Wagner (2016)).

The second branch of literature focuses on the *market value* of intermittent production technologies applied for instance in Joskow (2011), Fripp and Wiser (2008) and Hirth (2013). The market value widely serves as an indicator for the contributed value of renewables to the electricity markets. Hirth (2013) focuses on the estimation of the decreasing market value of wind (and solar) under a higher market share with empirically and numerically methods for different countries. This investigation is extended in Hirth (2016) (to account for hydro-electric storage potentials). Both analysis consider a country-wise investigation in contrast to the underlying regional, i.e. inner-country focus. Grothe and Müsgens (2013) extends the market value definition of Hirth (2013) and uses locational wind generation. They compare 37 exemplary wind parks within Germany and find that the locational profits of a wind turbine are affected (dependent on the subsidy scheme). Similar results are found by Elberg and Hagspiel (2015) who use a regional copula based methodology to estimated regional expected market values of wind in Germany. Both, Grothe and

Müsgens (2013) and Elberg and Hagspiel (2015) focus only on wholesale electricity market prices and neglect the influence of the transmission grid to the market value. As mentioned in Hirth et al. (2015) and as we see in the analytical analysis of Wagner (2016), the transmission situation might have strong impacts on capacity locations. Due to inner-German grid congestion, the values as well as the revenues are expected to deviate strongly with and without consideration of the transmission situation. This research considers, identifies and compares these distorting effects.

To achieve new insights, the underlying research is based on a nodal electricity market model with a DC load flow grid representation for Germany. This allows to consider the physical transmission situations, necessary for the assessment of the optimal wind locations. The main advantage of the underlying modeling methodology is the possibility to consider one electricity system with two different pricing regimes (zonal pricing and nodal pricing). Such a comparison is not possible with classic empirical methods since zonal and nodal pricing data do not exist simultaneously. Additionally, the endogeneity between wind production and electricity prices is represented in the present model which could be hard to include within empirical models (especially for future situations). The underlying methodology is applied for the modeled year 2014. However, the methodology is easily extendable to consider future years (regarding grid and capacity situations).

The present results are distinguished between the nodal pricing perspective, which internalizes physical transmission situations, and the zonal pricing perspective, which abstracts from electricity transmission. The zonal pricing regime represents the current design of most European electricity markets (among them Germany). The nodal pricing regime is applied for instance in the US electricity markets of PJM or ISO New England (Joskow (2005) or Litvinov (2010)). It can be considered as an economic benchmark compared to the zonal pricing, since costs for transmission and congestion are internalized Hogan (1999). For the nodal and zonal perspective, the wind revenues as well as the wind value factors are analyzed and compared.

The paper is organized as follows: Section 6.2 describes the methodology of the (nodal) electricity dispatch optimization model. Based on this, relevant data is derived to evaluate the revenues and value factors of wind. Section 6.3 compares the results under nodal pricing to the results under zonal pricing. The analysis is applied, first for the revenues and afterwards for the value factors. Section 6.4 discusses the results and shows the significance for locational signals as well as the design of subsidy schemes. Section 6.5 concludes and identifies further research.

6.2 Methodology

To identify optimal wind locations, high-resolution fundamental electricity market optimization model is applied (description in 6.2.1). A nodal model representation of Germany which respects inner-German transmission situations gives information about the optimal wind locations. In line with economic literature, the nodal model definition can be considered as the economic efficient benchmark due to internalized transmission costs (see for instance Schweppe et al. (1988) and later discussed in Hogan (1999), Chao et al. (2000), Green (2007), Leuthold et al. (2008), Burstedde (2012)).

In contrast to the theoretical efficient nodal representation, Germany and most other European countries have implemented a zonal (i.e. country-wise) market design with uniform pricing and neglect inner-country transmission situations in the wholesale market prices.

In zonal electricity markets, re-dispatch is a possible congestion management mechanism. As soon as the market-driven dispatch, i.e. the planned power plant utilization, leads to critical transmission line utilizations, an adjustment is performed. The responsible TSO instructs producers (regionally) before the grid congestion to reduce their production. In the same time, producers (regionally) behind the grid congestion are instructed to increase production. This production shift reduces the electrical power flow on the congested lines. A financial compensation for the shifting producers is payed which does not affect wholesale market prices. Especially the extension of wind and PV production have increased the problem of (weather-driven) grid congestion. In 2010, 1588 hours of re-dispatch were necessary. This number steadily increased in the subsequent years to 5030 hours in 2011, 7160 hours in 2012, 7965 hours in 2013 to 8453 hours in 2014 (see Bundesnetzagentur (2016)). As one main driver, the strong increase in northern wind production is mentioned.

In contrast to a zonal model with re-dispatch, a nodal model accounts implicitly for grid congestion and leads to market price deviations. These price deviations would direct give monetary incentives for electricity production, especially for northern wind producers. Thus, it is highly-relevant to analyze the market revenues for wind producers under a realistic nodal electricity valuation (which includes grid congestion externalities) instead of observing the artificial zonal wind valuation (with re-dispatch). To analyze the differences in wind valuation, the optimization model is applied with a nodal pricing configuration as well as a country-wise uniform (zonal) pricing configuration.

6.2.1 General model description

The applied fundamental electricity market model is a partial equilibrium model. Costs of electricity production are minimized under a inelastic demand function and subject to typical electricity market model restrictions (see next section). The model framework is PyPSA, which is an open source energy modeling framework.[2] The regional focus of the model is Germany with a nodal resolution. Neighboring countries are modeled simplified as one node without inner-country grid restrictions. Overall, the model incorporates 575 nodes and 854 connecting lines. The temporal focus is the year 2014 with an hourly resolution (8760 h). The model optimization assumes perfect foresight and neglects uncertainty for the corresponding timeframe. The considered network topology is shown in figure 6.1 and based on *SciGRID* (Matke et al., 2016, `www.scigrid.de`).

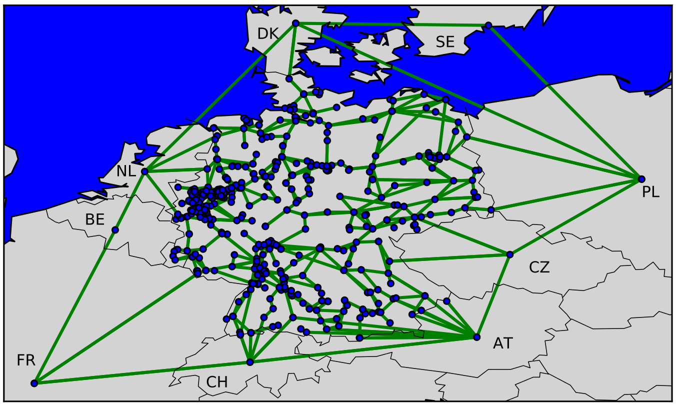

Figure 6.1: Network topology of the optimization model. The focus is a nodal resolution in Germany with its surrounding neighbor countries. Each dot represents one node, which are connected via transmission lines (220 kV and 380 kV).

[2]`http://pypsa.org/`, PyPSA Version 0.4.2, release date 17 Jun 2016

6.2.2 Fundamental equations

The model minimizes short run total system costs of the electricity production, which are the sum of the short run marginal generation costs times the generation over all nodes n, supply technologies s and timesteps t:

$$\min Totalcosts = \sum_{n,s,t} marginalCosts_{n,s,t} * gen_{n,s,t} \tag{6.1}$$

This is subject to following main restrictions:

- *Nodal power balances:* The electricity supply needs to equal the demand for each node n and each timestep t. Electricity supply can be provided by nodal generation $gen_{n,s,t}$ as well as electricity flow from connected nodes $flow_{l,t}$:

$$\forall n,t: \qquad \sum_{s} gen_{n,s,t} + \sum_{l} K_{n,l} flow_{l,t} = demand_{n,t} \tag{6.2}$$

  Here, $K_{n,l}$ denotes the incidence matrix which determines the connection of each line l to the corresponding nodes n. The generation $gen_{n,s,t}$ reflects production of conventional power plants, renewable power plants and storage units. Note that production by storage units and electricity flow can be negative in the case of storage uptake or power outflow, respectively.

- *Generation constraints:* Each generators' production (conventionals, renewables and storages) for each timestep t is restricted by its total capacity adjusted by the time-dependent availability:

$$\forall n,s,t: \qquad 0 \leq gen_{n,s,t} \leq availability_{n,s,t}\ capacity_{n,s}. \tag{6.3}$$

  The availability for renewable energies (i.e. wind and solar) is restricted to the exogenous capacity factors.

- *Storage constraints:* Each storage unit (e.g. pumped-hydro storage) is bounded by maximum and minimum storage levels (similar to equation (6.3)) as well as storage uptake and storage dispatch speeds and efficiencies. Storage inflow and losses may apply, dependent on the exact storage technology. Uncertainty is neglected, which generally tends to underestimate the value of storages (and flexible power plants).

- *Power flow:* Electricity transmission between nodes is only possible if a line exists. It is subject to line resistance and voltage magnitudes at the nodes. Note that the model is applied with a DC grid representation on voltage magnitudes. For a line l which is defined from node n to node m, the following equation holds:

$$\forall l, t: \qquad flow_{l,t} = \frac{\delta V_{n,t} - \delta V_{m,t}}{resistance_l} \tag{6.4}$$

in which $\delta V_{n,t}$ represents the voltage magnitude. For details, see for instance Gabriel et al. (2012, Appendix C). For the zonal pricing electricity model, inner-German line restrictions are neglected, which is consistent with the German electricity market design.

Further typical electricity market modeling restrictions apply which can be found at `pypsa.org`; among them efficiency losses or ramping constraints. The applied model is configured to not allow for capacity extensions of generators or lines.

6.2.3 Input Data

For conventional generation in Germany, the power plant list of the German regulator Bundesnetzagentur is used.[3] The power plants are matched to the nodes by its smallest distance. Neighboring countries are based on public available sources, e.g. Eurostat. Marginal costs of conventional generations are assumed as to Table 6.1 and have no regional differentiation.

Table 6.1: Model input: Marginal costs of production

Fuel	Marginal Costs [EUR/MWh]
Nuclear	8
Lignite	10
Hard coal	25
Gas	50
Oil	100

The demand time series is the hourly national demand from the ENTSO-e transparency platform for 2014. The German demand is distributed to the nodes via the share of the regional GDP and the regional population. A detailed description can be found in Appendix 6.6.1. The distribution accounts for annual values and neglects hourly demand variations.

[3] `https://www.bundesnetzagentur.de/SharedDocs/Downloads/DE/Sachgebiete/Energie/Unternehmen_Institutionen/Versorgungssicherheit/Erzeugungskapazitaeten/Kraftwerksliste/Kraftwerksliste_2016.xlsx`. Version of 03. Mar 2016, filtered for end of 2014 running power plants

The production profile of wind energy is based on a high-resolution meteorological weather model in combination with a wind park database and described in detail in Section 6.2.7. The production profile of solar energy is modeled based on the German solar production data of EEX in combination with a regionalization approach. This is described in Section 6.2.8

The transmission grid (i.e. 220 kV to 380 kV voltage levels) is based on the SciGRID dataset[4]. The distribution grid (i.e. voltage levels below 220 kV) cannot be considered due to insufficient data availability. Neighboring countries are considered as one node, such that no inner-country grid information is required. However, connections between neighboring countries are restricted by ENTSO-e transmission capacity data. Grid connections between neighboring countries and Germany are connected to the correspondent nodes in Germany and the typical grid characteristics (resistance, voltage magnitude) based on SciGRID.

The dispatch model is applied with two configurations which will be compared to each other in the latter analysis. First, the dispatch model will be applied with a nodal pricing configuration of Germany. The inner-German transmission restrictions must not be violated which results in different nodal prices. Second, the zonal pricing configuration is applied which means that no inner-German transmission restrictions hold. This is similar to the current German market design with one wholesale electricity price. In the real market, re-dispatch is applied to ensure network stability. In this modeled zonal pricing system, the consideration of re-dispatch is not necessary since the focus is on the market revenues and not on the technical feasibility of the load flows. Thus, the costs of re-dispatch (which increase total system costs but not the market revenues e.g. of wind production) are out of the scope of the investigation.

6.2.4 Model limitations

The model underlies some simplifications to make it tractable in reasonable computational time. The model is a linear optimization model and does not incorporate minimum load constraints as applied in unit commitment models (mixed integer linear programming, see e.g. Carrion and Arroyo (2006)). In contrast to unit commitment models, linear models have the relevant advantage that the dual variable of the electricity-balance equation can be interpreted as (perfectly competitive) marginal prices which is not possible in classical mixed integer models due to non-

[4] `www.scigrid.de`, release date 18. July 2016, Matke et al. (2016)

convexities (Bjørndal and Jörnsten, 2008, Ruiz et al., 2012). The model focuses on the short-term dispatch situations such that long-term effects as investments and capacity extensions are not included (as e.g. in Bertsch et al. (2016)). This reduces the model size and allows for a high number of inner-country nodes (>500 nodes and >800 lines) instead of a country-wise representation. The model has perfect information over each optimization interval and does not include e.g. stochasticity (as described for instance in Wallace and Fleten (2003) or Birge and Louveaux (1997)), which reduces model complexity. Heat production is neglected which implies that we overestimate in the model the cost of combined heat and power.

6.2.5 Revenues of wind

In the results chapter, we investigate and compare the revenues of wind turbines as these are the relevant criteria for the regional investment decisions of operators. Marginal costs of wind production are almost zero and thus profit maximization translates to revenue maximization. Regional site costs are assumed to not deviate across the nodes and are thus neglected. The wind revenues $R_{n,wind}$ at a given node n from the electricity market (without subsidies) can be expressed via:

$$R_{n,wind} = \sum_{t \in T} p_t \; gen_{n,wind,t} \tag{6.5}$$

$$\tilde{R}_{n,wind} = \sum_{t \in T} p_{n,t} \; gen_{n,wind,t} \tag{6.6}$$

where T is the total time span (here: 8760 hours of the year 2014), p_t is the electricity price [EUR/MWh] in hour t, and $gen_{n,wind,t}$ is the generation in [MWh] at bus n for supply tech $wind$ in hour t normed to 1 MW (for comparison reasons). Note that the difference between the revenues is the electricity price which is uniform in the first case and node-differentiated in the second case. Thus, R reflects the revenues under zonal pricing whereas $\tilde{R}$ reflects the revenues under nodal pricing and consideration of internal physical transmission situations. Note that the modeled revenues in general do not incorporate any subsidy payments. Figure 6.2 illustrates the difference between the zonal and nodal revenues with a simplified two-nodes example. In case of a grid congestion, the market prices are nevertheless identical in the zonal pricing regime, whereas price deviation could occur in the nodal pricing regime. Under identical wind production at both nodes, the revenues are identical under zonal pricing whereas the prices deviate under nodal pricing. Note that for the German case, typically, the northern wind production is higher due to higher wind

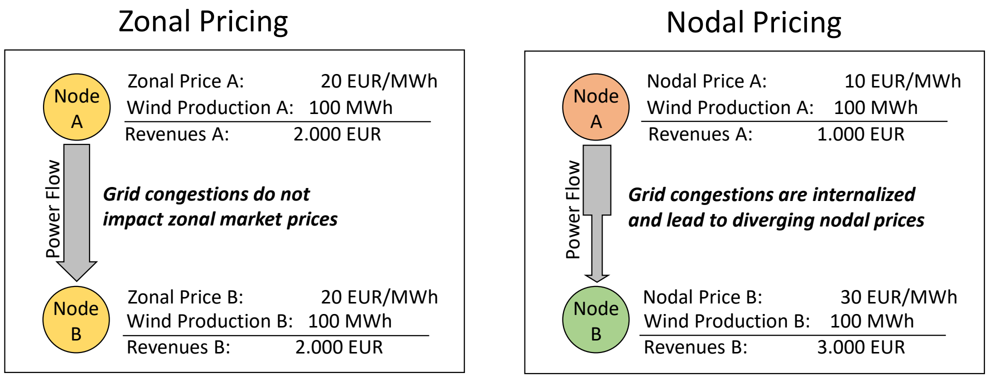

Figure 6.2: Simplified two-node illustration of the difference between the revenues under zonal pricing (left) and nodal pricing (right). Assume that we have two nodes which are connected by one transmission line. In the case where the transmission line is congested, we still face the same prices for Node A and Node B in the zonal pricing regime. The same situation could lead to price differences under nodal pricing. For identical wind production at both nodes, the revenues are identical in the zonal pricing regime (independent of the grid situation) and deviating in the nodal pricing regime.

speeds and higher wind power capacities. In windy situations, this leads to potential grid congestion from north to south. However, under zonal pricing, one MWh northern wind production is remunerated equally to one MWh southern wind production even in the case of grid congestion. Under nodal pricing, equally remuneration of one unit wind production is not necessarily the case. Thus, wind production recives the regional market price of energy.

6.2.6 Value of wind

We calculate the *market value factor of wind* according to the definition of Joskow (2011) and Hirth (2013). Thus, the market value factor of wind can be interpreted as the relation between the production-weighted wind revenues and the average market price.[5] It is defined as

$$\forall\ n: \qquad v_n := \frac{\mathbf{p}^T \mathbf{g}_n}{\mathbf{p}^T \mathbf{1}} = \frac{\left(\frac{\sum_t p_t \ gen_{n,wind,t}}{\sum_t gen_{n,wind,t}} \right)}{\left(\frac{1}{n} \sum_t p_t \right)} \tag{6.7}$$

where $\mathbf{p}$ is the vector of market prices (modeled system marginal costs), upper T denotes the transposition, $\mathbf{g}_n$ is the generation weights vector at node n, t denotes the

[5]The value factor is more suitable for later comparison since it is denominated by the base price and shows the relative value drop instead of the absolute value drop.

hours, and **1** is a vector of ones of corresponding length. The denominator of the average market price transforms the market value from EUR/MWh to a percental factor for comparability. A market value factor of 90% indicates that a producer is able to derive 90% of the average market price with its (volatile) production compared to a permanent operating producer. That could be the case, if the (volatile) production has a market price reducing effect, as it is the case of zero-marginal-cost renewable production like wind and PV. A market value factor of above 100% is possible, for instance if production is available in peak price situations. Due to different regional wind production profiles at each node, we derive different market value factors of wind even under a zonal pricing regime.

Since the market value factor of wind does not internalize inner-German grid situations, we define the *nodal market value factor of wind* which considers regional prices by:

$$\forall\ n: \qquad \tilde{v}_n := \frac{\mathbf{p}_n^T \mathbf{g}_n}{\mathbf{p}_n^T \mathbf{1}} = \frac{\left(\frac{\sum_t p_{n,t}\ \ gen_{n,wind,t}}{\sum_t gen_{n,wind,t}}\right)}{\left(\frac{1}{n}\sum_t p_{n,t}\right)}. \tag{6.8}$$

6.2.7 Description of wind data

Since this research focuses on the wind revenues and wind values, much emphasize is put on accurate wind production data. The data is based on Henckes et al. (2018). Here, the novel meteorological weather model COMSO-REA6 is applied, which calculates among others, high-resolution wind speeds for the analyzed year on a $6km \times 6km$ grid and several vertical layers. Henckes et al. (2018) uses the derived wind speed data in combination with a European wind park dataset, which includes locations (latitude, longitude), installed capacity, hub-height, turbine data (incl. cut-in and cut-off wind speeds) to calculate the correspondent power curves). A horizontal linear interpolation from the grid coordinates to the exact wind park location is used. On the vertical level, a logarithmic interpolation between the grid layers and the real hub-height of the wind turbines is performed. Overall, this enables to estimate high-detailed wind production per wind park in Germany (and Europe). Figure 6.3 visualizes the capacity distribution, the capacity factors as well as the regional production correlations (aggregated to hexagons) for Germany (cf. Henckes et al. (2018)). The hexagon's production correlation is compared to the total German production timeseries. The wind production per wind turbine is allocated to the nodes by the smallest distance in the electricity market model approach. The wind data of 2014 is chosen for this investigation from the total dataset (cov-

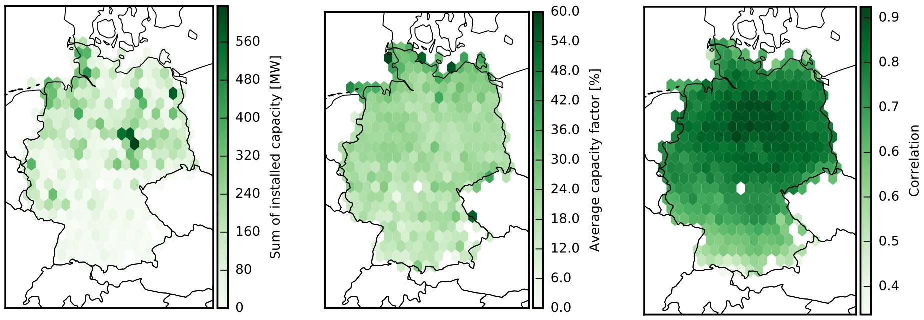

(i) Capacity (ii) Capacity factor (iii) Correlation

Figure 6.3: Wind data for Germany aggregated to hexagons: a) Sum of installed capacity within each hexagon, b) average capacity factor of wind turbines in each hexagon, and c) correlation of energy production in each hexagon with the total German wind energy production. Data from Henckes et al. (2018).

ering each year from 1995-2014 in hourly resolution). First reason is consistency to the demand and solar production year. The second reason is an almost average occurrence of extreme situations (low wind and high wind situations) as well as capacity factor in 2014 compared to the 20-year average (cf. Henckes et al. (2018)). The modeled wind production from Henckes et al. (2018) is equally scaled to the reported production of AG Energiebilanzen (2016), to compensate for the annual production difference.

6.2.8 Description of pv data

The PV production at each node is derived from the German ex-post PV production timeseries of the power exchange EEX in 2014. The total production was distributed via the regional installed capacities to the nodes. The regional installed PV capacities were taken from the *EEG Anlagestammdaten Register*, a register for all subsidized renewable production facilities in Germany. The register covers a total PV capacity of 35.19 GW in 2014 which corresponds to 92% of the total installed PV capacity (38.23 GW) in 2014. This regionalization approach has two drawbacks: (1) For whole Germany, the regional solar radiation is assumed to be the same and (2) the distribution of the installed capacities by the register is assumed to be fixed when the available installed PV capacity data is scaled to Germany's installed PV capacity. The first assumption of a regional invariant PV capacity factor is a rather strong assumption, since the solar radiation in the south of Germany is higher than in the north (see, for instance, the *Global Atlas for Renewable Energies* from IRENA `http:`

//irena.masdar.ac.ae/). However, solar radiation can not (yet) be derived by the used COSMO-REA6 model due to, e.g., instantaneous clouds, fogs or snow on the PV panels. Thus, in this approach, real production data is used but with the drawback of a unified capacity factor. The second assumption of a fixed distribution in the scaling process to Germany's total PV capacity is rather uncritical since the register covers 92 % of the total installed PV data.

6.3 Results

The results focus on two major indicators for the assessment of wind production. First, the regional wind revenues are analyzed. Afterwards, the wind value factors are analyzed.

6.3.1 Wind revenues

To assess regional wind location incentives, the wind revenues are analyzed. The (efficient) *nodal revenues of wind* are identified and compared to the *zonal revenues of wind* (current implemented design). Note that both revenues do not consider any subsidy payments and are based purely on market prices, i.e. a 100% market integration of wind energy.

The nodal revenues: Efficient benchmark with consideration of the transmission grid

Figure 6.4 shows the modeled wind revenues under nodal pricing, i.e. with consideration of the physical transmission characteristics. The revenues are in relative terms to the capacity weighted average German wind revenue.

Following aspects become obvious:

- Highest relative revenues are concentrated in the north-western area. The nodal revenues in the north-western area are mainly in the range between 100% and 200% (or higher) of the average German wind revenues and with peak-revenues up to 350%. However, the strongest wind speeds are typically located at the northern coast (cf. Henckes et al. (2018)). Due to the German transmission situation with mainly north-south congestion, the revenues in the north-western area are higher than the northern coast. The north-western

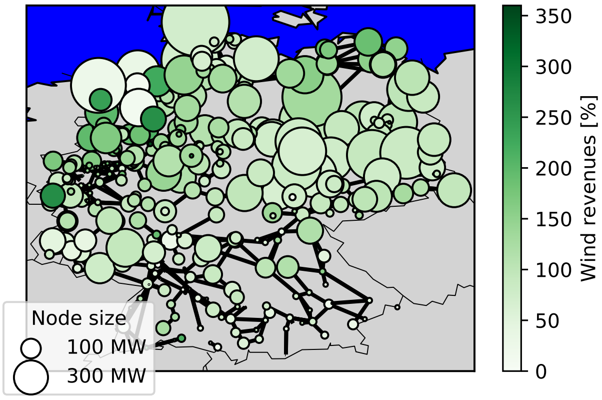

(i) Nodal revenues for all nodes

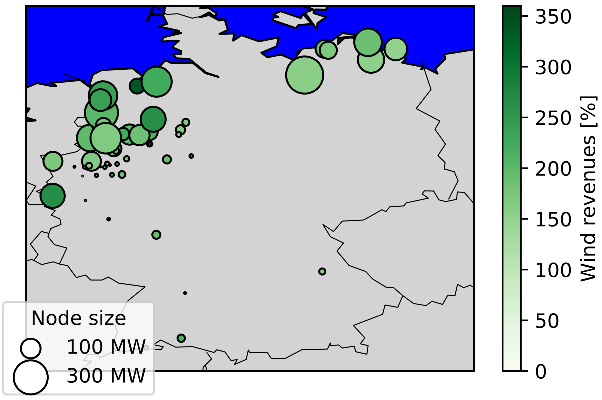

(ii) Nodal revenues for nodes with highest revenues (above 150%)

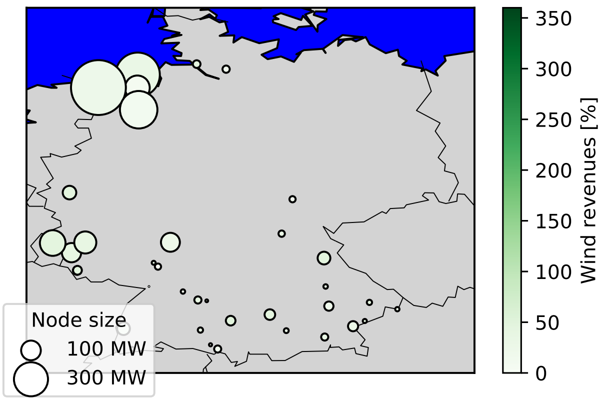

(iii) Nodal revenues for nodes with lowest revenues (below 50%)

Figure 6.4: Wind revenues per node within Germany under *nodal pricing*. (a) Different revenues at each node, (b) at nodes with revenues above 150%, (c) at nodes with revenues below 50%. All nodal revenues in percent compared to the capacity weighted average German revenue. Darker nodes represent higher percental revenues. The size of the nodes indicates the installed wind capacity per node.

wind locations are located slightly behind the mainly congested lines, which are also identified in Bundesnetzagentur (2016).

- Most of the low revenues are concentrated in the southern area but a few are located at the northern coast. In these northern nodes, typically high wind situations occur. Nevertheless, several revenues are below 50% of the capacity weighted German average revenues. This can be explained via the before mentioned grid situation. Additionally high installed capacities lead to simultaneity production and thus strongly reduce electricity prices. These effects are also denoted as cannibalization effects and may further decrease revenues.
- The eastern area with highest installed wind capacities (cf. Figure 6.3) has mostly revenues below 100%, but no extreme high or low revenues. Those effects are mainly driven by the cannibalization effects.

The modeled revenues under nodal pricing can be considered as efficient benchmark with internalization of the power flow characteristics. Under this assumption, regional advantageous and disadvantageous locations are identified.

The market revenues: Today's market situation in Germany (without subsidies)

Figure 6.5 performs the same calculation like before but considers zonal pricing which is the current applied market pricing regime in Germany and does not consider physical transmission flow characteristics. The modeled revenues are relative to the capacity weighted average German wind revenues.

The scale is identical to the former results to guarantee comparability, although the maximum and minimum market revenues have a smaller range and lower deviations. The main findings of the market revenues are the following.

- The concentration of the highest relative revenues are at the northern coastal area with few representatives in the western area. Only few revenues exceed 150% of the capacity weighted average German wind revenue.
- Almost all of the lowest values are in the southern area.
- Many nodes show only slight deviations (between 50% and 150%) to the German average revenue. Locations with a high concentration of the installed capacity (i.e. the eastern-central area) are not below 50% and thus not shown in Figure 6.5iii.

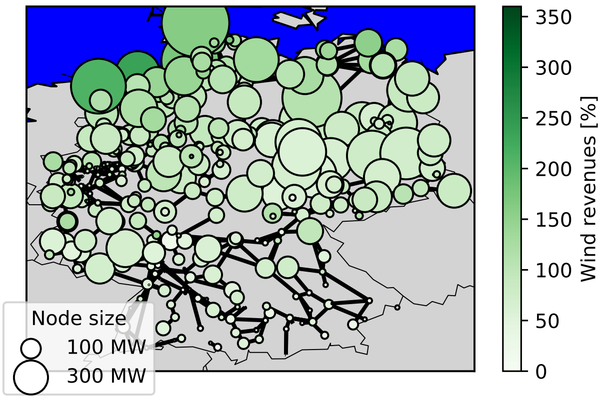

(i) Zonal revenues for all nodes

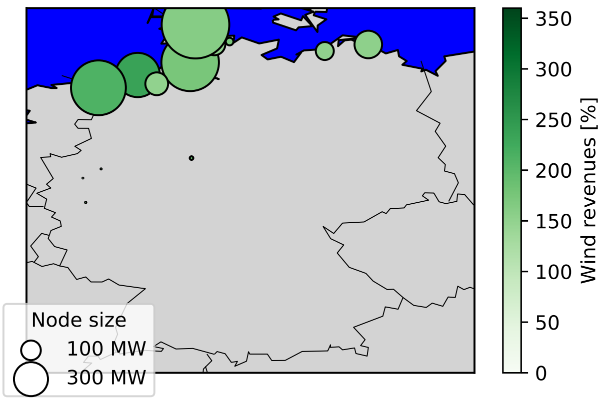

(ii) Zonal revenues for nodes with highest revenues (above 150%)

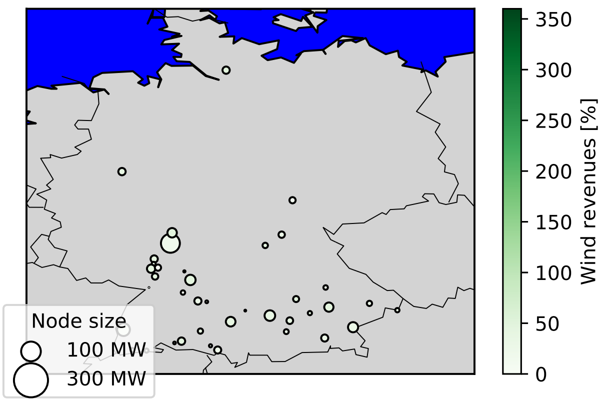

(iii) Zonal revenues for nodes with lowest revenues (below 50%)

Figure 6.5: Wind revenues per node within Germany under *zonal pricing*. (a) Different revenues at each node, (b) at nodes with revenues above 150%, (c) at nodes with revenues below 50%. All revenues in percent to the capacity weighted average German revenue. Darker nodes represent higher percental revenues. The size of the nodes indicates the installed wind capacity per node.

Comparison of the revenues under nodal pricing to the revenues under zonal pricing: Zonal revenues might incentivize inefficient wind locations

Figure 6.6 compares the revenues under zonal pricing to the revenues under zonal pricing (zonal pricing revenues minus nodal pricing revenues). The revenues are relative to the capacity-weighted German average wind revenue per MW (both for nodal and zonal pricing, respectively). The modeled relative nodal pricing revenues deviate strongly from the modeled relative zonal pricing revenues. The capacity-weighted average nodal pricing revenue is 21% higher than the capacity-weighted average zonal pricing revenue (107% compared to 86%). Differences between the zonal pricing revenues and the nodal pricing revenues can be up to ±200%-points. Additionally, the nodal pricing revenues have a broader range (standard deviation of 56%) compared to the zonal pricing revenues (standard deviation of 35%). Detailed statistics can be found in 6.2 in the Appendix 6.6.2. The regional differences deviate regionally. The nodal pricing revenues tend to be higher in the western and southern area and lower at the northern coastal area than the zonal pricing revenues. Cannibalization effects (which have a strong impact on the nodal pricing revenues) are mainly smoothed across Germany, since no transmission congestion restrict the inner-German exchange.

Implications of the revenues

The regional differences between the nodal pricing revenues and the zonal pricing revenues are driven by the regional deviating electricity situation in combination with the transmission characteristics. The well-known German north-south transmission congestion leads to price differences in several (i.e. windy) situations. The electricity price differences induce a differentiation in the wind revenues. Additionally, the cannibalization effects decrease the revenues of certain locations which have high concentrations of installed wind capacities. Both reasons imply that wind capacities in the western area are higher valuated to the electricity system under consideration of the physical transmission characteristics. Northern coastal areas seem to be high valuated locations under the current market design but under consideration of the grid situations they face lower revenues.

As wind operators act profit maximizing, they aim for building new wind capacities at most profitable locations. Under *nodal pricing revenues*, wind investments seem to be more profitable in the western area than in the northern are as identified under *zonal pricing revenues*. This points to a locational discrepancy of profit optimal wind

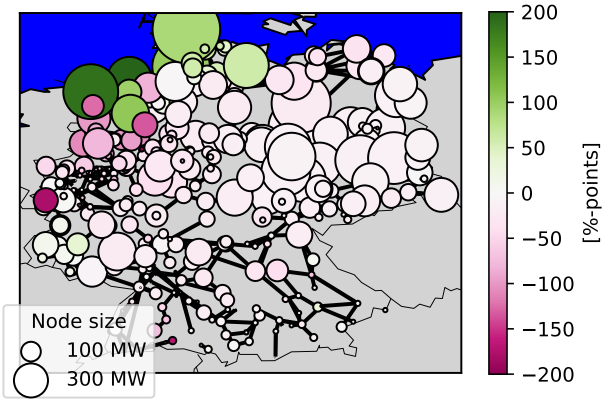

(i) Deltas for all nodes

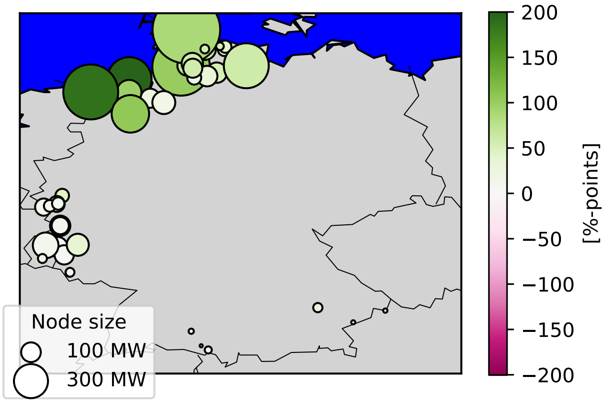

(ii) Nodes with a positive deltas (which are above 5%-points)

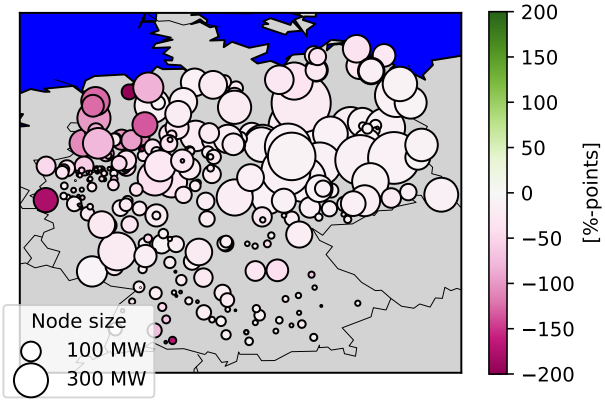

(iii) Nodes with a negative deltas (which are below -5%-points)

Figure 6.6: Difference of relative wind revenues between zonal pricing and nodal pricing for each node within Germany. Wind revenues are relative to the capacity-weighted German average wind revenue under zonal/nodal pricing and than differentiated. A positive value indicates higher market revenues under zonal pricing. The size of the nodes indicates the installed wind capacity per node. The size of the nodes indicates the installed wind capacity per node. Results are for (a) all nodes, (b) nodes with a positive delta, and (c) nodes with a negative delta.

locations between both pricing regimes. Thus, the neglecting of the transmission situation in the current market design causes wind capacities at system-unfavorable locations. Under a future increase in wind capacities, to tackle this inefficiency may become more important.

6.3.2 Value factor of wind

From an operators' perspective, the wind revenues are the main aspect to assess the value of wind production. However, the market value of wind is widely used as an indicator to assess the value of wind to the electricity markets (e.g. Ackermann (2005), Hirth (2013), Hirth et al. (2015), Lamont (2008), Obersteiner and Saguan (2011)). A similar indicator is the electricity base price, which neglects time structure information as well but provides aggregated information. Thus, the investigation of the market value with its aggregated information is of high interest. The following section provides an analysis of the nodal pricing value factors of wind as well as the zonal pricing value factors of wind (cf. Section 6.2.6 for details of the definition). For comparison reasons, the focus lies on the value factor (instead of the value itself), which is denominated by the (regional) base prices.

Nodal pricing value factor of wind

The modeled nodal pricing value factor of wind production as to definition (6.8) is calculated under a nodal pricing regime with respect to physical power flow characteristics. The resulting nodal pricing value factors of wind production are shown in Figure 6.7. Statistics can be found in Appendix 6.6.3. Note that for comparison reasons, the lower range of the scale is limited to the 1%-quantile threshold of the results, which represents a nodal pricing value factor of wind of 75%. The upper range limit is chosen symmetric to this (i.e. 125%), although the maximum nodal pricing value factor does not exceeds 111%.

A structural difference between northern and southern nodes becomes obvious. The structural break crosses Germany along an imaginary diagonal line from north-west to south-east. Most northern nodes under nodal pricing have value factors of wind between 75% and 90% whereas southern nodes have in general higher values, in the range from 95% to 100% (up to 110%). The structural break represents insufficient grid transmission capacities which leads to regional price differences, e.g. in hours of high wind feed-in. Breuer et al. (2013) and Burstedde (2012) identi-

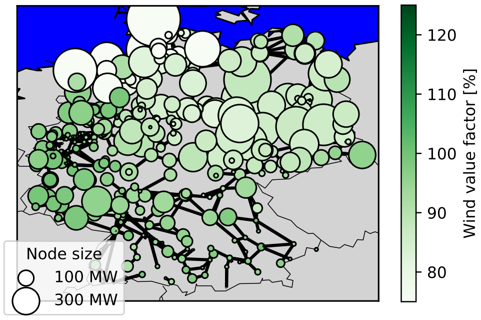

Figure 6.7: Markte value factor of wind production under nodal pricing for each node within Germany. The size of the nodes indicates the installed wind capacity per node.

fied similar structural breaks caused by insufficient the grid capabilities. The mainly congested lines are reported in Bundesnetzagentur (2016) and correspond to the congested lines which are identified within this model.[6]

Comparison of the market value factor for wind under nodal pricing to zonal pricing

Figure 6.8 shows the modeled regional value factor of wind under nodal pricing and zonal pricing. Note that the colormaps are cut to the range from 75% to 125% for

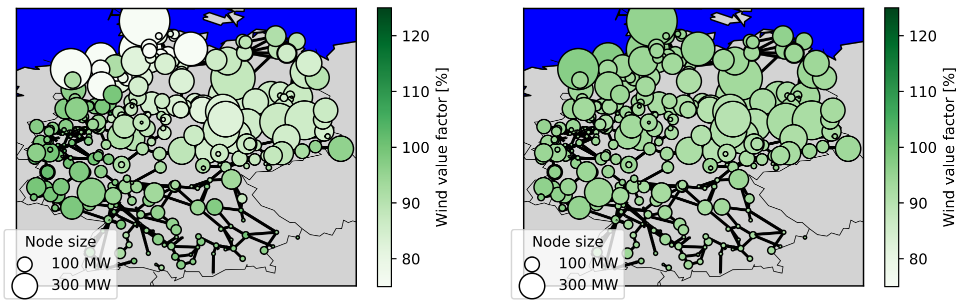

(i) Market value factor of wind under nodal pricing per node

(ii) Market value factor of wind under zonal pricing per node

Figure 6.8: Comparison of the regional market value factors of wind production for each node within Germany: (a) under nodal pricing, (b) under zonal pricing. The size of the nodes indicates the installed wind capacity per node.

[6]Further research on the effects of a German market splitting assume a separation along a horizontal line further southwards based on some heuristics, e.g. re-dispatch amount or reported congestion (Egerer et al., 2016, Trepper et al., 2015). Based on own calculations, the paper in in line with research on optimal zone configurations of (Breuer et al., 2013) or Burstedde (2012) with a mainly diagonal congestion structure.

comparison reasons and that, for the nodal pricing value factor of wind, wind values down to 30% exist (cf. 6.10 in the appendix). The regional value factor of wind has an average value of 94% and a smaller standard deviation of 1% under zonal pricing compared to nodal pricing (mean: 91%, standard deviation: 10%). Details can be found in 6.3. The lowest zonal pricing value factors of wind are concentrated in the eastern-central area in Germany. In contrast to the zonal pricing value factors of wind, the nodal pricing value factors of wind are low in that area as well, but are even lower at the northern coast.

Differences in the nodal pricing and zonal pricing value factors

The difference between the regional wind value factor under nodal pricing and zonal pricing is shown in Figure 6.6. For comparison, the colormaps are restricted to ±10%-points. The total differences are shown in a line plot in Figure 6.11.

The value factor may strongly deviate between zonal and nodal pricing. Differences up to -17%-points and +63%-points may arise. Additionally, the zonal pricing smooths the regional effects which, in contrast, exist in the nodal pricing regime. For the investigated case, the zonal pricing value factor has a 3%-points higher mean and a 9%-points lower standard deviation compared to the value factor under nodal pricing.

The difference in the value factors arises mainly due to the internalization of the physical power flow characteristics of the grid to the dispatch model. The internalized cost of transmission lead to different market prices (i.e. nodal prices) and finally to a different value of wind. Especially windy situations cause such grid congestion.

Implications of the value factor analysis

The comparison shows that the market value factor of wind under zonal pricing overestimates the value of wind in the northern area and underestimates it in the southern area in comparison to the nodal pricing value factor of wind. The zonal pricing value factor does not reflect the value of wind under consideration of the transmission characteristics. Thus it is not suitable to assess the value of wind to electricity systems. The nodal pricing value factor considers physical flow restrictions and is therefore much more suitable to assess the value of wind to the electricity system.

The value factor neglects the real production. It is not sufficient for detailed assess-

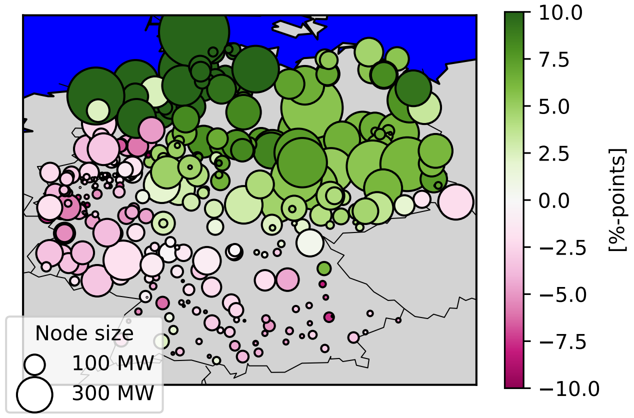

(i) Deltas for all nodes

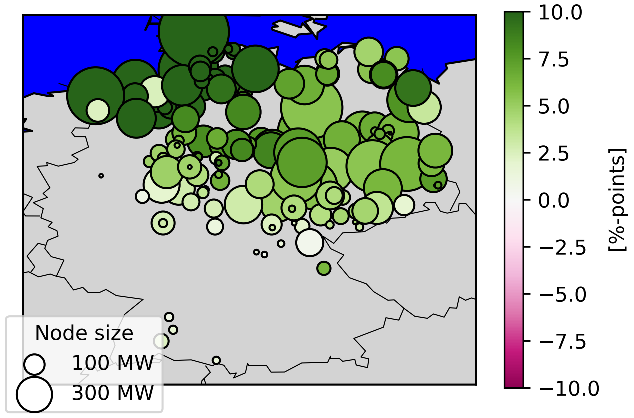

(ii) Nodes with positive deltas

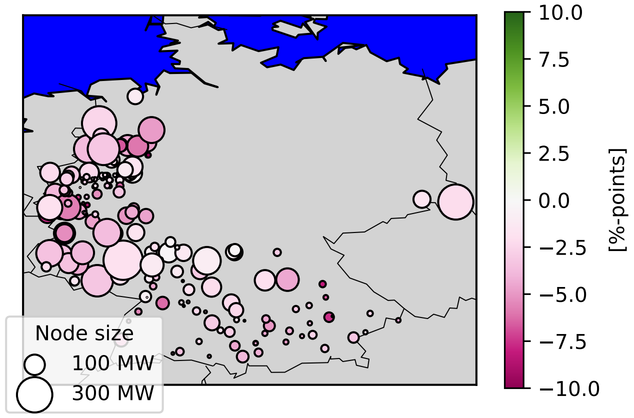

(iii) Nodes with negative deltas

Figure 6.9: Difference between the market value factor of wind production under zonal pricing to nodal pricing within Germany. A positive value indicates a higher market value factor under zonal pricing. The size of the nodes indicates the installed wind capacity per node.

ments. For this, the wind revenues are recommended (as discussed in Section 6.3.1). However, the value factors may serve as a rough indicator, e.g. to compare the wind contribution of different countries to each other.

6.4 Discussion

The results have highly relevant implications on different aspects of wind energy.

- Market revenues under zonal pricing incentivize inefficient locations compared to the market revenues under nodal pricing. The revenues for wind under zonal pricing do not consider the grid situations. Thus, zonal pricing revenues would favor windy locations. Under consideration of the grid situation (nodal pricing), different locations are favorable which are identified within this analysis. Optimal wind locations should thus be estimated under consideration of the grid situations. The underlying approach with a nodal pricing optimization model reflects one opportunity to identify optimal wind locations.
- The value factor may serve as an indicator but does not reflect the wind revenues accurately. The discrepancy between the revenues (cf. Figure 6.4i) and value factor (cf. Figure 6.7) might serve as an example. The reason is that the value factor does not consider the actual wind production. The definition of the value factor is solely an aggregation of the wind-production-weighted electricity prices. Thus, the value factor is not sufficient to assess locational investment decisions in detail. However, the aggregated information in the value factor might be suitable for various other investigation and is a widely used indicator.
- The derived results are highly relevant for the design and implementation of subsidy schemes. Wind capacity extensions are usually incentivized by additional subsidy payments. It is not finally answered which design of a subsidy scheme is economically beneficial in which situation. This is subject of current research (e.g. Pechan (2017) and Wagner (2016)). The underlying research provides new insights for the design of optimal subsidy schemes. It shows that market integrated subsidy schemes could be distorting if they do not incorporate the physical transmission situation. Thus, the transmission situation should be considered in the subsidy scheme definition. Furthermore, subsidy schemes which are partially or fully based on the wind production (e.g. fixed

feed-in tariffs, fixed feed-in premiums) and have no grid component might incentivize non-system-favorable locations. This could lead to more grid congestion and should be avoided. The German government tries to avoid over-investment of wind in system-unfavorable northern areas by a politically given capacity restriction (cf. Bundesnetzagentur (2017)). The underlying approach allows to identify and evaluate such suggestions. Moreover, in combination with an adjusted subsidy scheme, a market driven solution could be implemented to avoid over-investments. Dependent on the subsidy adjustment, more risk is transferred to the wind producers (i.e. operators). The increased risks could lead to increased investment costs. Therefore, adjustments should be applied carefully.

However, the derived results have a drawback. The performed analysis is static, i.e. a one-shot analysis of a current state without investment decisions. The modeled wind results (revenues and value factors) are dependent on (1) the grid structure and (2) complementary installed (wind) capacities. Further investments may change the regional revenues and value factors of wind. Additionally, further wind capacities at the same or near-by nodes cause additional correlation effects. This cannibalization effect would tend to decrease the regional revenues as well as the regional value factors.

6.5 Conclusion

This paper investigates the modeled wind revenues and modeled wind value factors under two pricing regimes: zonal pricing and nodal pricing. Focus is the German electricity market due to a high share of wind production and regional different wind speed structures. The revenues and the value factors of wind are assessed (1) under *nodal pricing* with internalized transmission situations and (2) under *zonal pricing* without internalized transmission situations. The nodal pricing regime is considered as the economic efficient benchmark whereas the zonal pricing regime represents the current European market design.

The contribution to existing literature is twofold: First, the regional revenues for wind production under nodal pricing and zonal pricing are quantified and compared. The revenues show strong deviations dependent on the transmission situations. The revenues incentivize wind locations. Under zonal pricing (without grid consideration) the regional incentives are identified as system-unfavorable. This might lead to congestion increasing wind investments.

Second, the value factor is identified. It does not reflect the operators' revenue-optimal locations. Thus, the value factor is not suitable as a detailed indicator. Furthermore, the market value factor under zonal pricing overestimates windy locations in contrast to the nodal pricing regime.

The derived results are highly relevant for the design and adjustment of wind energy subsidy schemes which should consider the grid situations to achieve system optimal wind locations.

Further research is necessary to account for dynamic investment decisions and to find long-run optimal wind locations. This is technically possible with the underlying model but simplifications might be necessary to guarantee tractable model size. Another extension would consider the interdependency between the grid extension and the capacity extension and analyze the robustness of a dynamic solution.

6.6 Appendix

6.6.1 Load Distribution

For the nodal electricity market model, all relevant location parameters have to be matched to the nodes. For electricity production this is performed by the smallest distance approach of the production's location to the nodes. For the load distribution, this approach is not suitable. Thus, a regression is performed which estimates the load consumption based on GDP and population.

The load distribution weights are derived via a least squares estimation of the dependent variable load by the independent variables GDP and population, i.e.

$$Load_i = \alpha + \beta_1 GDP_i + \beta_2 population_i + \varepsilon_i \qquad \text{, for country i.} \tag{6.9}$$

The observations are on a European national level based on public available data from Eurostat for the years 2011 to 2014. The estimated coefficients are $\beta_1 = 0.41$ and $\beta_2 = 0.59$. Those coefficienty represent the weights which are used to distribute the total German load to the German counties (NUTS-3 areas), for which the GDP and the population are known but the load is unknown. For each German county, this reads as

$$Load_{county} = Load_{Germany} \cdot \left[0.41 \frac{GDP_{county}}{GDP_{Germany}} + 0.59 \frac{Population_{county}}{Population_{Germany}} \right]. \tag{6.10}$$

Furthermore, the areas are upsampled to the specific nodes by Voronoi diagrams. For each node a surrounding area is determined which is characterized such that no other node is closer for the surrounding area. In this way, complete Germany is partitioned. In a second step, the calculated load distribution of the counties (NUTS-3 areas) are matched to the nodes dependent on the share of the overlapping Voronoi areas. That means, if a county contains two nodes with equal area of the belonging Voronoi diagrams, both nodes derive 50% of the county's load. If the Voronoi diagram of a node also contains other counties' shares, the counties' corresponding load share is added.

6.6.2 Statistics of the wind revenues per node under nodal pricing and zonal pricing

Table 6.2 shows statistics of the nodal and zonal wind production revenues which are compared in Figure 6.8. The wind revenues are relative to the capacity-weighted average wind revenue for Germany. The average wind revenue under a nodal pricing is 107% and above the zonal pricing average wind revenue of 87%. Note that the revenues reflect the unweighted average of each node. Since more nodes are behind the typical wind-driven grid congestion, the average wind revenue is higher under nodal pricing. The statistics show that the nodal pricing leads to a broader range of wind revenues compared to zonal pricing. The minimum and maximum are more extreme as well.

Table 6.2: Statistics of the wind revenues under nodal pricing, zonal pricing and the difference (zonal − nodal pricing) per node. Percentage to the capacity-weighted average wind revenues under nodal or zonal pricing, respectively. The nodes are not weighted, i.e. each node counts as one observation.

	Nodal pricing wind revenues [%]	Zonal pricing wind revenues [%]	Difference between zonal and nodal wind revenues [%-points]
mean	107	87	-21
std	56	35	45
min	6	5	-214
25%	75	64	-31
50%	97	84	-18
75%	131	106	-9
max	361	279	205

6.6.3 Statistics of the market value factor of wind per node under nodal pricing and zonal pricing

Table 6.3: Statistics of the wind value factor per node under nodal pricing, zonal pricing and the difference (zonal value factor - nodal value factor).

	Market value factor under nodal pricing [%]	Market value factor under zonal pricing [%]	Difference between the market value factor of zonal to nodal pricing [%-points]
mean	91	94	3
std	10	1	10
min	31	89	-17
25%	87	93	-3
50%	94	94	-1
75%	98	94	6
max	111	98	63

Figure 6.10 shows the histograms of the market value factor of wind under nodal and zonal pricing. The value factor under nodal pricing has a broader range and

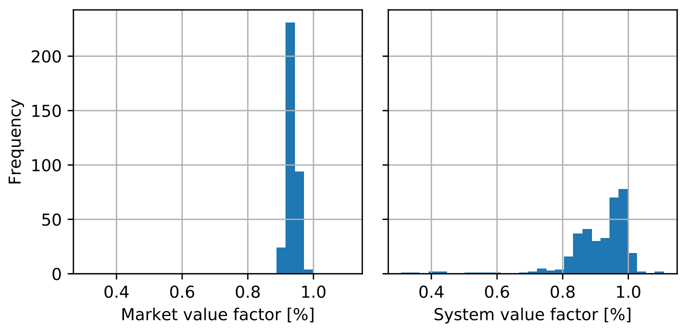

Figure 6.10: Histogram of the modeled market values of wind production per node under zonal pricing (left) and nodal pricing (right)

less values around 100% in comparison to zonal pricing.

Figure 6.11 shows the differences between the market value factor of wind production under nodal pricing and zonal pricing for each node in a lineplot (sorted ascending).

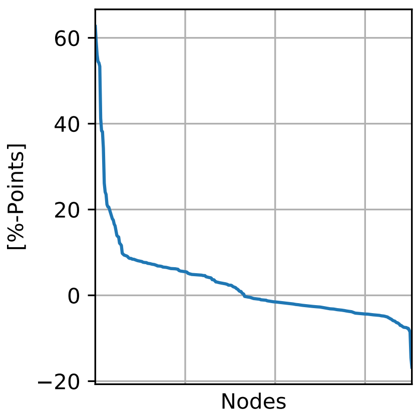

Figure 6.11: Lineplot of the difference between the market value factor of wind production per node under nodal pricing and zonal pricing. Values are the percental point difference of the market value factors of zonal to nodal pricing.

Bibliography

50Hertz (2017). Extrapolated actual wind power feed-in - 50hertz Transmission GmbH. Online; Accessed 26-Jul-2017; http://www.50hertz.com/en/Grid-Data/Wind-power/Extrapolated-actual-wind-power-feed-in.

Acemoglu, D., Kakhbod, A., and Ozdaglar, A. (2017). Competition in Electricity Markets with Renewable Energy Sources. *The Energy Journal*, 38(01).

Ackermann, T. (2005). Wind Power in Power Systems. In *Wind Power in Power Systems*. John Wiley & Sons, Ltd.

AG Energiebilanzen (2016). Bruttostromerzeugung in Deutschland ab 1990 nach Energieträgern.

AG Energiebilanzen (2017). Bruttostromerzeugung in Deutschland ab 1990 bis 2016 nach Energieträgern.

Allaz, B. (1992). Oligopoly, uncertainty and strategic forward transactions. *International Journal of Industrial Organization*, 10(2):297–308.

Allaz, B. and Vila, J.-L. (1993). Cournot Competition, Forward Markets and Efficiency. *Journal of Economic Theory*, 59(1):1–16.

Amprion (2017). Photovoltaic infeed. Online; Accessed 26-Jul-2017; https://www.amprion.net/Grid-Data/Photovoltaic-Infeed/.

APG (2017). Market Information - Generation Forecast. Online; Accessed 26-Jul-2017; https://www.apg.at/en/market/Markttransparenz/generation/generation-forecast.

Ausubel, L. M., Cramton, P., Pycia, M., Rostek, M., and Weretka, M. (2014). Demand Reduction and Inefficiency in Multi-Unit Auctions. *The Review of Economic Studies*.

Bathurst, G., Weatherill, J., and Strbac, G. (2002). Trading wind generation in short term energy markets. *IEEE Transactions on Power Systems*, 17(3):782–789.

Bertsch, J., Hagspiel, S., and Just, L. (2016). Congestion management in power systems. *Journal of Regulatory Economics*, 50(3):290–327.

Bessembinder, H. and Lemmon, M. L. (2002). Equilibrium Pricing and Optimal Hedging in Electricity Forward Markets. *The Journal of Finance*, 57(3):1347–1382.

Birge, J. and Louveaux, F. (1997). *Introduction to stochastic programming*, volume 9. Springer-Verlag.

Bissolli, P. and Dittmann, E. (2001). The objective weather type classification of the German Weather Service and its possibilities of application to environmental and meteorological investigations. *Meteorologische Zeitschrift*, 10(4):253–260.

Bjørndal, M. and Jörnsten, K. (2008). Equilibrium prices supported by dual price functions in markets with non-convexities. *European Journal of Operational Research*, 190(3):768–789.

Bloys van Treslong, A. and Huisman, R. (2010). A comment on: Storage and the electricity forward premium. *Energy Economics*, 32(2):321–324.

Bollmeyer, C., Keller, J. D., Ohlwein, C., Wahl, S., Crewell, S., Friederichs, P., Hense, A., Keune, J., Kneifel, S., Pscheidt, I., Redl, S., and Steinke, S. (2015). Towards a high-resolution regional reanalysis for the European CORDEX domain. *Quarterly Journal of the Royal Meteorological Society*, 141(686):1–15.

Borenstein, S., Bushnell, J. B., and Wolak, F. A. (2002). Measuring Market Inefficiencies in California's Restructured Wholesale Electricity Market. *The American Economic Review*, 92(5):1376–1405.

Botterud, A., Wang, J., Bessa, R., Keko, H., and Miranda, V. (2010). Risk management and optimal bidding for a wind power producer. In *2010 IEEE Power and Energy Society General Meeting*.

Breuer, C., Seeger, N., and Moser, A. (2013). Determination of alternative bidding areas based on a full nodal pricing approach. In *2013 IEEE Power Energy Society General Meeting*, pages 1–5.

Bundeskartellamt (2011). Sektoruntersuchung Stromerzeugung und -großhandel. Technical Report Abschlussbericht gemäß § 32e GWB, Bundeskartellamt.

Bundesnetzagentur (2014). *Kraftwerksliste zum NEP 2014*.

Bundesnetzagentur (2016). Monitoring Report 2015. Technical report, Bundesnetzagentur.

Bundesnetzagentur (2017). Aenderungsverordnung_eeav.

Bundesregierung (1991). Gesetz über die Einspeisung von Strom aus erneuerbaren Energien in das öffentliche Netz (Stromeinspeisungsgesetz) vom 07. Dezember 1990 (BGBl I S. 2633).

Bundesregierung (2012). Gesetz zur Neuregelung des Rechtsrahmens für die Förderung der Stromerzeugung aus erneuerbaren Energien Vom 28. Juli 2011.

Bundesregierung (2014). Erneuerbare-Energien-Gesetz vom 21. Juli 2014 (BGBl. I S. 1066), das durch Artikel 1 des Gesetzes vom 13. Oktober 2016 (BGBl. I S. 2258) geändert worden ist.

Bundesregierung (2017). Gesetz zur Einführung von Ausschreibungen für Strom aus erneuerbaren Energien und zu weiteren Änderungen des Rechts der erneuerbaren Energien Vom 13. Oktober 2016.

Bunn, D. W. and Chen, D. (2013). The forward premium in electricity futures. *Journal of Empirical Finance*, 23:173–186.

Burke, D. J. and O'Malley, M. J. (2008). Optimal Wind Power Location on Transmission Systems - A Probabilistic Load Flow Approach. In *Proceedings of the 10th International Conference on Probabilistic Methods Applied to Power Systems, 2008. PMAPS '08*, pages 1–8.

Burke, D. J. and O'Malley, M. J. (2011). A Study of Optimal Nonfirm Wind Capacity Connection to Congested Transmission Systems. *IEEE Transactions on Sustainable Energy*, 2(2):167–176.

Burstedde, B. (2012). From nodal to zonal pricing: A bottom-up approach to the second-best. In *2012 9th International Conference on the European Energy Market*, pages 1–8.

Bushnell, J. (2007). Oligopoly equilibria in electricity contract markets. *Journal of Regulatory Economics*, 32(3):225–245.

Bushnell, J. B. and Oren, S. S. (1994). Bidder cost revelation in electric power auctions. *Journal of Regulatory Economics*, 6(1):5–26.

Cameron, L. and Cramton, P. (1999). The Role of the ISO in U.S. Electricity Markets. *The Electricity Journal*, 12(3):71–81.

Cannon, D. J., Brayshaw, D. J., Methven, J., Coker, P. J., and Lenaghan, D. (2015). Using reanalysis data to quantify extreme wind power generation statistics: A 33 year case study in Great Britain. *Renewable Energy*, 75:767–778.

Carrion, M. and Arroyo, J. M. (2006). A computationally efficient mixed-integer linear formulation for the thermal unit commitment problem. *IEEE Transactions on Power Systems*, 21(3):1371–1378.

Cartea, l. and Villaplana, P. (2008). Spot price modeling and the valuation of electricity forward contracts: The role of demand and capacity. *Journal of Banking & Finance*, 32(12):2502–2519.

Chao, H.-p., Peck, S., Oren, S., and Wilson, R. (2000). Flow-Based Transmission Rights and Congestion Management. *The Electricity Journal*, 13(8):38–58.

Chao, H.-P. and Wilson, R. (2002). Multi-Dimensional Procurement Auctions for Power Reserves: Robust Incentive-Compatible Scoring and Settlement Rules. *Journal of Regulatory Economics*, 22(2):161–183.

Chen, C., Duan, S., Cai, T., and Liu, B. (2011). Online 24-h solar power forecasting based on weather type classification using artificial neural network. *Solar Energy*, 85(11):2856–2870.

Cludius, J., Hermann, H., Matthes, F. C., and Graichen, V. (2014). The merit order effect of wind and photovoltaic electricity generation in Germany 2008–2016: Estimation and distributional implications. *Energy Economics*, 44:302–313.

Conejo, A. J., Plazas, M. A., Espinola, R., and Molina, A. B. (2005). Day-ahead electricity price forecasting using the wavelet transform and ARIMA models. *IEEE Transactions on Power Systems*, 20(2):1035–1042.

Contreras, J., Espinola, R., Nogales, F. J., and Conejo, A. J. (2003). ARIMA models to predict next-day electricity prices. *IEEE Transactions on Power Systems*, 18(3):1014–1020.

Cosseron, A., Gunturu, U. B., and Schlosser, C. A. (2013). Characterization of the Wind Power Resource in Europe and its Intermittency. *Energy Procedia*, 40:58–66.

Couto, A., Costa, P., Rodrigues, L., Lopes, V. V., and Estanqueiro, A. (2015). Impact of Weather Regimes on the Wind Power Ramp Forecast in Portugal. *IEEE Transactions on Sustainable Energy*, 6(3):934–942.

Couture, T. and Gagnon, Y. (2010). An analysis of feed-in tariff remuneration models: Implications for renewable energy investment. *Energy Policy*, 38(2):955–965.

Davis, M. J. (2010). Contrast coding in multiple regression analysis: Strengths, weaknesses, and utility of popular coding structures. *Journal of Data Science*, 8(1):61–73.

de Frutos, M.-A. and Fabra, N. (2012). How to allocate forward contracts: The case of electricity markets. *European Economic Review*, 56(3):451–469.

Dena (2014). *Systemdienstleistungen 2030 - Sicherheit und Zuverlässigkeit einer Stromversorgung mit hohem Anteil erneuerbarer Energien*. Berlin.

Dickey, D. A. and Fuller, W. A. (1979). Distribution of the Estimators for Autoregressive Time Series with a Unit Root. *Journal of the American Statistical Association*, 74(366a):427–431.

Douglas, S. and Popova, J. (2008). Storage and the electricity forward premium. *Energy Economics*, 30(4):1712–1727.

DWD (2017). The objective weather type classification. Online; Accessed 26-Jul-2017; https://www.dwd.de/EN/ourservices/wetterlagenklassifikation/wetterlagenklassifikation.html

Egerer, J., Weibezahn, J., and Hermann, H. (2016). Two price zones for the German electricity market — Market implications and distributional effects. *Energy Economics*, 59:365–381.

Elberg, C. and Hagspiel, S. (2015). Spatial dependencies of wind power and interrelations with spot price dynamics. *European Journal of Operational Research*, 241(1):260–272.

Elzinga, K. G. and Mills, D. E. (2011). The Lerner Index of Monopoly Power: Origins and Uses. *The American Economic Review*, 101(3):558–564.

EPEX SPOT (2017). Intraday Continuous German/Austria. Online; Accessed 26-Jun-2017; https://www.epexspot.com/en/market-data/intradaycontinuous/intraday-table/-/DE.

EU Comission (2009). Official Journal of the European Union, L 140, 05 June 2009.

EU Comission (2013). European Commission guidance for the design of renewables support schemes Accompanying the document Communication from the Commission Delivering the internal market in electricity and making the most of public intervention - Comission Staff Working Document.

EUR-lex (2004). Guidelines on the assessment of horizontal mergers under the Council Regulation on the control of concentrations between undertakings.

European Commission (2017). Commission Regulation (EU) establishing a guideline on electricity balancing (Proposal).

Fabra, N., von der Fehr, N.-H., and Harbord, D. (2006). Designing electricity auctions. *The RAND Journal of Economics*, 37(1):23–46.

Foley, A. M., Leahy, P. G., Marvuglia, A., and McKeogh, E. J. (2012). Current methods and advances in forecasting of wind power generation. *Renewable Energy*, 37(1):1–8.

Fripp, M. and Wiser, R. H. (2008). Effects of Temporal Wind Patterns on the Value of Wind-Generated Electricity in California and the Northwest. *IEEE Transactions on Power Systems*, 23(2):477–485.

Furió, D. and Meneu, V. (2010). Expectations and forward risk premium in the Spanish deregulated power market. *Energy Policy*, 38(2):784–793.

Gabriel, S. A., Conejo, A. J., Fuller, J. D., Hobbs, B. F., and Ruiz, C. (2012). *Complementarity Modeling in Energy Markets*. Springer Science & Business Media. Google-Books-ID: Lu1L5wUea8IC.

Gerstengarbe, F.-W., Werner, P. C., Hess, P., and Brezowsky, H. (2010). *Katalog der Großwetterlagen Europas nach Paul Hess und Helmuth Brezowsky:(1881-2004)*. PIK.

Green, R. (2007). Nodal pricing of electricity: how much does it cost to get it wrong? *Journal of Regulatory Economics*, 31(2):125–149.

Green, R. J., Lorenzoni, A., Perez, Y., and Pollitt, M. G. (2006). Benchmarking Electricity Liberalisation in Europe. Working Paper, Faculty of Economics, University of Cambridge, UK.

Green, R. J. and Newbery, D. M. (1992). Competition in the British Electricity Spot Market. *Journal of Political Economy*, 100(5):929–953.

Grothe, O. and Müsgens, F. (2013). The influence of spatial effects on wind power revenues under direct marketing rules. *Energy Policy*, 58:237–247.

Grothe, O. and Schnieders, J. (2011). Spatial dependence in wind and optimal wind power allocation: A copula-based analysis. *Energy Policy*, 39(9):4742–4754.

Growitsch, C., Höffler, F., and Wissner, M. (2010). Marktkonzentration und Marktmachtanalyse für den deutschen Regelenergiemarkt. *Zeitschrift für Energiewirtschaft*, 34(3):209–222.

Gunturu, U. B. and Schlosser, C. A. (2012). Characterization of wind power resource in the United States. *Atmos. Chem. Phys.*, 12(20):9687–9702.

Hagspiel, S., Knaut, A., Peter, J., and others (2017). Reliability in Multy-Regional Power Systems-Capacity Adequacy and the Role of Interconnectors. Technical report, Energiewirtschaftliches Institut an der Universitaet zu Koeln (EWI).

Hallgren, W., Gunturu, U. B., and Schlosser, A. (2014). The Potential Wind Power Resource in Australia: A New Perspective. *PLOS ONE*, 9(7):e99608.

Haucap, J., Heimeshoff, U., and Jovanovic, D. (2012). Competition in Germany's minute reserve power market: An econometric analysis. *DICE Discussion Paper*, 75.

Heffner, G. (2008). Loads Providing Ancillary Services: Review of International Experience. *Lawrence Berkeley National Laboratory*.

Heim, S. and Götz, G. (2013). Do pay-as-bid auctions favor collusion? Evidence from Germany's market for reserve power. *ZEW Discussion Paper*, 13-035.

Henckes, P., Knaut, A., Obermüller, F., and Frank, C. (2018). The benefit of long-term high resolution wind data for electricity system analysis. *Energy*, 143:934–942.

Henriot, A. (2014). Market design with centralized wind power management: handling low-predictability in intraday markets. *The Energy Journal*, 35(1):99–117.

Hirschman, A. O. (1964). The Paternity of an Index. *The American Economic Review*, 54(5):761–762.

Hirth, L. (2013). The market value of variable renewables: The effect of solar wind power variability on their relative price. *Energy Economics*, 38:218–236.

Hirth, L. (2016). The benefits of flexibility: The value of wind energy with hydropower. *Applied Energy*, 181:210–223.

Hirth, L. and Müller, S. (2016). System-friendly wind power: How advanced wind turbine design can increase the economic value of electricity generated through wind power. *Energy Economics*, 56:51–63.

Hirth, L., Ueckerdt, F., and Edenhofer, O. (2015). Integration costs revisited – An economic framework for wind and solar variability. *Renewable Energy*, 74:925–939.

Hirth, L. and Ziegenhagen, I. (2015). Balancing power and variable renewables: Three links. *Renewable and Sustainable Energy Reviews*, 50:1035–1051.

Hogan, W. A. (1999). Transmission congestion the nodal-zonal debate revisited.

Hogan, W. W. (1997). A Market Power Model with Strategic Interaction in Electricity Networks. *The Energy Journal*, 18(4):107–141.

IEA (2016). Next Generation Wind and Solar Power.

ISO New England (2011). Overview of New England's Wholesale Electricity Markets.

Ito, K. and Reguant, M. (2016). Sequential Markets, Market Power, and Arbitrage. *American Economic Review*, 106(7):1921–1957.

Jamasb, T. and Pollitt, M. (2005). Electricity Market Reform in the European Union: Review of Progress toward Liberalization & Integration. *The Energy Journal*, 26:11–41.

James, P. M. (2007). An objective classification method for Hess and Brezowsky Grosswetterlagen over Europe. *Theoretical and Applied Climatology*, 88(1-2):17–42.

Jägemann, C. (2015). An Illustrative Note on the System Price Effect of Wind and Solar Power: The German Case. *Zeitschrift für Energiewirtschaft*, 39(1):33–47.

Joskow, P. L. (2005). Markets for Power in the United States: An Interim Assessment. SSRN Scholarly Paper ID 845785, Social Science Research Network, Rochester, NY.

Joskow, P. L. (2011). Comparing the Costs of Intermittent and Dispatchable Electricity Generating Technologies. *The American Economic Review*, 101(3):238–241.

Joskow, P. L. and others (2008). *Lessons Learned from the Electricity Market Liberalization*. Massachusetts Institute of Technology, Center for Energy and Environmental Policy Research.

Just, S. (2011). Appropriate contract durations in the German markets for on-line reserve capacity. *Journal of Regulatory Economics*, 39(2):194–220.

Just, S. and Weber, C. (2008). Pricing of reserves: Valuing system reserve capacity against spot prices in electricity markets. *Energy Economics*, 30(6):3198–3221.

Kaimal, J. C. and Finnigan, J. J. (1994). *Atmospheric Boundary Layer Flows: Their Structure and Measurement*. Oxford University Press. Google-Books-ID: C7LnCwAAQBAJ.

Kaiser-Weiss, A. K., Kaspar, F., Heene, V., Borsche, M., Tan, D. G. H., Poli, P., Obregon, A., and Gregow, H. (2015). Comparison of regional and global reanalysis near-surface winds with station observations over Germany. *Adv. Sci. Res.*, 12(1):187–198.

Kiesel, R. and Paraschiv, F. (2017). Econometric analysis of 15-minute intraday electricity prices. *Energy Economics*, 64:77–90.

Knaut, A. and Obermüller, F. (2016). How to sell renewable electricity: Interactions of the intraday and day-ahead market under uncertainty. EWI Working Paper 16/04, Energiewirtschaftliches Institut an der Universitaet zu Koeln (EWI).

Knaut, A., Obermüller, F., and Weiser, F. (2017). Tender Frequency and Market Concentration in Balancing Power Markets. EWI Working Paper 2017-4, Energiewirtschaftliches Institut an der Universitaet zu Koeln (EWI).

Knaut, A. and Paschmann, M. (2017a). Decoding Restricted Participation in Sequential Electricity Markets. EWI Working Paper 17/05, Energiewirtschaftliches Institut an der Universitaet zu Koeln (EWI).

Knaut, A. and Paschmann, M. (2017b). Price Volatility in Commodity Markets with Restricted Participation. EWI Working Paper 17/02, Energiewirtschaftliches Institut an der Universitaet zu Koeln (EWI).

Knaut, A. and Paulus, S. (2017). When are consumers responding to electricity prices? An hourly pattern of demand elasticity. Technical Report 2016-7, Energiewirtschaftliches Institut an der Universitaet zu Koeln (EWI).

Kreuz, S. and Müsgens, F. (2017). The German Energiewende and its roll-out of renewable energies: An economic perspective. *Frontiers in Energy*, pages 1–9.

Kunz, F. (2013). Improving Congestion Management: How to Facilitate the Integration of Renewable Generation in Germany. *Energy Journal*, 34(4):55–78.

Lamont, A. D. (2008). Assessing the long-term system value of intermittent electric generation technologies. *Energy Economics*, 30(3):1208–1231.

Lange, M. and Heinemann, D. (2002). Accuracy of short term wind power predictions depending on meteorological conditions.

Lange, M. and Waldl, H.-P. (2001). Assessing the uncertainty of wind power predictions with regard to specific weather situations (PDF Download Available).

Leuthold, F., Weigt, H., and von Hirschhausen, C. (2008). Efficient pricing for European electricity networks – The theory of nodal pricing applied to feeding-in wind in Germany. *Utilities Policy*, 16(4):284–291.

Litvinov, E. (2010). Design and operation of the locational marginal prices-based electricity markets. *IET Generation, Transmission & Distribution*, 4(2):315–323.

Longstaff, F. A. and Wang, A. W. (2004). Electricity forward prices: a high-frequency empirical analysis. *The journal of finance*, 59(4):1877–1900.

Matke, C., Medjroubi, W., and Kleinhans, D. (2016). *SciGRID - An Open Source Reference Model for the European Transmission Network (v0.2)*.

McClendon, M. (1994). *Multiple Regression and Causal Analysis*. F E Peacock Pub - Better World Books.

MISO (2016). Energy and Operating Reserve Markets: Business Practices Manual (BPM-002-r16). Technical report.

Monforti, F., Gaetani, M., and Vignati, E. (2016). How synchronous is wind energy production among European countries? *Renewable and Sustainable Energy Reviews*, 59:1622–1638.

Morales, J., Conejo, A., and Perez-Ruiz, J. (2010). Short-Term Trading for a Wind Power Producer. *IEEE Transactions on Power Systems*, 25(1):554–564.

Morales, J. M., Conejo, A. J., Madsen, H., Pinson, P., and Zugno, M. (2013). *Integrating Renewables in Electricity Markets: Operational Problems*. Springer Science & Business Media. Google-Books-ID: QF24BAAAQBAJ.

Morales-España, G., Latorre, J. M., and Ramos, A. (2013). Tight and Compact MILP Formulation of Start-Up and Shut-Down Ramping in Unit Commitment. *IEEE Transactions on Power Systems*, 28(2):1288–1296.

Motta, M., Barthelmie, R. J., and Vølund, P. (2005). The influence of non-logarithmic wind speed profiles on potential power output at Danish offshore sites. *Wind Energy*, 8(2):219–236.

Müsgens, F. and Ockenfels, A. (2011). Design von Informationsfeedback in Regelenergiemärkten. *Zeitschrift für Energiewirtschaft*, 35(4):249–256.

Müsgens, F., Ockenfels, A., and Peek, M. (2014). Economics and design of balancing power markets in Germany. *International Journal of Electrical Power & Energy Systems*, 55:392–401.

Müsgens, P. D. F., Ockenfels, P. D. A., and Peek, M. (2012). Balancing Power Markets in Germany: Timing Matters. *Zeitschrift für Energiewirtschaft*, 36(1):1–7.

Newey, W. K. and West, K. D. (1987). Hypothesis Testing with Efficient Method of Moments Estimation. *International Economic Review*, 28(3):777–787.

Obermüller, F. (2017a). Build Wind Capacities at Windy Locations? Assessment of System Optimal Wind Locations. EWI Working Paper 17/09, Energiewirtschaftliches Institut an der Universitaet zu Koeln (EWI).

Obermüller, F. (2017b). Explaining Electricity Forward Premiums - Evidence for the Weather Uncertainty Effect. EWI Working Paper 17/10, Energiewirtschaftliches Institut an der Universitaet zu Koeln (EWI).

Obersteiner, C. and Saguan, M. (2011). Parameters influencing the market value of wind power – a model-based analysis of the Central European power market. *European Transactions on Electrical Power*, 21(6):1856–1868.

Ocker, F., Braun, S., and Will, C. (2016). Design of European balancing power markets. In *2016 13th International Conference on the European Energy Market (EEM)*, pages 1–6.

Ostrowski, J., Anjos, M. F., and Vannelli, A. (2012). Tight Mixed Integer Linear Programming Formulations for the Unit Commitment Problem. *IEEE Transactions on Power Systems*, 27(1):39–46.

Overall, J. E. and Spiegel, D. K. (1969). Concerning least squares analysis of experimental data. *Psychological Bulletin*, 72(5):311.

Paraschiv, F., Fleten, S.-E., and Schürle, M. (2015). A spot-forward model for electricity prices with regime shifts. *Energy Economics*, 47:142–153.

Paschmann, M. (2017). Economic Analysis of Price Premiums in the Presence of Non-convexities - Evidence from German Electricity Markets. EWI Working Papers.

Pechan, A. (2015). The Effect of Market Design on Spatial Distribution of Wind Energy Installation. *Oldenburg: Carl von Ossietzky Universität*.

Pechan, A. (2017). Where do all the windmills go? Influence of the institutional setting on the spatial distribution of renewable energy installation. *Energy Economics*, 65:75–86.

Pinson, P., Chevallier, C., and Kariniotakis, G. (2007). Trading Wind Generation From Short-Term Probabilistic Forecasts of Wind Power. *IEEE Transactions on Power Systems*, 22(3):1148–1156.

PJM (2017). PJM Manual 11: Energy & Ancillary Services Market Operations (Revision: 88). Technical report.

Richter, J. (2012). On the interaction between product markets and markets for production capacity: The case of the electricity industry. *EWI Working Paper*, 11/09.

Ritter, M. and Deckert, L. (2017). Site assessment, turbine selection, and local feed-in tariffs through the wind energy index. *Applied Energy*, 185, Part 2:1087–1099.

Roques, F., Hiroux, C., and Saguan, M. (2010). Optimal wind power deployment in Europe—A portfolio approach. *Energy Policy*, 38(7):3245–3256.

Ruiz, C., Conejo, A. J., and Gabriel, S. A. (2012). Pricing Non-Convexities in an Electricity Pool. *IEEE Transactions on Power Systems*, 27(3):1334–1342.

Saloner, G. (1987). Cournot duopoly with two production periods. *Journal of Economic Theory*, 42(1):183–187.

Schill, Pahle, G. (2016). DIW Berlin: On Start-up Costs of Thermal Power Plants in Markets with Increasing Shares of Fluctuating Renewables.

Schweppe, F. C., Tabors, R. D., Caraminis, M. C., and Bohn, R. E. (1988). Spot pricing of electricity.

Sensfuß, F., Ragwitz, M., and Genoese, M. (2008). The merit-order effect: A detailed analysis of the price effect of renewable electricity generation on spot market prices in Germany. *Energy Policy*, 36(8):3086–3094.

Shi, J., Lee, W. J., Liu, Y., Yang, Y., and Wang, P. (2012). Forecasting Power Output of Photovoltaic Systems Based on Weather Classification and Support Vector Machines. *IEEE Transactions on Industry Applications*, 48(3):1064–1069.

Staffell, I. and Pfenninger, S. (2016). Using bias-corrected reanalysis to simulate current and future wind power output. *Energy*, 114:1224–1239.

Stull, R. B., editor (1988). *An Introduction to Boundary Layer Meteorology*. Springer Netherlands, Dordrecht.

Swider, D. J. and Weber, C. (2007). The costs of wind's intermittency in Germany: application of a stochastic electricity market model. *European Transactions on Electrical Power*, 17(2):151–172.

Tennet (2017). Actual and forecast photovoltaic energy feed-in | Tennet. Online; Accessed 26-Jul-2017; https://www.tennettso.de/site/en/Transparency/publications/network-figures/actual-and-forecast-photovoltaic-energy-feed-in_land?

The Wind Power (2016). *Europe wind farms database*.

TransnetBW (2017). Key figures | TransnetBW GmbH. Online; Accessed 26-Jul-2017; https://www.transnetbw.com/en/transparency/market-data/key-figures.

Transparency, E. (2017). Transparency in Energy Markets - Solar & Wind Power Production.

Trepper, K., Bucksteeg, M., and Weber, C. (2015). Market splitting in Germany – New evidence from a three-stage numerical model of Europe. *Energy Policy*, 87:199–215.

Twomey, P., Green, R. J., Neuhoff, K., and Newbery, D. (2006). A Review of the Monitoring of Market Power The Possible Roles of TSOs in Monitoring for Market Power Issues in Congested Transmission Systems. Working Paper.

Twomey, P. and Neuhoff, K. (2010). Wind power and market power in competitive markets. *Energy Policy*, 38(7):3198–3210.

US Department of Justice, Federal Trade Commission (2010). Horizontal Merger Guidelines (08/19/2010).

Usaola, J. and Angarita, J. (2007). Bidding wind energy under uncertainty. In *International Conference on Clean Electrical Power, 2007. ICCEP '07*, pages 754–759.

Vandezande, L., Meeus, L., Belmans, R., Saguan, M., and Glachant, J.-M. (2010). Well-functioning balancing markets: A prerequisite for wind power integration. *Energy Policy*, 38(7):3146–3154.

Viehmann, J. (2011). Risk premiums in the German day-ahead Electricity Market. *Energy Policy*, 39(1):386–394.

Viehmann, J. (2017). State of the German Short-Term Power Market. *Zeitschrift für Energiewirtschaft*, 41(2):87–103.

Vlachos, A. and Biskas, P. (2013). Demand Response in a Real-Time Balancing Market Clearing With Pay-As-Bid Pricing. *IEEE Transactions on Smart Grid*, 4(4):1966–1975.

von der Fehr, N.-H. and Harbord, D. (1998). Competition in Electricity Spot Markets. Economic Theory and International Experience. Working Paper 05/1998, Memorandum, Department of Economics, University of Oslo.

Wagner, J. (2016). Grid Investment and Support Schemes for Renewable Electricity Generation. EWI Working Paper 2016-8, Energiewirtschaftliches Institut an der Universitaet zu Koeln (EWI).

Wallace, S. W. and Fleten, S.-E. (2003). Stochastic Programming Models in Energy. In A. Ruszczynski, a. A. S., editor, *Handbooks in Operations Research and Management Science*, volume Volume 10, pages 637–677. Elsevier.

Wang, Q., Zhang, C., Ding, Y., Xydis, G., Wang, J., and Østergaard, J. (2015). Review of real-time electricity markets for integrating Distributed Energy Resources and Demand Response. *Applied Energy*, 138:695–706.

Weron, R. (2007). *Modeling and Forecasting Electricity Loads and Prices: A Statistical Approach*. John Wiley & Sons. Google-Books-ID: cXcWdMgovvoC.

WindEurope (2017). *Wind in power: 2016 European statistics*.

Zhang, B., Johari, R., and Rajagopal, R. (2015). Competition and Coalition Formation of Renewable Power Producers. *IEEE Transactions on Power Systems*, 30(3):1624–1632.

Zhang, Y., Wang, J., and Wang, X. (2014). Review on probabilistic forecasting of wind power generation. *Renewable and Sustainable Energy Reviews*, 32:255–270.